January 1966

Application of Electronic Analog Computer to Solution of Hydrologic and River Basin Planning Problems: Utah Simulation Model II

J. Paul Riley

Duane G. Chadwick

Jay M. Bagley

APPLICATION OF ELECTRONIC ANALOG COMPUTER TO SOLUTION OF HYDROLOGIC AND RIVER-BASIN-PLANNING PROBLEMS: UTAH SIMULATION MODEL II

by

J. Paul Riley
Duane G. Chadwick
Jay M. Bagley

The work reported by this project completion report was supported in part with funds provided by the Department of the Interior, Office of Water Resources Research under P. L. 88-379, Project Number-B-005-Utah, Agreement Number-14-0001-864, Investigation Period-September 1, 1965, to September 30, 1966

Utah Water Research Laboratory
College of Engineering
Utah State University
Logan, Utah

October 1966

ACKNOWLEDGMENTS

This publication represents the final report of a project which was supported in part with funds provided by the Office of Water Resources Research of the United States Department of the Interior as authorized under the Water Resources Research Act of 1964, Public Law 88-379. The work was accomplished by personnel of the Utah Water Research Laboratory in accordance with a research proposal which was submitted to the Office of Water Resources Research through the Utah Center for Water Resources Research at Utah State University. This University is the institution designated to administer the programs of the Office of Water Resources Research in Utah.

The authors acknowledge the technical advice and suggestions which were provided by Mr. Creighton N. Gilbert and Erland Warnick of the Sevier River Basin Investigation Party at Richfield, Utah. Others of various agencies have also provided useful suggestions for which appreciation is expressed.

Special thanks are extended to Mr. Neil W. Morgan, Mr. Kanaan Haffar, and other students who helped with the computer modifications, to Mr. Eugene K. Israelsen who assisted with the programming and operation of the computer, to Miss Donna Higgins for her helpful assistance in editing the manuscript, and to Mrs. Dorothy Riley and other secretaries for their careful typing of it.

J. Paul Riley
Duane G. Chadwick
Jay M. Bagley

LIST OF TABLES

LIST OF FIGURES

LIST OF FIGURES (Continued)

PARTIAL LIST OF SYMBOLS FOR A HYDROLOGIC MODEL[1]

Symbol	Definition
E_r	actual evaporation rate
E_{cr}	potential evaporation rate on evaporation capacity
ET_r	actual evapotranspiration rate
ET_{cr}	potential evapotranspiration rate or evapotranspiration capacity
F_r	actual infiltration rate
F_{cr}	infiltration capacity or maximum infiltration rate
G_r	deep percolation rate to the groundwater basin (inflow to storage)
G_s	quantity of water stored within the groundwater basin
I_r	rate at which precipitation is entering interception storage
M_s	quantity of water stored within the root zone and available for plant use
M_{cs}	root zone storage capacity of water available to plants
M_{es}	limiting root zone available moisture content below which the actual evapotranspiration rate becomes less than the potential rate

[1] Notes:
1) All parameters are functions of time
2) The subscript "r" denotes a rate of change with respect to time
3) The subscript "s" denotes a stored quantity
4) Values of all parameters are greater than or equal to zero
5) Symbols not included in this list are defined within the text of the report

CHAPTER I

INTRODUCTION

The rapid growth in recent years of a variety of demands upon available water resources has led to an increasing interest in the science of hydrology. In every hydrologic system each upstream use has some effect on the quantity of flow occurring at downstream points. Because many of the factors which affect hydrologic flow systems are subject to management or regulation, the optimum use of an existing water supply depends upon an accurate quantitative assessment of the possible management alternatives.

A hydrologic system is relatively easy to describe from a qualitative standpoint. However, the extension of this qualitative knowledge to obtain specific quantitative results is a difficult problem. The complex interrelation and variable nature of the many different processes occurring simultaneously within a hydrologic system make this so. In addition, compared to many other fields of science, few basic quantitative concepts exist as yet in the area of hydrology. Thus, there is need both to describe the various hydrologic processes in mathematical terms and to develop a practical method of combining these expressions into models which will facilitate a quick and easy examination of hydrologic parameters as they are affected by management and other changes within a prototype basin.

In an attempt to find a solution to this problem, research workers in recent years have turned to modern high-speed electronic computers. Through these devices comprehensive simulation models of the entire hydrologic system are being formulated. Considerable progress in digital computer simulation has been made at Stanford University (1, 7, 8). A simplified digital model of the hydrologic and water quality system of the Lost River in northern California has been developed (51), and work is now in progress on digital models at several universities (37).

Simulation of hydrologic systems by means of electronic analog computers is also under development. In the area of flood runoff, Shen (32) discusses the applicability of analog models for analyzing flood flows. The Hydraulic Laboratory of the University of California has built an analog model for the purpose of routing floods in a particular river system (15). In addition, an analog computer program has been developed for simulating flood conditions on the Kitakami River of Japan (24).

Research in electronic analog models of hydrologic systems began at Utah State University in 1963 (2). Professors Bagley and Chadwick envisioned model simulation of an entire watershed and recommended the design and formulation of a pilot model. These recommendations were accepted, and the Soil Conservation Service and the Utah Water and Power Board provided funding to proceed with the construction of a test model. An electronic analog computing device was subsequently designed and built at Utah State University, and completed in November of 1964 (3).

The design of this first hydrologic model developed at Utah State University was relatively simple. Thus, requirements in terms of hydrologic definition and analog computer capacity were not high. A primary objective was to demonstrate the validity of the analog computer approach to modeling in terms of the basic physical processes which occur in any hydrologic system, and which are not specific to any particular geography. Experimental and analytic results were used wherever possible to assist in establishing the mathematical relationships. The operation of these relationships was then observed and improved by verification studies on both analog and digital computers. This model has proved to be entirely satisfactory for the study of interbasin effects and other hydrologic problems where somewhat gross simulation is sufficient.

The success of this project encouraged further work, and led to the study reported herein. The objectives of this project may be briefly stated as follows:

1. The development of improved relations for describing the various hydrologic processes and the interconnecting links between those processes.
2. The development of an electronic analog computer having a high degree of flexibility and capability for the solution of hydrologic and related problems.

The problem presented by the first objective was approached by attempting to describe each physical process in terms of its characteristic variables. From a practical standpoint, only those variables were considered which might be available in a sparse data situation. The second objective was met by adding needed equipment to the original model of the analog computer (3).

While comprehensive simulation models of hydrologic systems are a recent development, they are, of necessity, broad in scope and thus very dependent upon previous work in hydrology. The works of many authors have influenced the model described by this report, and it is hoped that adequate credit has been given in all cases.

Chapter II deals with the basic concepts that are incorporated into the development of an electronic analog model of a hydrologic system. Chapter III contains the mathematical descriptions of the various components of the model, and Chapter IV discusses the added capability resulting from improvements to the analog computer that were made during the course of this project. Chapter V describes briefly the verification of both the mathematical model and the computer design by the simulation of a particular watershed, and finally Chapter VI reviews the present status and future prospects of simulation techniques involving electronic analog computers at Utah State University.

CHAPTER II

ANALOG COMPUTER SIMULATION OF HYDROLOGIC SYSTEMS

Characteristics of the analog computer

Simulation is a technique for investigating the behavior or response of a dynamic system subject to particular constraints and input functions. This technique is usually performed by means of both physical and electronic models. Physical models and also those consisting of electrical resistor-capacitor networks have been used to investigate hydraulic and hydrologic phenomena for many years. However, simulation by means of high-speed electronic computers is a relatively new technique.

As indicated in Chapter I, digital computers have been used successfully for the simulation of hydrologic phenomena. However, for a problem of this nature the electronic analog computer has several important advantages. This type of computer solves problems by behaving electronically in a manner analogous with the problem solution, and is therefore a much faster computing machine than the digital computer. Moreover, the analog computer is a parallel device in that all computations proceed simultaneously. If the size of a problem is doubled, the amount of analog equipment required is also approximately doubled, but the time for solution remains the same. On the other hand, the digital computer, which is a sequential machine, takes twice as long when the problem size is doubled.

Many of the processes which occur in nature are time dependent and as such are differential in form. It is in the solution of differential equations that the great speed of the analog computer is particularly apparent because it can integrate the problem variables continuously instead of using numerical approximations. Frequently, design optimization problems or those involving stochastic variables require differential equations to be solved repeatedly, each with slightly different parameters or functions. Because of its tremendous speed, problems of this nature can be undertaken feasibly by the analog computer when all other methods would require unacceptable lengths of time.

Output on an analog computer is presented in graphical form as a continuous plot of the variable quantities involved. The operator can visualize results as being the actual dynamic responses of the physical system under investigation. Also, the results of possible alternative ways of combining the various components of the entire system can be quickly defined as an aid to determining the changes in specific processes that might be necessary to meet prototype conditions. Thus, the analog is very helpful during the exploratory phases of developing both component relationships and a composite model of a hydrologic system.

The only available independent variable on an analog computer is time, and computations are performed continuously throughout the integration period. It is for this reason that differential equations with respect to time are very applicable to this type of computer. For example, in the case of precipitation, intensity or rate is given by the following differential expression:

$$P_r = \frac{dP}{dt} \quad \ldots\ldots\ldots\ldots\ldots \quad 2.1$$

From equation 2.1 the total precipitation occurring during a period of time, n, is given as follows:

$$P(n) = \int_{t_o}^{t_n} P_r \, dt \quad \ldots\ldots\ldots\ldots\ldots \quad 2.2$$

It is recognized that meteorological data are frequently recorded in digital format over finite time intervals. For example, precipitation information might be available as inches per day or per month, which is expressed in finite form as follows:

$$\overline{P}_r = \frac{\Delta P}{\Delta t} \quad \ldots\ldots\ldots\ldots\ldots \quad 2.3$$

in which $\overline{P}_r$ designates the average rate of precipitation during the time period Δt, and ΔP is the precipitation which occurred during this period. In many cases it is very convenient to input to the analog computer the data in its digital format, and this is possible if the period of integration coincides with the finite period over which the record was obtained. In this case equation 2.2 becomes:

$$P(n) = \overline{P}_r \int_o^1 dt = \overline{P}_r \, (1) \quad . \; . \; . \; . \; . \; . \; . \; . \; . \; . \; . \; . \quad 2.4$$

This function is, of course, continuous only within a particular finite period. A solution over a longer period of time is achieved, however, because conditions existing at the end of period n then become initial conditions for integration over period (n + 1), and so on. As a second alternative for the input of digital information, continuous functions of time can be developed from digital data by interpolation techniques. These functions are then input to the computer by means of electronic function generating devices.

Throughout this report the subscript r applied to any parameter is used to designate the variation of that parameter with respect to time, whether it be an instantaneous rate or an average value occurring over a finite time interval, such as a day or a month.

Concepts of a hydrologic model

The fundamental requirements of a computer model of a hydrologic system are that:

1. It simulates on a continuous basis all important processes and relationships within the system that it represents.
2. It is nonunique with respect to space. This implies that it can be easily applied to different geographic areas with existing hydrologic data.

3. The computing equipment possess a high degree of capacity and capability.

Requirements one and two are approached by developing a preliminary model from an analysis of published information and established concepts. Through operation of the model, quantitative relationships and hydrologic concepts are further defined and improved. At the same time, the third requirement is met through improvements in equipment design and modeling techniques. For example, consideration is now being given at Utah State University to the development of a hybrid computer which will incorporate the advantages of both the analog and the digital computing systems.

When the model is properly verified so that it accurately simulates a particular system, input and individual model parameters can be varied, and the effects of these changes can be observed at any point in the system. The general research philosophy involved in the development of a simulation model of a dynamic system, such as a hydrologic unit, is shown by the flow diagram of figure 2. 1.

A dynamic system consists of three basic components, namely the medium or media acted upon, a set of constraints, and an energy supply or driving forces. In a hydrologic system water in any one of its three physical states is the medium of interest. The constraints are applied by the physical nature of the hydrologic basin, and the driving forces are supplied by both direct solar energy and gravity and capillary

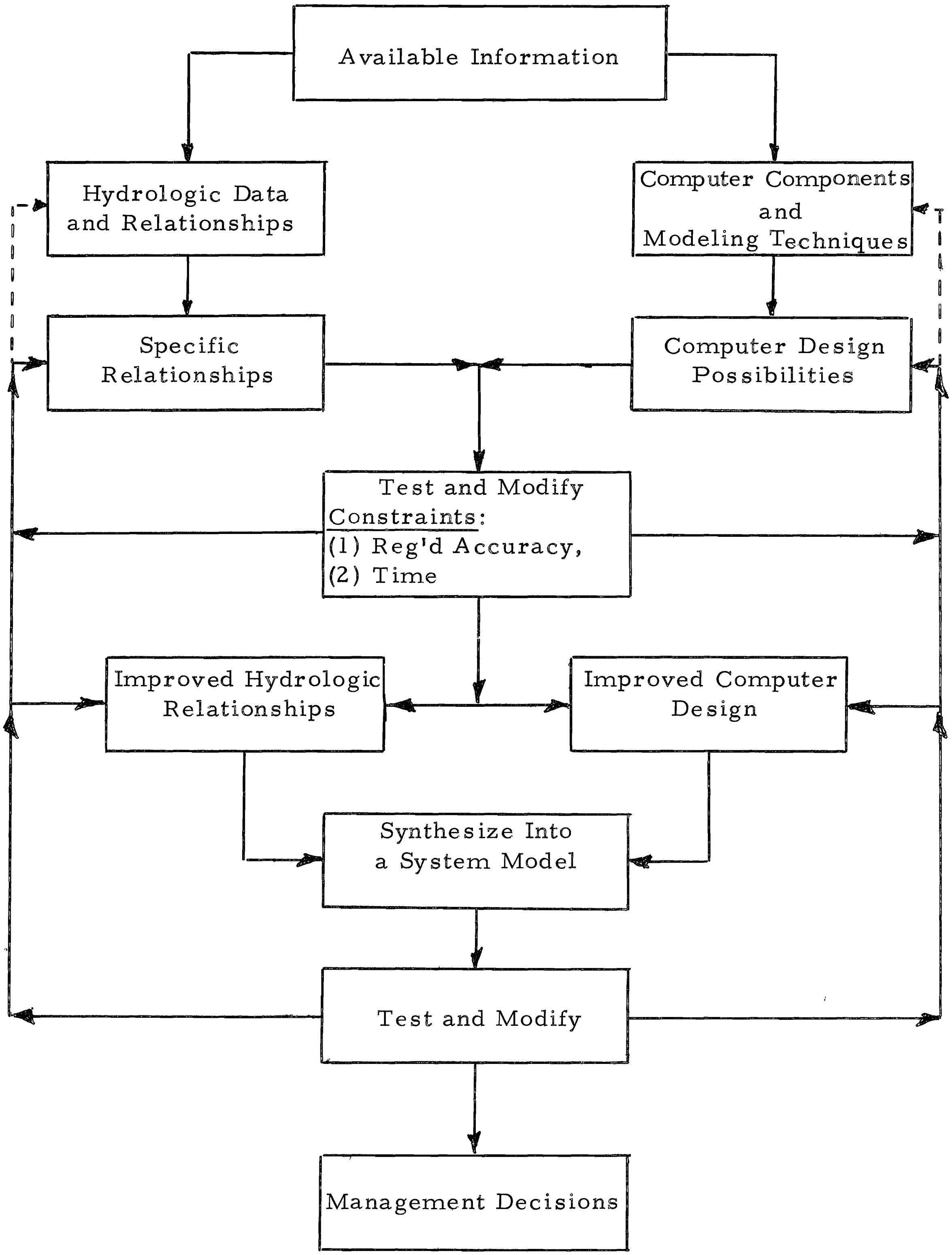

Figure 2.1. Development process of a hydrologic model.

potential fields. The various functions and operations of the different parts of the system are interrelated by the concepts of continuity of mass and momentum. Unless relatively high velocities are encountered, such as in channel flow, the effects of momentum are negligible, so that for many hydrologic models continuity of mass is the only link between the various processes within the system.

Continuity of mass is expressed by the general equation:

$$\text{Input} = \text{Output} + \text{Change in Storage} \quad . \quad . \quad . \quad . \quad . \quad . \quad . \quad . \qquad 2.5$$

A hydrologic balance is the application of this equation in order to achieve an accounting of physical hydrologic measurements within a particular unit. Through this means and the application of appropriate translation or routing functions, it is possible to predict the movement of water within a system in terms of its occurrence in space and time.

The concept of the hydrologic balance is pictured by the block diagram of figure 2.2. The inputs to the system are precipitation and surface and groundwater inflow, while the output quantity is divided among surface outflow, groundwater outflow, and evapotranspiration. As water passes through this system, storage changes occur on the land surface, in the soil moisture zone, in the groundwater zone, and in the stream channels. These changes occur rapidly in surface locations and more slowly in the subsurface zones.

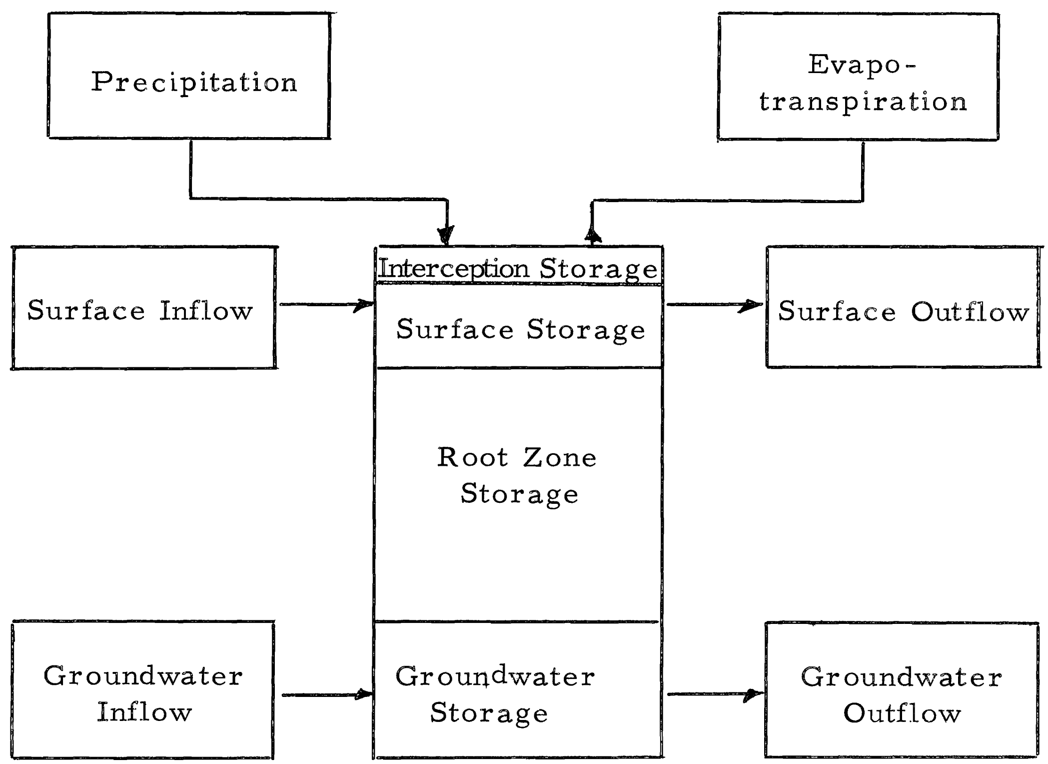

Figure 2.2. A simplified diagram of the hydrologic balance.

A further examination of figure 2.2 indicates that the hydrologic balance as represented by equation 2.5 can be written in more detailed form as follows:

$$P = I \pm \Delta M_s + SRO \pm \Delta G_s + GWO + ET \pm \Delta S_s - SRI - GWI \quad . . . . \quad 2.6$$

in which

P = precipitation

I = interception loss

ΔM_s = change in soil moisture storage

SRI = surface inflow

SRO = surface runoff

ΔS_s = change in surface storage

ΔG_s = change in groundwater storage

GWI = groundwater inflow

GWO = groundwater outflow

ET = evapotranspiration

Figure 2.2 and equation 2.6 both emphasize the importance of precipitation and other water inflow parameters to the hydrologic system. Because it is applied as an index of energy, temperature is also a very significant quantity. Net energy influences both evapotranspiration and the snow accumulation and ablation processes. Not shown, but also an important means of comparing available energy on the various facets of a landscape is potential insolation. A third fundamental hydrologic process is translation storage or routing. This process governs the movement of surplus water through a hydrologic system. Each of these basic hydrologic parameters and processes is discussed further in the next chapter.

Time and space considerations in a hydrologic model

Practical data limitations and problem constraints require that increments of both time and space be considered by a model design. Data, such as temperature and precipitation readings, are usually available as point measurements in terms of time and space, and integration in both dimensions is usually most easily accomplished by the method of finite increments.

The complexity of a model designed to represent a hydrologic system largely depends upon the magnitudes of the time and spatial increments utilized in the model. In particular, when large increments are applied, the scale magnitude is such that the effects of phenomena which change over relatively small increments of space and time are insignificant. For instance, on a monthly time increment interception rates and changing snowpack temperatures are neglected. In addition, sometimes the time increment chosen coincides with the period of cyclic changes in certain hydrologic phenomena. In this event net changes in these phenomena during the time interval are usually negligible.

For example, on an annual basis storage changes within a hydrologic system are often insignificant, whereas on a monthly basis the magnitudes of these changes are frequently appreciable and need to be considered. As time and spatial increments decrease, improved definition of the hydrologic processes is required. No longer can short-term transient effects or appreciable variations in space be neglected, and the mathematical model therefore becomes increasingly more complex, with an accompanying increase in the requirements of computer capacity and capability.

As already indicated, the design of the first hydrologic model developed under the analog simulation research program at Utah State University was relatively simple. This objective was accomplished by the use of rather large increments of time and space (2, 3). The study reported herein constitutes the second stage of the overall research program, and deals with the development and testing of both equations and equipment designed to model a hydrologic system in terms of large time increments of, for example, one month, but rather small geographic areas or zones. The areal extent of these zones is selected on the basis that within each zone important characteristics, such as slope, soil type, vegetative cover, and meteorological factors, can be assumed to be reasonably constant. By means of averaging techniques it is also possible to apply the relationships of this model to rather extensive geographic increments. All equations used in the model are included in the following chapter.

CHAPTER III

THE HYDROLOGIC MODEL

A block flow diagram of a typical hydrologic system for which input data and consequently output information are based on large time increments is shown in figure 3. 1. The model is sufficiently general to include all of the phenomena which occur in any hydrologic system. Each parameter and process depicted by this figure is discussed in the sections which follow.

Temperature

Average temperature values for the zone or area being considered are required. Integration techniques are necessary in order to utilize point measurements for the estimation of effective or average temperature for an area. For those cases where watershed temperature records are available, this integration is accomplished by preparing area charts showing isothermal lines for particular periods of time. Average zone temperatures are then computed from these charts and a relationship is thus established between these and temperatures at one or more selected index stations. In some cases it is necessary to develop different relationships for different periods of the year. Consideration is now being given to the development of an analog input device which will integrate over a given area point measurements of temperature or precipitation at particular locations.

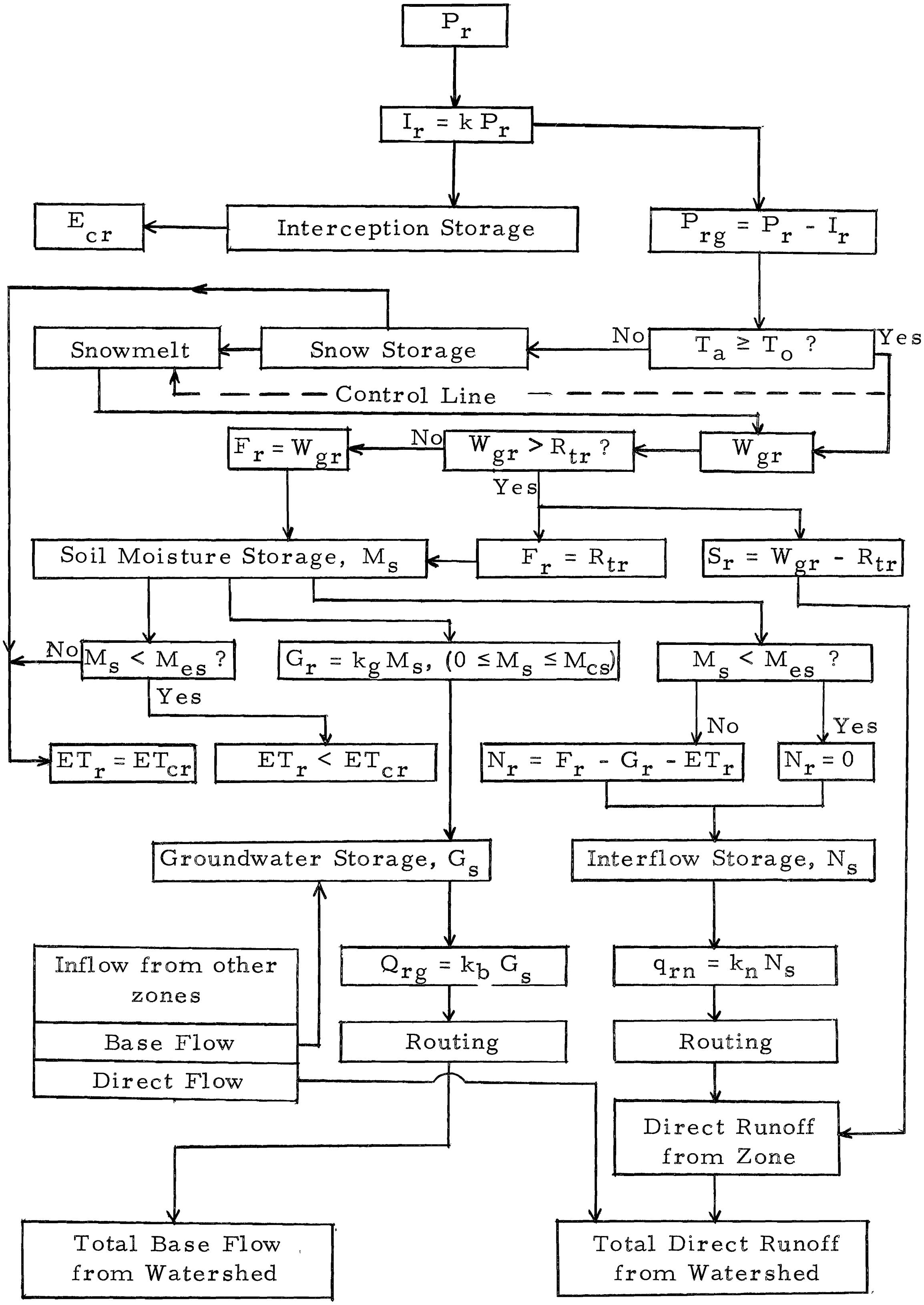

Figure 3.1. Flow diagram for a typical hydrologic model using large time increments.

For watersheds where temperature data are lacking, records from an index station on the valley floor are "lapsed" to the zone under consideration. The adiabatic lapse rate of approximately -3.5^{o} per 1,000 feet elevation increase varies considerably. However, average monthly lapse rates for a particular location can be established from radiosonde data (42) applied in conjunction with valley temperature records. Figure 3.2 illustrates computed average monthly temperature lapse rates between elevations 6,000 and 10,000 feet for the vicinity of Circleville, Utah. The average annual lapse rate for the 14-year period investigated (1950-1963) was -3.8^{o} F per 1,000 feet.

Precipitation

Average zone precipitation. Average precipitation values as a function of time for a zone are computed by procedures which are similar to those applied to obtain average temperatures. Where watershed precipitation data are available, isohyetal charts, plotted from monthly records for particular storms, permit the establishment of relationships between average precipitation for the zone under study and concurrent records from one or more index stations. For cases where records are available for only the valley floor, isohyetal charts showing average precipitation values are employed to establish a lapse rate between the valley stations and the watershed zones. Thus:

$$P_i(z) = k_j(z)\, P_i(v) \quad \ldots \ldots \ldots \ldots \quad 3.1$$

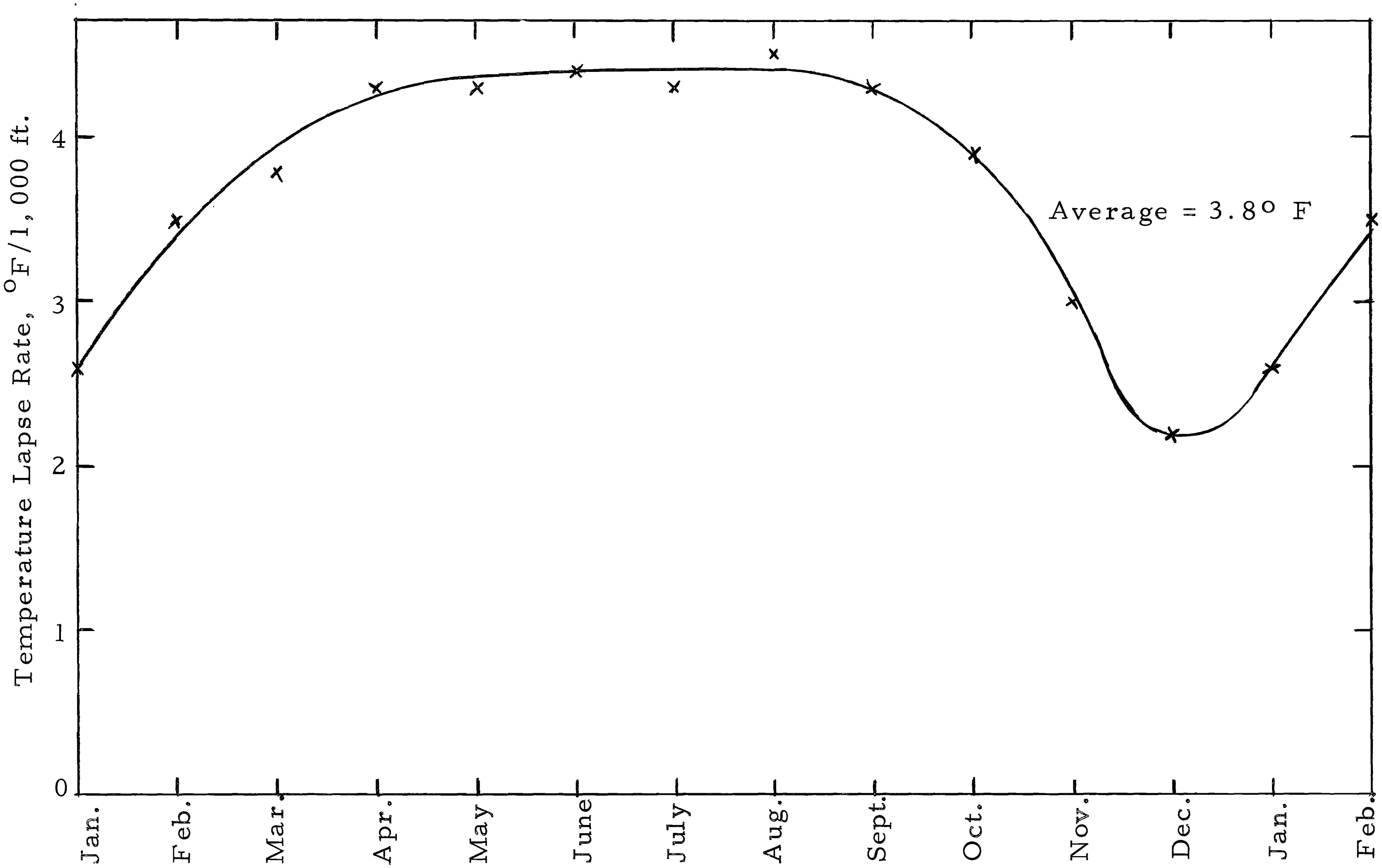

Figure 3.2. Average temperature lapse rate with elevation as a function of time at Circle Valley, Utah.

in which

$P_i(z)$ = the estimated precipitation in inches of water for zone z and for a particular month, i

$P_i(v)$ = the measured precipitation on the valley floor for the same month

$k_j(z)$ = the lapse rate constant applicable to zone z during a particular period, j

The length of the period j depends upon available information. For Utah isohyetal charts covering the state have been prepared (43). These indicate lines of equal average precipitation for the two periods, May to September and October to April. Lapse rates can, therefore, be determined for these two periods. Table 3.1 illustrates the application of this procedure for a particular watershed zone within the Sevier River basin of Utah.

Table 3.1. Precipitation lapse constants, Circleville, Utah

Period	Average zone precipitation (From isohyetal charts)	Average valley precipitation (From records)	Lapse constant
May to September	5.4	3.2	1.7
October to April	10.3	4.3	2.4

Thus, the multiplication of a particular monthly precipitation quantity recorded at Circleville would yield an estimate of the average precipitation on the appropriate watershed zone for this same month. Obviously, estimates are considerably improved if sufficient information is available to permit the development of lapse rates on at least a monthly basis.

Forms of precipitation. Only two forms of precipitation, rain and snow, are considered in this study, with a temperature criterion being applied to establish the occurrence of these two forms. Temperature is not an ideal index of the form of precipitation since there is no single temperature above which it always rains and below which it always snows. Unless a better indication as to form of precipitation is present, surface air temperature seems to be the best available index. A chart indicating the probability of the occurrence of snow at various air temperatures is shown by figure 3.3. (40). On the basis of this figure at a temperature of 35° F there is a 50 percent chance that precipitation will be in the form of snow. When the average temperature elevation lapse rate and the average falling rate of a snowflake are considered, this temperature seems to be a reasonable criterion, and precipitation at surface air temperatures less than this value is considered to be in the form of snow.

Potential insolation

Potential insolation is used as a means of comparing the energy flux among the different facets of a landscape (12, 19, 35, 36). In the concept of potential insolation the earth's atmosphere is ignored. Thus,

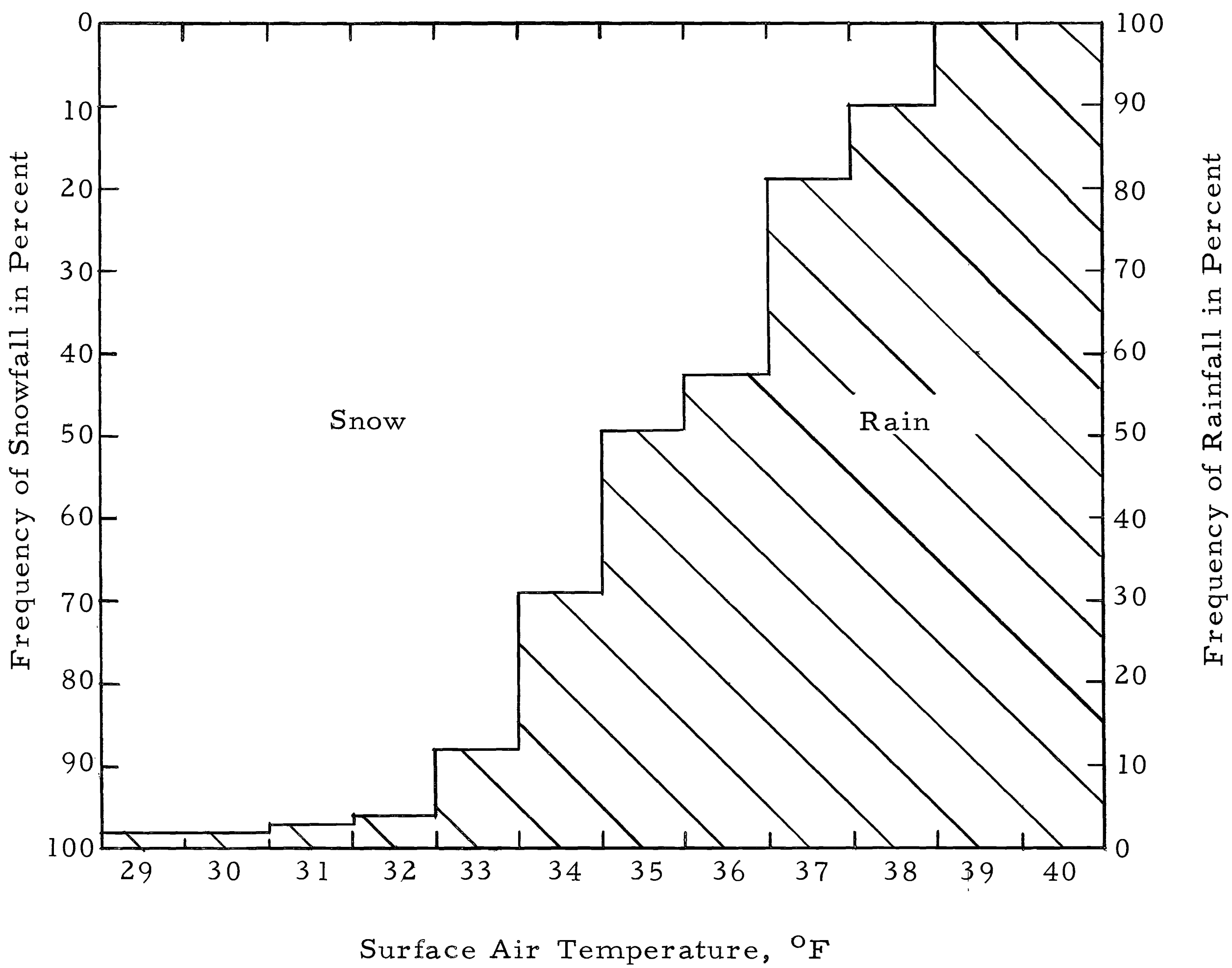

Figure 3.3. Frequency distribution showing rain and snow forms of precipitation.

irradiation of a surface by direct sunshine is considered to be only a function of the angle between the surface and the sun's rays. This angle, in turn, is a function only of the geometric relationships between the surface and the sun as expressed by latitude, degree of slope and aspect of the surface, and the declination and hour angle of the sun. For a given site the only variation in instantaneous potential insolation will be perfectly cyclical with time, depending upon the changes in hour angle and declination. Thus, the use of potential insolation as a parameter of a surface is sufficiently simple to make feasible its wide application.

Consider first the following symbols:

D = declination of the sun in degrees, north (+) and south (-). This angle is a function of time

e = ratio of the earth to sun distance at any time and the mean of this distance

h = azimuth (degrees), measured clockwise from north

I_o = the solar constant, 2.00 gm cal/cm^2 min (langleys/min)

I_q = quantity of insolation (langleys)

I_p = maximum potential insolation, or I_o/e^2

RI = radiation index, percent I_q of I_p

θ = slope inclination in degrees or percent

L = latitude of observation in degrees, north (+) and south (-)

T = longitude of observation in degrees

τ = number of days from January 1 of each year

t_1 = minutes from true solar noon to sunrise

t_2 = minutes from true solar noon to sunset

ω = angular velocity of the earth's rotation in radians per minute

N = the number of days from the nearest equinox (Sept. 23 or March 21), in degrees

ψ = angle between the sun's rays and the normal to the irradiated surface, degrees. This angle is a function of time.

In the discussion which follows, true solar noon is taken as being the zero or reference point. Thus, time intervals before solar noon are assigned negative values, while those after solar noon are assumed to be positive. In general terms, the values of t_1 are negative, while those of t_2 are positive.

The quantity of insolation received at a surface for any particular day is given by:

$$I_q = \frac{I_o}{e^2} \int_{t_1}^{t_2} \cos \psi \, dt \quad . \quad . \quad . \quad . \quad . \quad . \quad . \quad . \quad . \quad . \quad . \quad . \quad 3.2$$

Cos ψ is obtained by taking the dot product of the vector representing the sun's rays and the normal vector to the irradiated surface. Thus, for a horizontal surface:

$$\cos \psi = \cos D \cos L \cos \omega t + \sin D \sin L \quad . \quad . \quad . \quad . \quad . \quad . \quad 3.3$$

from which

$$I_q = \frac{I_o}{e^2} \int_{t_1}^{t_2} (\cos D \cos L \cos \omega\ t + \sin D \sin L)\, dt$$

$$= \frac{I_o}{e^2} \left[\frac{1}{\omega} \cos D \cos L (\sin \omega\ t_2 - \sin \omega\ t_1) + (t_2 - t_1) \sin D \sin L \right] \quad . \quad . \quad . \quad . \quad . \quad . \quad . \qquad 3.4$$

The change in declination with time is approximated by the following equation:

$$D = 23.5 \sin N \quad . \quad . \quad . \quad . \quad . \quad . \quad . \quad . \quad . \quad . \quad . \quad . \quad . \qquad 3.5$$

and values of I_o/e^2 are estimated by the expression:

$$\frac{I_o}{e^2} = 0.07 \cos \tau + 2.00 \quad . \quad . \quad . \quad . \quad . \quad . \quad . \quad . \quad . \qquad 3.6$$

The insolation equations for sloping or inclined surfaces are much more complex than those for horizontal surfaces. However, the theory of "equivalent slope" offers a simple approach to this problem. This concept is derived from the fact that every inclined surface on the face of a sphere is parallel to some horizontal surface whose location is mathematically defined. The determination of the location of this equivalent slope in terms of increments of latitude and longitude requires the solution of a terrestrial spherical triangle. The difference in longitude between the location of a given slope and that of an equivalent horizontal area is given by:

$$\Delta T = \tan^{-1}\left(\frac{\sin h \cdot \sin \theta}{\cos \theta \cdot \cos L - \cos h \cdot \sin \theta \cdot \sin L}\right) \quad . \quad . \quad 3.7$$

The latitude of the equivalent slope is given by:

$$L' = \sin^{-1}(\sin \theta \cdot \cos h \cdot \cos L + \cos \theta \cdot \sin L) \quad . \quad . \quad . \quad 3.8$$

It will be noted that in the above equations h defines the direction or aspect of the given slope.

The potential insolation of the given slope can now be computed from equation 3.4 in terms of its equivalent horizontal slope providing the appropriate length of day can be established. On the basis that the earth rotates at the rate of 15^{o} per hour, the time shift in minutes between the given and equivalent slopes is equal to $4(\Delta T)$. For a horizontal surface both t_1 and t_2 are given by:

$$t = 4 \cos^{-1}(-\tan L \tan D) \quad . \quad . \quad . \quad . \quad . \quad . \quad . \quad . \quad . \quad 3.9$$

Now, in the case of an east-facing slope, the sunrise will obviously occur at the same time as for a horizontal surface at the same location. Thus, t_1 is given by equation 3.9. In this case the time from solar noon to sunrise at the equivalent slope, represented by t'_1, is established from the local time at the actual slope and is given by:

$$t'_1 = t_1 + 4(\Delta T) \quad . \quad . \quad . \quad . \quad . \quad . \quad . \quad . \quad . \quad . \quad . \quad . \quad 3.10$$

Combining equations 3.9 and 3.10 yields

$$t'_1 = 4 \left[\cos^{-1} (-\tan L \tan D) + \Delta T \right] \quad . \quad . \quad . \quad . \quad . \quad . \quad . \qquad 3.11$$

The time between solar noon and sunset, t'_2, at an equivalent site for an east-facing slope is given by equation 3.9 as follows:

$$t'_2 = 4 \cos^{-1} (-\tan L' \tan D) \quad . \quad . \quad . \quad . \quad . \quad . \quad . \quad . \quad . \qquad 3.12$$

The afternoon sun will leave the surfaces of the horizontal equivalent slope and the east-facing actual slope at the same time. The period between solar noon and sunset at the actual slope is given by:

$$t_2 = t'_2 - 4(\Delta T) \quad . \quad . \quad . \quad . \quad . \quad . \quad . \quad . \quad . \quad . \quad . \quad . \quad . \qquad 3.13$$

For a west-facing slope t_2 is determined by equation 3.9 and t'_2 by either equation 3.10 or 3.11. In this case equations 3.12 and 3.13 establish the time periods t'_1 and t_1 respectively. It is again emphasized that in most cases t'_1 represents a period before solar noon and is usually negative, while t'_2 most frequently occurs after solar noon and is usually positive in value. From the appropriate values of t'_1, t'_2, and L', the potential insolation received on the given sloping surface over the period of time $(t_2 - t_1)$ is now computed by substitution into equation 3.4 as follows:

$$I_q = \frac{I_o}{e^2} \left[\frac{1}{\omega} \cos D \cos L' \left(\sin \omega t'_2 - \sin \omega t'_1 \right) + \left(t'_2 - t'_1 \right) \sin D \sin L \right] \quad . \quad . \quad . \quad . \quad . \quad . \quad . \quad . \qquad 3.14$$

It will be noted that for a particular surface, ΔT and L remain constant so that the daily values of I_q are computed from equations 3.5, 3.6, 3.9, 3.10, 3.12, and 3.14, respectively.

Because mapped areas represent the horizontal projection of sloping surfaces, the computed potential insolation per unit area on a sloping surface is adjusted to account for this factor. Thus:

$$I_q(H) = I_q \sec\theta \quad . \; . \; . \; . \; . \; . \; . \; . \; . \; . \; . \; . \; . \; . \quad 3.15$$

where $I_q(H)$ represents the potential insolation in langleys on the horizontal projection of the sloping surface.

The radiation index for a surface for any particular day is given by the following ratio:

$$RI = \frac{100\, I_q(H)}{I_p\,(2t)} = \frac{100\, I_q(H)}{I_o/e^2\,(2t)} \quad . \; . \; . \; . \; . \; . \; . \; . \quad 3.16$$

where t is the time in minutes from noon to either sunrise or sunset for a horizontal surface at the particular location. Substituting for $I_q(H)$ its equivalent from equations 3.14 and 3.15

$$RI = \frac{50}{t} \sec\theta \left[\frac{1}{\omega} \cos D \cos L' \,(\sin\omega\, t'_2 - \sin\omega\, t'_1) + (t'_2 - t'_1) \sin D \sin L' \right] \quad . \; . \; . \; . \; . \; . \; . \quad 3.17$$

A digital computer program has been written incorporating the equations presented in this section. From this program it is possible to compute the variation of potential insolation with solar declination for any surface established by latitude, aspect, and degree of slope. Figure 3.4 illustrates a computer plot of the radiation index calculated from

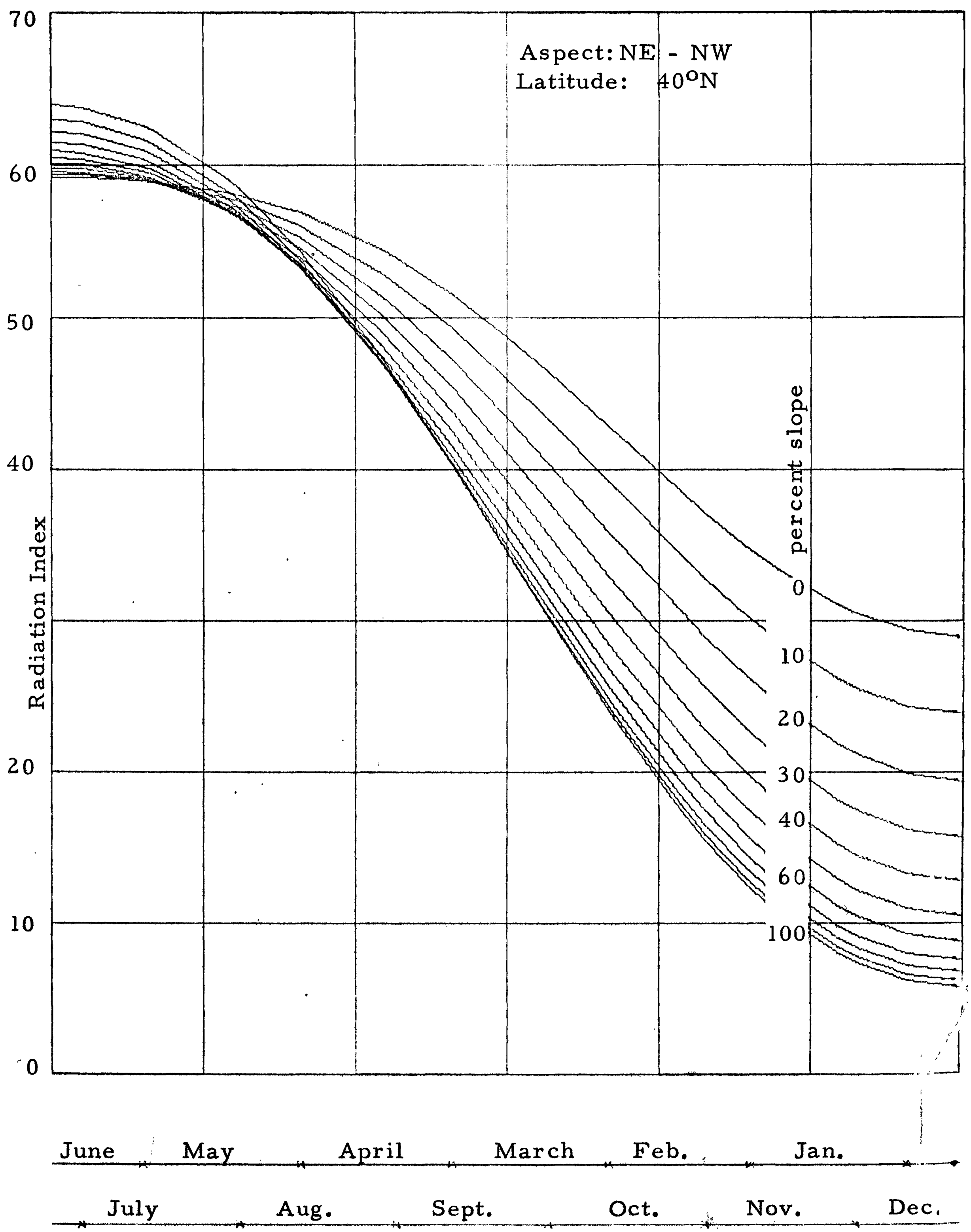

Figure 3.4. Radiation index values as a function of slope inclination and time of year.

equation 3.17 for a particular aspect and expressed as a function of slope inclination and solar declination. The latitude is 40° N. Because direct radiation is equal upon facets that show symmetry with respect to a north-south axis, two aspects are represented by this figure. The digital computer program together with some sample output and an additional computer plot (figure A1) are included within appendix A of this report.

The application of the theory presented in this section to watershed studies requires that for each zone or area under consideration the orientation and slope of an effective plane surface be defined such that this surface receives as nearly as possible the same potential insolation as is received by the particular zone.

Interception loss

Much of the precipitation falling during the early stages of a storm is stored on the vegetative cover and returned to the atmosphere by evaporation. Evaporation losses from the falling precipitation itself are not considered because these losses are assumed to be uniform over the particular area or zone and, of course, are not measured as an input quantity to the system. The magnitude of the interception loss is dependent largely upon the type and density of forest canopy and the relative extent of the forested land within the area. Interception losses during a large time period of say one month are commonly expressed as a fraction of the precipitation during this same period (40). Thus:

$$I_r = k_i C_d F_d P_r \quad \ldots\ldots\ldots\ldots \quad 3.18$$

in which the undefined terms are:

k_i = a constant

C_d = canopy density. In the case of deciduous vegetation this value will vary with the season of the year.

F_d = forest cover density within the watershed zone under consideration

Limited studies (17, 40) indicate that the most probable average value of k_i is 0.4 for both rain and snow falling on coniferous trees. This same value is also applicable to deciduous trees during the summer months, but during the winter months interception losses by deciduous vegetation are insignificant. The forest cover density F_d is given by:

$$F_d = \frac{A_c}{A_z} \quad \ldots\ldots\ldots\ldots \quad 3.19$$

in which

A_c = area of the watershed zone covered by forest vegetation

A_z = total area of the zone

Thus, for an area containing i types of vegetation

$$I_r = \frac{k_i}{A_z} \left[a_1 C_d(1) + a_2 C_d(2) + \ldots + a_i C_d(i) \right] P_r$$

$$= k_i C_v P_r \quad \ldots\ldots\ldots\ldots \quad 3.20$$

The value of C_v is computed for each zone and represents an input value to the computer. C_d is assumed to equal zero for grasses.

The rate at which precipitation reaches the ground, P_{rg}, is obtained by subtracting interception losses from the precipitation rate. Thus, from equation 3.20:

$$P_{rg} = P_r - k_i C_v P_r$$

$$= P_r (1 - k_i C_v), (k_i C_v < 0) \quad . \quad . \quad . \quad . \quad . \quad . \quad . \quad . \quad . \quad 3.21$$

Snowmelt

Both the complex nature of snowmelt and data limitations prevent a strictly analytical approach to this process. In particular, for the computation of melt on the basis of large time increments, such as a month, a rather empirical approach seemed most suitable. Accordingly, a relationship was proposed which states that the rate of melt is proportional to the available energy and the quantity of precipitation stored as snow. Expressed as a differential equation the relationship appears:

$$\frac{d[W_s(t)]}{dt} = - k_s (T_a - 35) \frac{RI_s}{RI_h} W_s(t) \quad . \quad . \quad . \quad . \quad . \quad . \quad . \quad 3.22$$

in which the undefined terms are:

k_s = a constant

RI_s = the radiation index on a surface possessing a known degree and aspect of slope

RI_h = the radiation index for a horizontal surface at the same latitude as the particular watershed under study

From an analysis of snow course data from various parts of Utah, the value of k_s was determined to be approximately 0.10. The independent variables on the right side of equation 3.22 can be expressed either as continuous functions of time or as step functions consisting of mean constant values applicable throughout a particular time increment. In this model a time increment is being utilized with the integration being performed in steps over each successive period. Thus, the final value of $W_s(t)$ at the end of the period becomes the initial value for the integration process over the following period. On this basis the integral form of equation 3.22 is:

$$\int_{W_s(0)}^{W_s(1)} \frac{dW_s}{W_s} = -0.10\,(T_a - 35)\,\frac{RI_s}{RI_h} \int_0^1 dt \quad . \quad . \quad . \quad 3.23$$

or

$$W_s(1) = W_s(0) \exp\left[-0.10\,(T_a - 35)\, RI_s/RI_h \right] \quad . \quad . \quad . \quad 3.24$$

A test of equation 3.22 is illustrated by figure 3.5 which indicates both predicted and actual rates of snowmelt for a watershed in Montana.

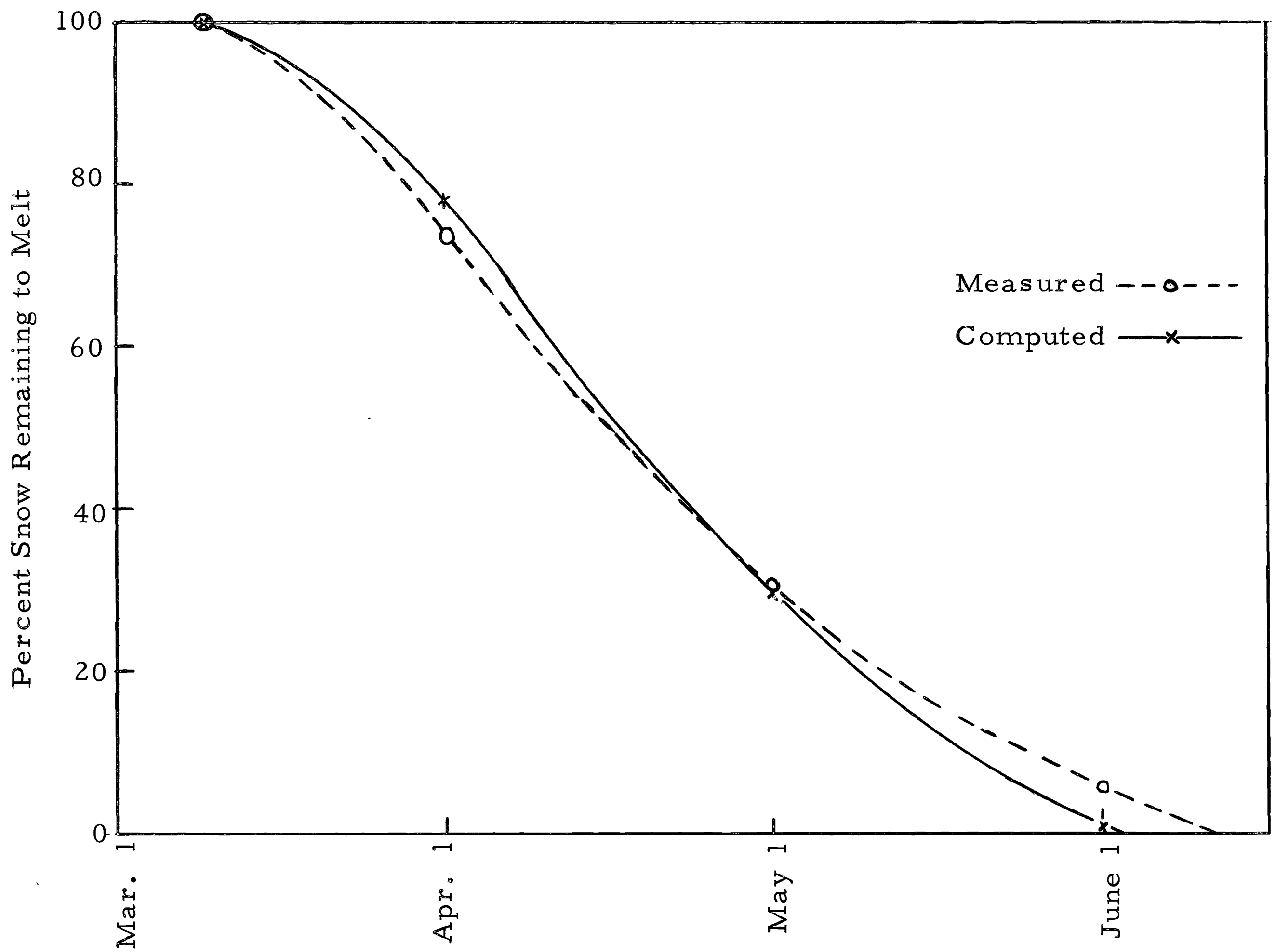

Figure 3.5. Measured and computed snowmelt rate curves for the Middle Fork Flathead River, Montana, 1947.

Surface runoff

This quantity is provided for by establishing for each watershed zone a limiting rate of surface runoff for any particular period of time. If this value is exceeded by snowmelt, rainfall, or irrigation, or by any combination of these, the surplus becomes surface runoff. Surface runoff records enable the value of the limiting rate to be estimated for each particular watershed or zone during verification of the model. In equation form the rate of surface runoff during a particular period of time, n, is given by:

$$S_r = W_{gr} - R_{tr} \quad , \quad (S_r \geq 0) \quad . \; . \; . \; . \; . \; . \; . \; . \; . \; . \; 3.25$$

in which the previously undefined term R_{tr} represents the limiting or threshold rate of surface supply at which surface runoff begins to occur.

The values of the threshold surface runoff rate, R_{tr}, are dependent upon variables, such as soil surface conditions, soil moisture, and storm characteristics, which in terms of a long time increment of, for example one month, are very probabilistic in nature. This situation could be accounted for in the model by assuming a normal distribution pattern and generating probability functions about the average values of R_{tr} determined for each particular time period. However, in a sparse data situation and where computing equipment is limited, the deterministic approach or use only of average values of R_{tr} generally should yield satisfactory results.

Depression storage

Water retained in puddles, ditches, and other depressions in the soil surface is termed depression storage. Outflow from this form of storage occurs either as direct evaporation or infiltration into the soil where the moisture is subject to use by the plants. In this model where large increments of time are involved, water retained temporarily in depression storage is assumed to be a part of the evapotranspiration loss from the area and thus is not considered as a separate entity.

Available soil moisture storage

The two soil moisture equilibrium points which are of greatest interest to the hydrologist are field capacity and wilting point. The field capacity is the moisture content of soil after gravity drainage is essentially complete, while the wilting point represents the soil moisture content at the time that plants can no longer extract sufficient water from the soil to meet their requirements and permanent wilting occurs. The difference between these two points is termed the available moisture, and it represents the useful storage capacity of the soil or the maximum water available to plants.

Under usual circumstances, additions to available soil moisture storage result from infiltration, while abstractive quantities are evapotranspiration losses, deep percolation, and interflow. Thus, soil moisture storage at any time, t, is given by the expression:

$$M_s(t) = \int (F_r - ET_r - G_r - N_r)\, dt \quad . \; . \; . \; . \; . \; . \; . \quad 3.26$$

Each of the four phenomena represented on the right side of the above equation will be discussed in the following sections.

Infiltration

Infiltration is the passage of water through the soil surface into the soil. In this model all water which occurs on the soil surface, except surface runoff, is assumed to enter the soil, and the rates of infiltration over a particular period of time are therefore given by:

$$F_r = W_{gr} \quad , \quad (W_{gr} < R_{tr}) \quad . \; . \; . \; . \; . \; . \; . \; . \; . \quad 3.27$$

$$F_r = R_{tr} \quad , \quad (W_{gr} \geq R_{tr}) \quad . \; . \; . \; . \; . \; . \; . \; . \; . \quad 3.28$$

Evapotranspiration

This process is often defined briefly as the sum of the water transpired by growing plants and that which evaporates from the soil, snow, and interceptive surfaces. Potential evapotranspiration is that which occurs under conditions of complete crop cover by actively growing plants, and where moisture supplies are not limiting.

Elevation effects on evapotranspiration. Frequently elevation differences on a watershed are substantial, and it is conceivable that these differences might produce significant effects on the evapotranspiration process. Under this heading only the evaporation portion of the process is considered. The same general principles which govern evaporation apply also to plant transpiration except that in this case plant effects are involved, and these are considered in a subsequent section. It is further pointed out that in this discussion elevation is not regarded as an independent parameter in the evaporation process. The rate at which this process occurs is influenced mainly by solar radiation, air temperature, vapor pressure, and wind (20). However, frequently all of these factors are altered by elevation changes within a watershed. Each factor is subject to independent measurement, but in many areas data are inadequate or entirely lacking. Air temperature, a commonly measured parameter, is utilized in several relationships which have been developed for predicting evaporation and evapotranspiration. The dependency of evaporation upon vapor pressure is demonstrated by the Dalton mass transfer equation (11). In turn, vapor pressures are a function of temperature (20). Air temperatures are not directly related to wind or air movement, a parameter which can substantially influence the vapor pressure gradient above an evaporating surface. However, in general, the importance of wind is greatly lessened under regional considerations of evaporation rates as opposed to local or point rates (23). Evaporation is profoundly influenced by total insolation since this energy represents the driving function in the process (6, 16, 18). Particularly within the region of a continental climate, there exists a high degree of correlation between total insolation and air temperature (31).

However, under stable and equilibrium air-mass conditions an increase in elevation, on a watershed for example, causes a reduction in air temperature due to adiabatic cooling, and, on the other hand, produces an increase in insolation because of the reduced atmospheric transmission losses (20, 21). Thus, within the local area, air temperatures cease to be entirely indicative of the incoming energy supply available for the evapotranspiration process on the watershed. For this reason, a correction or adjustment seems appropriate to evaporation equations based primarily on the temperature parameter. Theoretically this adjustment should compensate for the joint effects of adiabatic cooling of the air and increasing total insolation with height above the base elevation of the land surface or valley floor. The following discussion develops a basis for a correction factor of this nature.

The energy budget for an evaporation surface may be expressed as follows (20):

$$Q_s - Q_r - Q_b - Q_h - Q_e = Q_\theta - Q_v \quad . \quad . \quad . \quad . \quad . \quad . \quad . \qquad 3.29$$

in which

Q_s = solar and sky radiation reaching the surface

Q_r = reflected short wave radiation

Q_b = long wave radiation lost to the atmosphere

Q_h = heat conduction to the atmosphere

Q_c = the energy used for evaporation

Q_θ = the increase in stored energy within the evaporating body

Q_v = net energy content of inflowing and outflowing water (advected energy)

For particular levels of extraterrestrial radiation and atmospheric transmissivity the quantity of solar and sky radiation reaching a surface is dependent upon the length of the atmospheric path traversed by the sun's rays in reaching the surface (21). A parameter designated optical air mass is a measure of this distance. Thus, at any given time an increase in elevation causes an increase in the Q_s term, with the average increase being a linear function of atmospheric density as indicated by barometric pressure (21). The only other terms in equation 3.29 which are dependent upon elevation or barometric pressure are Q_h and Q_e. These two terms are related by a ratio, termed the Bowen ratio:

$$R = \frac{Q_h}{Q_e} \quad . \ . \ . \ . \ . \ . \ . \ . \ . \ . \ . \ . \ . \ . \quad 3.30$$

where

$$R = 0.61 \left[\frac{T_s - T_a}{e_s - e_a} \right] \frac{p}{1000} \quad . \ . \ . \ . \ . \ . \ . \ . \ . \ . \quad 3.31$$

in which

p = the barometric pressure in millibars

T_a = the temperature of the air in degrees C

e_a = the vapor pressure of the air in millibars

T_s = the water surface temperature in degrees C

e_s = the saturation vapor pressure in millibars corresponding to T_s

This ratio was conceived because sensible-heat transfer cannot be readily observed or computed and the Bowen ratio permits the elimination of this term from the budget equation. By applying the Bowen ratio equation 3.29 can be written:

$$Q_e = \frac{Q_s - Q_r - Q_b + Q_v - Q_\theta}{(1 + R)} \quad \ldots\ldots\ldots \quad 3.32$$

Equation 3.31 indicates that if temperature and the vapor pressure deficit are held constant, a reduction in barometric pressure causes a decrease in the values of R and consequently an increase in the energy loss by evaporation. However, in this analysis, the temperature of the water surface is considered equal to that of the air, so that the value of R becomes zero. For a given set of equilibrium conditions the values of Q_r, Q_b, Q_v, and Q_θ can be considered constant so that equation 3.32 can then be written:

$$Q_e = Q_s - C \quad \ldots\ldots\ldots \quad 3.33$$

in which C represents a constant. From equation 3.33 a change in energy available for evaporation can be related to a change in insolation:

$$\Delta Q_e = \Delta Q_s \quad \ldots\ldots\ldots \quad 3.34$$

Letting H_v represent the latent heat of vaporization of water and ρ its density, equation 3.34 can be written

$$\Delta E = \frac{\Delta Q_s}{H_v \rho} = K \Delta Q_s \quad . \ . \ . \ . \ . \ . \ . \ . \ . \ . \ . \ . \quad 3.35$$

in which E is the evaporation in depth units.

As indicated, for particular conditions the quantity of solar and sky radiation reaching a surface is dependent upon the length of the atmospheric path traversed by the sun's rays in reaching that surface. Figure 3.6 illustrates the radiation intensity reaching a horizontal surface at sea level for cloudless conditions as a function of the optical air mass. Because the optical air mass is a function of the zenith angle of the sun (21), the terrestrial radiation intensity at a particular latitude and solar declination can be related to the hour angle as shown by figure 3.7. It will be noted that for a given latitude (in this case 40° N) the intensity of radiation is dependent upon not only the hour angle and declination of the sun, but also the precipitable moisture content of the atmosphere. The variation in total daily insolation received on a horizontal surface at sea level as a function of atmospheric moisture content and solar declination is illustrated by figure 3.8. Also shown for comparison is a plot of the extraterrestrial radiation received on a horizontal surface. For the same three levels of precipitable atmospheric moisture, namely 0, 2.0, and 5.0 centimeters, and a latitude of 40° N, figure 3.9 indicates the mean monthly losses of radiant energy by

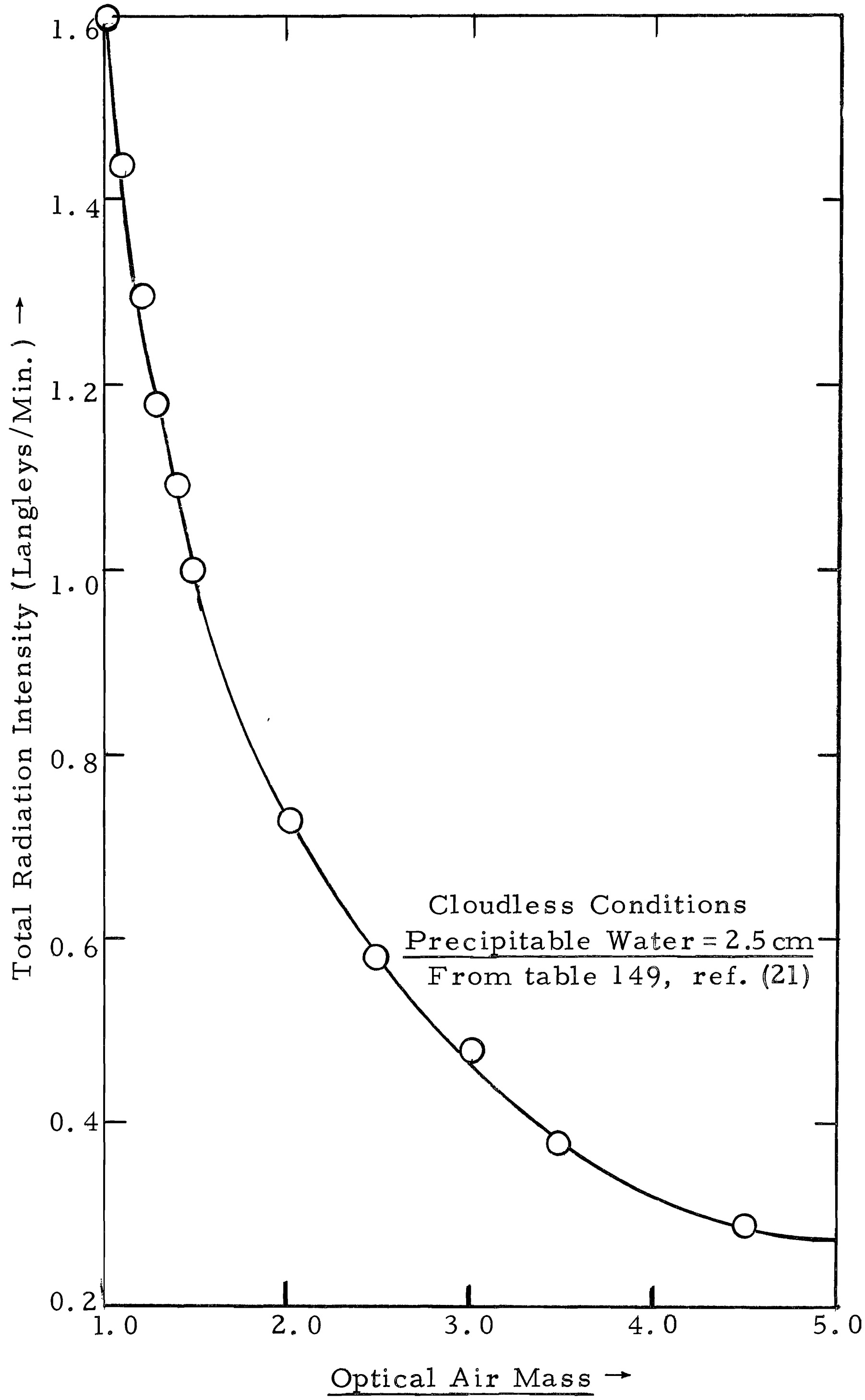

Figure 3.6. Total solar and sky radiation on a horizontal surface at sea level during cloudless conditions as a function of the optical air mass.

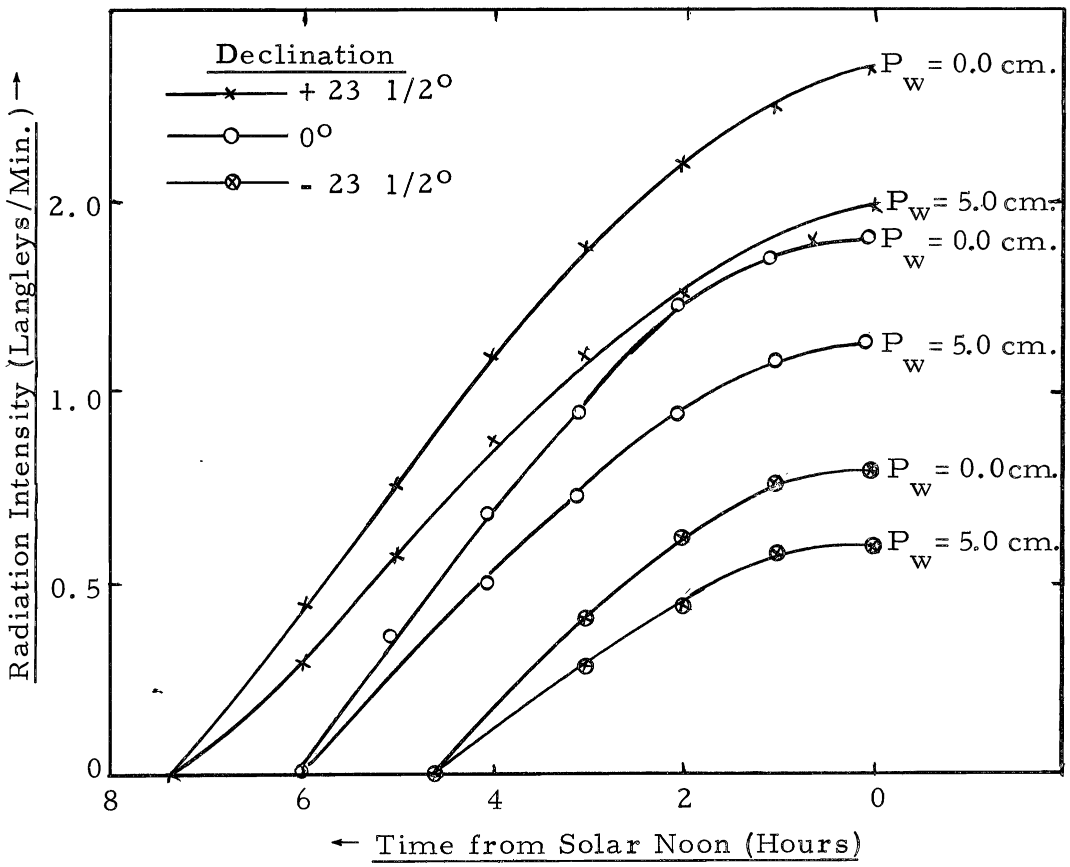

Figure 3.7. Total radiation intensity upon a horizontal surface at sea level under cloudless conditions as a function of time at a latitude of 40°N.

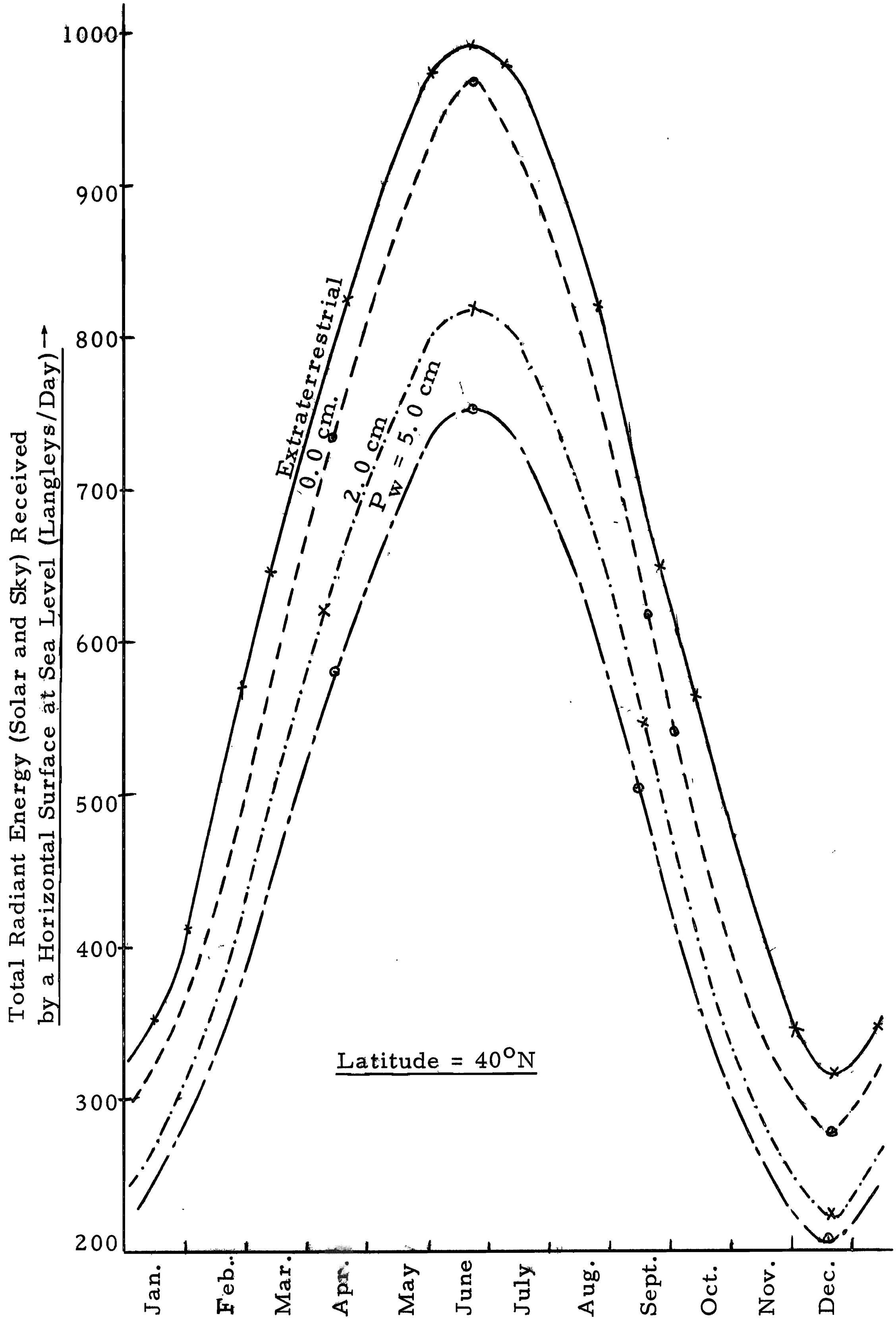

Figure 3.8. Radiation intensity as a function of time and atmospheric precipitable water content.

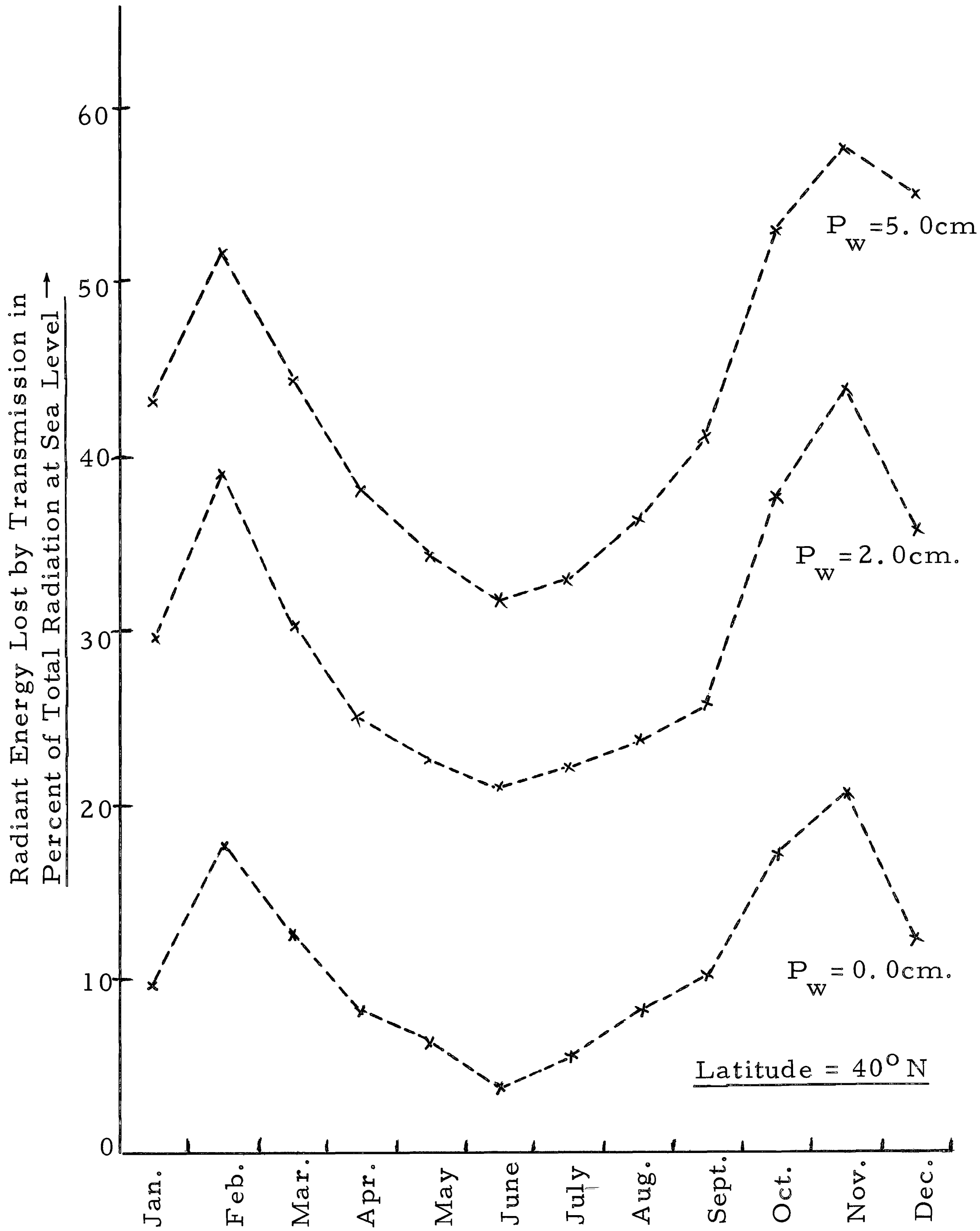

Figure 3.9. Radiation transmission losses as a function of time and atmospheric precipitable water content.

transmission through a cloudless atmosphere expressed as a percentage of the total radiation received on a horizontal surface at sea level. Transmission losses expressed as a function of precipitable moisture are shown by figure 3.10. It will be noted that for a precipitable moisture content of 2.5 centimeters (approximately one inch) the average annual atmospheric transmission loss at a latitude of 40^{o} N is approximately 33 percent of the total received at sea level.

For stations at elevations greater than sea level the values of optical air mass corresponding to a particular zenith angle are multiplied by the ratio P_i/P_o, where P_i represents the barometric pressure at the station in question and P_o indicates the barometric pressure at a base elevation, such as sea level (21). Thus, for a particular latitude and precipitable moisture content, the time variation in total radiation intensity on a horizontal surface can be estimated for any desired elevation. Figure 3.11 illustrates this variation for an elevation of 10,000 feet, a latitude of 40^{o} N, and a precipitable moisture content of 2.0 centimeters.

On the basis of the relationship between barometric pressure and insolation received, equation 3.35 can be modified to read:

$$\Delta E = \frac{Q_E - Q_o}{H_v \rho} \left[1 - \frac{P_i}{P_o} \right] \quad . \ . \ . \ . \ . \ . \ . \ . \ . \ . \quad 3.36$$

in which

ΔE = the evaporation increase in centimeters per day

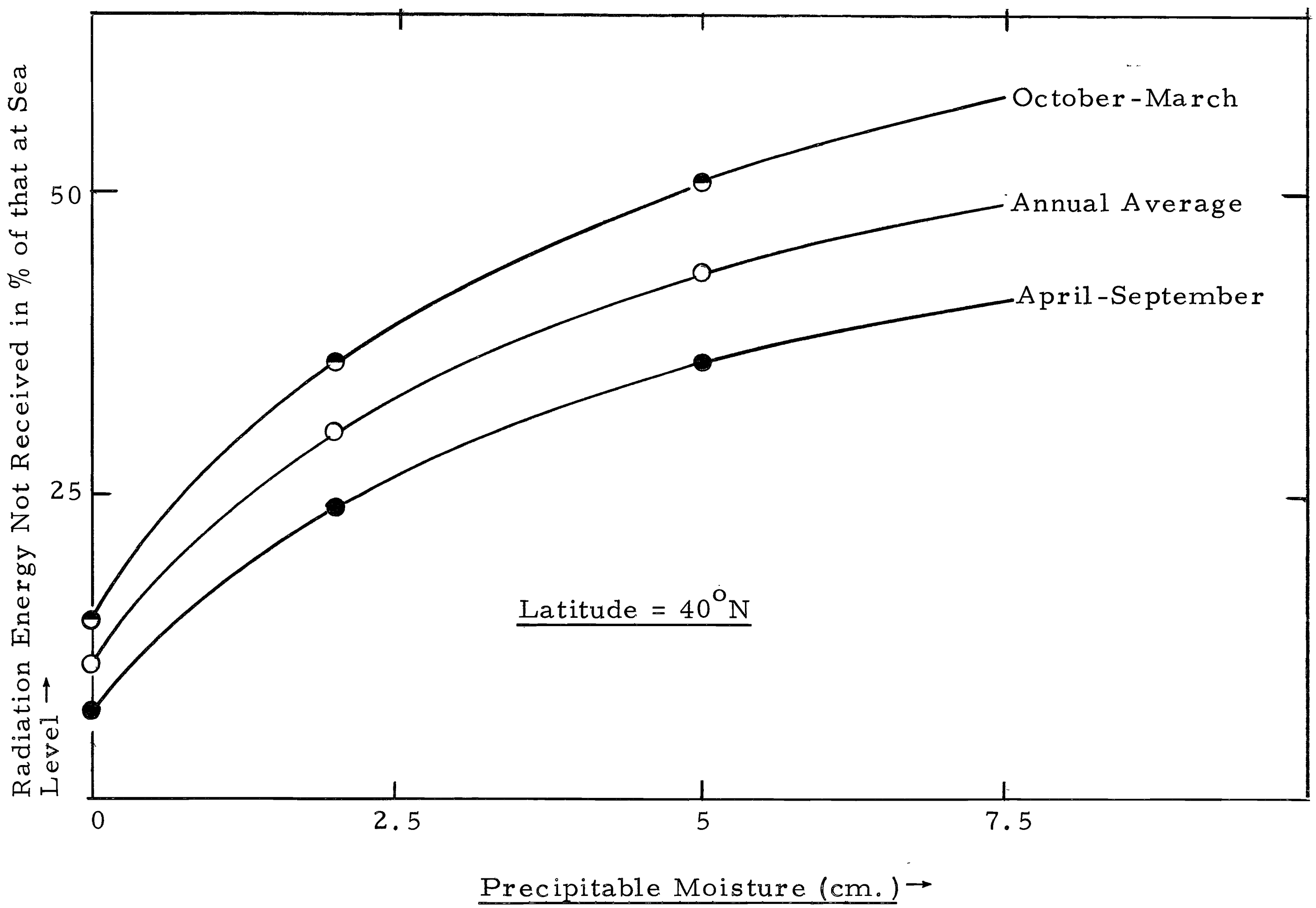

Figure 3.10. Seasonal and annual radiation transmission losses as a function of atmospheric precipitable water content.

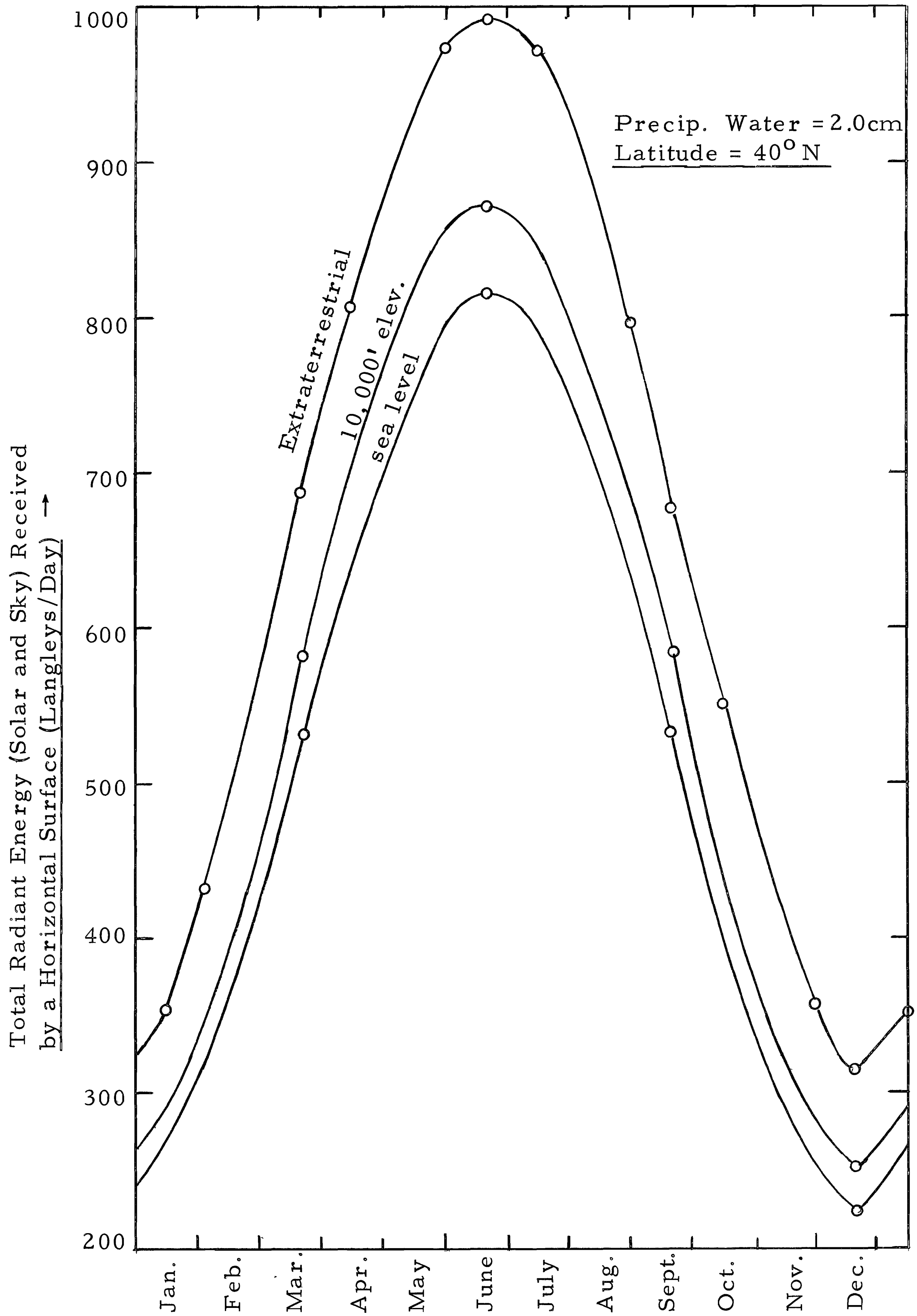

Figure 3.11. Total radiant energy as a function of elevation.

Q_E = the extraterrestrial radiation in langleys per day

Q_o = radiation in langleys per day on a horizontal surface at a given base

and the other variables have been defined previously.

Within the elevation range between sea level and 12,000 feet the ratio P_i/P_o is fairly linear with elevation so that a good estimate of ΔE expressed in inches per day per 1,000 feet elevation increase can be determined from equation 3.36 and expressed in the following relationship:

$$\Delta E = \frac{Q_E - Q_o}{(12)(2.54)\, H_v \rho} \left(1 - \frac{P_{12}}{P_o}\right)$$

$$= (Q_E - Q_o)\, 2.23 \times 10^{-5} \quad \ldots\ldots\ldots\ldots \quad 3.37$$

From equation 3.37 and figure 3.8, monthly values of ΔE were computed for three levels of precipitable moisture. These computations are shown by table 3.2.

From the average values shown at the bottom of table 3.2, figure 3.12 was plotted. A comparison of figures 3.11 and 3.12 indicates that on a percentage basis energy transmission losses during the winter months exceed those of the summer months. On the other hand, the magnitudes of the summer losses are considerably higher than those of the winter months. In both cases seasonal differences become more pronounced with increasing levels of precipitable moisture.

Table 3.2. Evaporation rate as a function of elevation and atmospheric precipitable moisture.[1]

Month	Monthly avg. rad. on horiz. surface (l/day)				$Q_E - Q_o$ (langleys/day)			$\Delta E \times 10^{-4}$ (in./day/1000')		
	Q_E (Extra-terrestrial)	Q_o at sea level								
		P_w = 0.0 cm	P_w = 2.0 cm	P_w = 5.0 cm	P_w = 0.0cm	P_w = 2.0 cm	P_w = 5.0 cm	P_w = 0.0 cm	P_w = 2.0 cm	P_w = 5.0cm
January	350	320	270	245	30	80	105	6.7	17.8	23.4
February	500	425	360	330	75	140	170	16.7	31.2	37.9
March	665	590	510	460	75	155	205	16.7	34.5	45.7
April	800	740	640	580	60	160	220	13.4	35.6	49.0
May	920	865	750	685	55	170	235	12.3	37.8	52.4
June	980	945	810	745	35	170	235	7.8	37.8	52.4
July	970	920	795	730	50	175	240	11.1	39.0	53.5
August	865	800	700	635	65	165	230	14.5	36.8	51.2
September	705	640	560	500	65	145	205	14.5	32.3	45.7
October	550	470	400	360	80	150	190	17.8	33.4	42.3
November	410	340	285	260	70	125	150	15.6	27.8	33.4
December	325	290	240	210	35	85	115	7.8	19.0	25.6
Averages										
Annual								13.0	31.9	42.8
Ap.-Sept.								12.3	36.5	50.8
Oct.-Mar.								13.6	27.3	34.7

[1] Notes: (1) Cloudless conditions.
(2) Latitude = 40°N.
(3) P_w = precipitable water within the atmosphere in centimeters.
(4) Table applicable between sea level and an elevation of 12,000 feet.

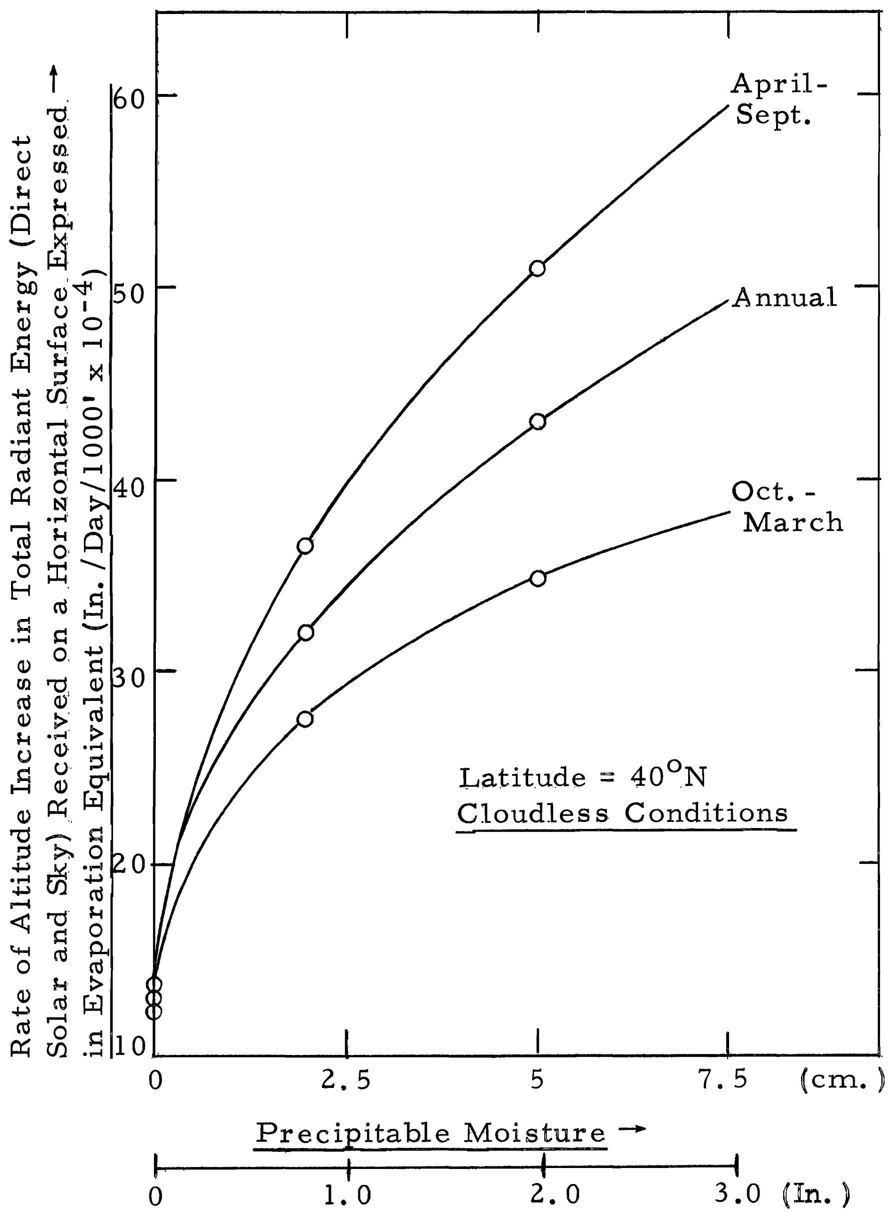

Figure 3.12. Seasonal and annual values of radiant energy as a function of atmospheric precipitable moisture and elevation.

For a given moisture level, magnitudes of transmission losses and seasonal differences both decrease with decreasing latitude. However, even at the 40° N latitude the magnitude of the incremental evaporation with increasing elevation is rather small. For example, at a precipitable moisture level of 2.54 centimeters (one inch), figure 3.12 indicates the average annual value of ΔE to be approximately 0.0035 inch per day per 1,000 feet, or about 0.10 inch per month per 1,000 feet elevation increase above the floor of the valley. In terms of absolute magnitude, variations from this figure on both a seasonal basis and with precipitable moisture are small.

Average monthly values of the precipitable water content of the atmosphere over the continental United States are shown by table 3.3 (44). These figures apply to a vertical column of air extending eight kilometers (26,300 feet) above the earth's surface. The annual average for the United States is 0.78 inch, with seasonal values of 0.54 inch for the winter months and 1.03 inches for the summer. Included in table 3.3 are corresponding average monthly values of the precipitable water within the atmosphere at Ely, Nevada, where the annual average figure is 0.382 inch, with seasonal averages of 0.30 inch during the winter period and 0.465 inch for the summer. Corresponding average values of precipitable water for the intermountain region, including eastern Nevada, Utah, and southern Idaho, were estimated from constant moisture charts (44) as being 0.43 inch, 0.35 inch, and 0.55

Table 3.3. Average values of precipitable water, surface to eight kilometers.[1]

Month	Total Precipitable Water in Inches		
	Average for continental U. S.	Ely, Nevada	Average for Intermountain Region
Jan.	0.44	0.275	0.32
Feb.	0.45	0.277	0.32
Mar.	0.49	0.282	0.33
Apr.	0.64	0.351	0.41
May	0.84	0.378	0.45
June	1.11	0.441	0.52
July	1.26	0.580	0.69
Aug.	1.26	0.563	0.66
Sept.	1.05	0.479	0.57
Oct.	0.79	0.387	0.45
Nov.	0.57	0.285	0.33
Dec.	0.51	0.290	0.34
Annual	0.78	0.382	0.45
Winter	0.54	0.300	0.35
Summer	1.03	0.465	0.55

[1]From reference (44).

inch, respectively (table 3.3). On the basis of these values, within the intermountain region incremental evaporation per 1,000 feet elevation increase varies from an annual average of 0.0027 inch per day (0.081 inch per month) to 0.0026 inch per day during the winter and 0.0029 inch per day during the summer months. These figures indicate that for most applications within this region use of the average annual value throughout the entire year would yield satisfactory results.

Computation of evapotranspiration. A large number of formulas have been developed for estimating evapotranspiration, and many of these were investigated with regard to their application to this study. The rate of evapotranspiration depends on several factors, such as crop, climate, soil moisture supply, salinity, and vegetative cover. Climatic conditions usually considered are solar radiation, precipitation, temperature, daylight hours, humidity, wind velocity, and length of growing season. The quantity of water transpired by plants is also thought to depend upon the availability of moisture within the root zone, the stage of plant development, the foliage cover, and the nature of the leaf surfaces. Many of these various factors are interrelated, and their individual effects on evapotranspiration are difficult to determine.

The methods which have been developed for estimating evapotranspiration can be grouped into three general categories, depending upon the approach employed in their development, namely vapor transfer, energy balance, and empirical.

The vapor transfer process assumes that the moisture flow through a layer of air near the ground or water surface can be measured. It requires simultaneous measurements of wind velocity, temperature, and vapor pressure at different heights above the surface. Of the equations reviewed only that proposed by Papadakis (25) can be considered to fall into this category. Working in Argentina he developed the following relationship:

$$E_n = 0.5625\,(e_{ma} - e_d) \quad . . . . \quad 3.38$$

in which

E_n = monthly potential evapotranspiration in centimeters

e_{ma} = saturation vapor pressure corresponding to the average daily maximum temperature of the month, in millibars

e_d = vapor pressure that corresponds to dewpoint, in millibars

Under the energy balance technique an attempt is made to establish relationships for the flow of energy which produces evapotranspiration. The assumption is made that the energy received by a surface through radiation must equal (1) the energy used for evaporation, (2) heating the air, (3) heating the soil, and (4) any extraneous or advective energy. It is usually felt that for short periods, such as daily and monthly balances, items (3) and (4) can be neglected without seriously affecting the accuracy of the results. In general, an equation developed under this approach requires parameters which are often not measured at meteorological stations; in addition, calculations tend to be somewhat complicated.

Penman's formula (27), which includes a large number of parameters, is perhaps the best known of these rational relationships. For many areas his formula yields satisfactory estimates of evapotranspiration, but because the equation does not provide for the advective transfer of energy, results are inclined to be low for regions of high temperatures and low humidity.

The formulas which fall into the category of empirical relationships make up by far the largest group of those which have been proposed to estimate evapotranspiration. The equations were developed from primarily empirical relationships between experimental data and various climatic and water supply measurements. For illustrative purposes the most common equations from among the many reviewed are included in this discussion.

The Lowry-Johnson formula (22) expresses evapotranspiration losses in terms of an effective heat factor.

$$U = 0.8 + 0.156\, F \qquad 3.39$$

in which

U = the "valley" consumptive use or evapotranspiration in acre-feet per acre for the period under consideration

F = "effective heat" for the period in thousands of day degrees. Effective heat is defined as the accumulation, in day degrees, of maximum daily growing season temperatures above 32° F.

This relationship was developed for the purposes of estimating valley consumptive use on an annual basis. However, Criddle (9) adapted the Lowry-Johnson technique to estimate monthly consumptive use by using the proportion of monthly heat units to annual heat units. Thus, monthly values of consumptive use are given by:

$$u = \left(\frac{f}{F}\right) U \quad . \; . \; . \; . \; . \; . \; . \; . \; . \; . \; . \; . \; . \qquad 3.40$$

in which f is the effective heat in thousands of day degrees (above 32° F) for the month.

Thornthwaite (38) developed the following expression:

$$PET_n = 1.6\ L_n \frac{10T_n}{I}^{a} \quad , \quad \text{for } T > -1^{\circ}\text{ C} \quad . \; . \; . \qquad 3.41$$

in which

PET_n = potential evapotranspiration in inches during the month, n

L_n = mean possible duration of sunlight in the month, n, expressed in units of 30 days of 12 hours each

I = heat index

$$= \sum_{n=1}^{12} i_n \quad , \quad i_n = \left(\frac{T_n}{5}\right)^{1.514}$$

a $= 6.75 \times 10^{7} I^{3} - 7.71 \times 10^{5} I^{2} + 1.792 \times 10^{-2} I + 0.49239$

T_n = mean monthly temperature in degrees C. $PET_n = 0$ for $T_n \leq -1^{\circ}$ C

The Blaney-Criddle formula (4) was proposed as follows:

$$U = kF \qquad 3.42$$

in which

U = seasonal crop consumptive use in inches

k = a seasonal coefficient which varies with type of crop and location

F = sum of the monthly consumptive use factors, f, for the growing season

$$f = \frac{tp}{100} \qquad 3.43$$

in which t is mean monthly temperature in degrees F, and p is monthly percentage of daylight hours of the year.

Phelan and other personnel of the Soil Conservation Service (28, 29) developed a modification of the Blaney-Criddle formula whereby the monthly coefficient, k, is divided into two parts, k_c and k_t. k_t is a function of temperature and is expressed as

$$k_t = (0.0173\ t - 0.314) \qquad 3.44$$

in which t is mean monthly temperature in degrees F. It is considered that k_c is a function mainly of the physiology and stage of growth of the crop, but it is recognized that it no doubt still contains some climatological influences.

This modification has accomplished the following:

1. enabled the application of the formula over a wide area for known values of k_c,
2. largely explained the variation in k for a given month from year to year, and
3. enabled the establishment of the beginning of the growing season on the basis of mean monthly air temperatures. The growing season for most annual crops is ended before the first 32° F frost in the fall.

Because of its simplicity and wide acceptance, and because through it evapotranspiration losses for individual crops can be estimated, the Blaney-Criddle formula as modified by Phelan and others was selected for this study. The equation is expressed as follows:

$$ET_{cr} = k_c \, k_t \frac{T_a \, p}{100} \quad \ldots\ldots\ldots\ldots \quad 3.45$$

It is again emphasized that the independent variables on the right side of the above relationship can be expressed either as continuous functions or as step functions consisting of constant mean values for a particular time increment. The estimated potential evapotranspiration rate function is established accordingly. For example, if mean monthly values of the independent parameters are used, the relationship yields an estimate of the mean potential evapotranspiration rate during each month.

Plots indicating k_c values as a function of time have been prepared for a number of different agricultural plant varieties. Typical examples are those for alfalfa and spring grain shown by figures 3.13 and 3.14, respectively. In addition, preliminary k_c curves for various species of phreatophytic and other forms of native vegetation have been developed from the limited water-use information which is available for these plants (33, 39, 41, 52). The k_c curve for grass pasture shown by figure 3.15 seems applicable to many species of native vegetation. As indicated by figure 3.14, in the case of perennial crops the available curves included only the growing season. Since for any given area evapotranspiration continues throughout the entire year, the k_c curves for all annual varieties have been extended to include the full year (34, 47). During the noncropping season evapotranspiration from bare ground and snow surfaces is estimated.

The two parameters of temperature and percent daylight hours which appear in equation 3.45 are indices of the total energy available to surfaces subject to the evapotranspiration process. Values of p on a monthly basis are available in a number of references, one of which is cited (10). These indices integrate total energy received on a regional basis and the equation is applicable to horizontal surfaces. In order to provide an adjustment for sloping land surfaces, such as

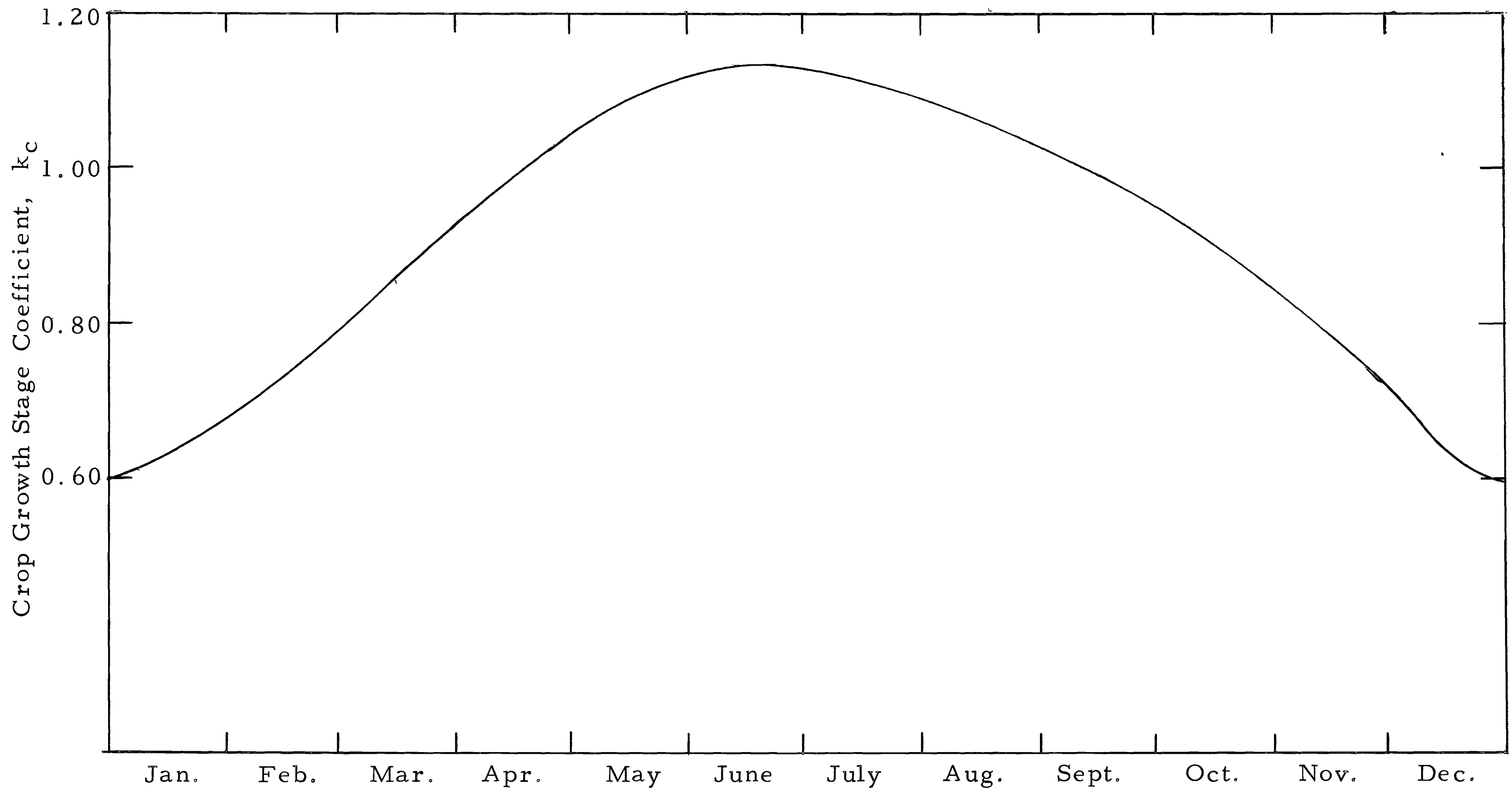

Figure 3.13. Crop growth stage coefficient curve for alfalfa.

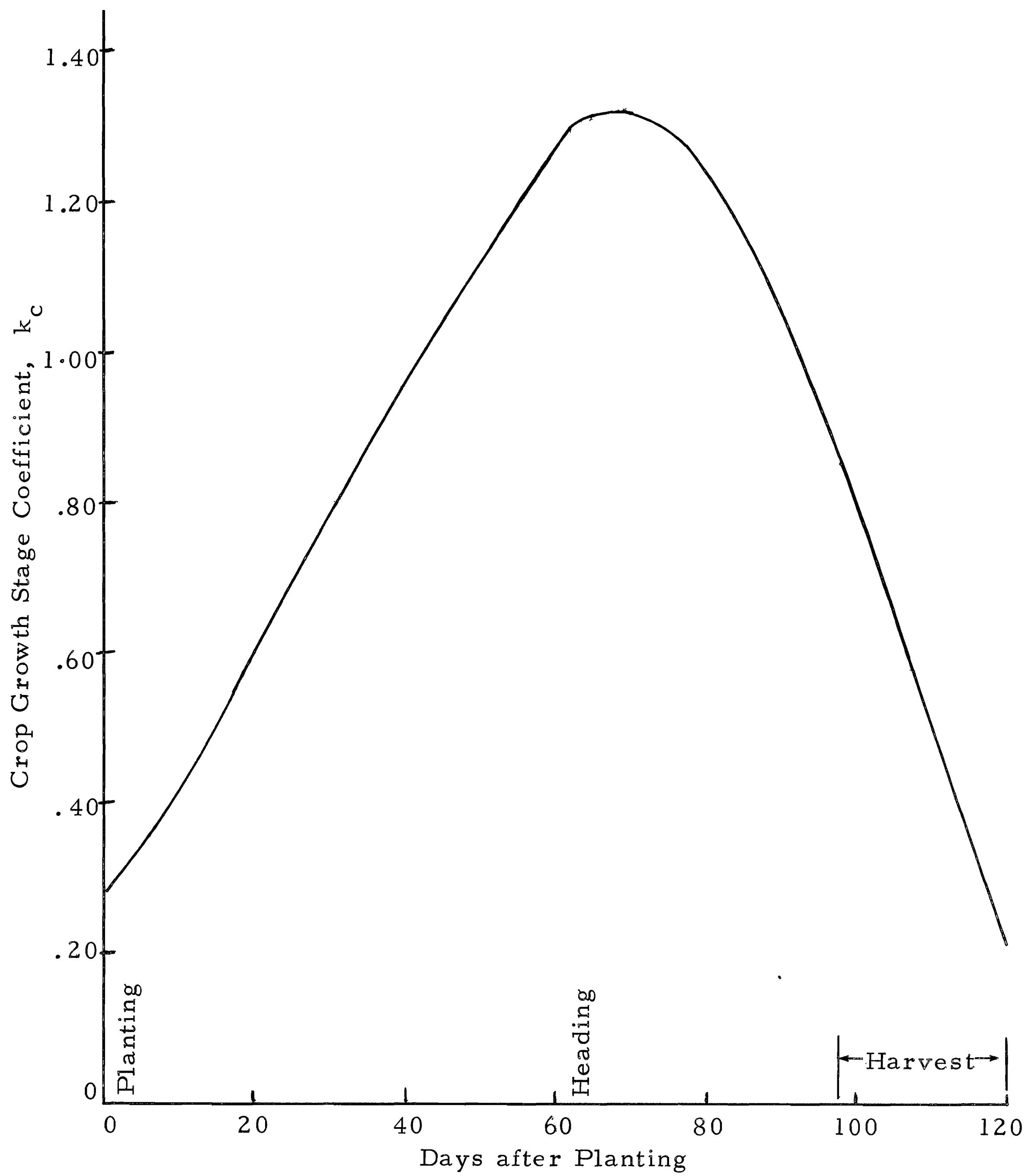

Figure 3.14. Crop growth stage coefficient curve for spring grain.

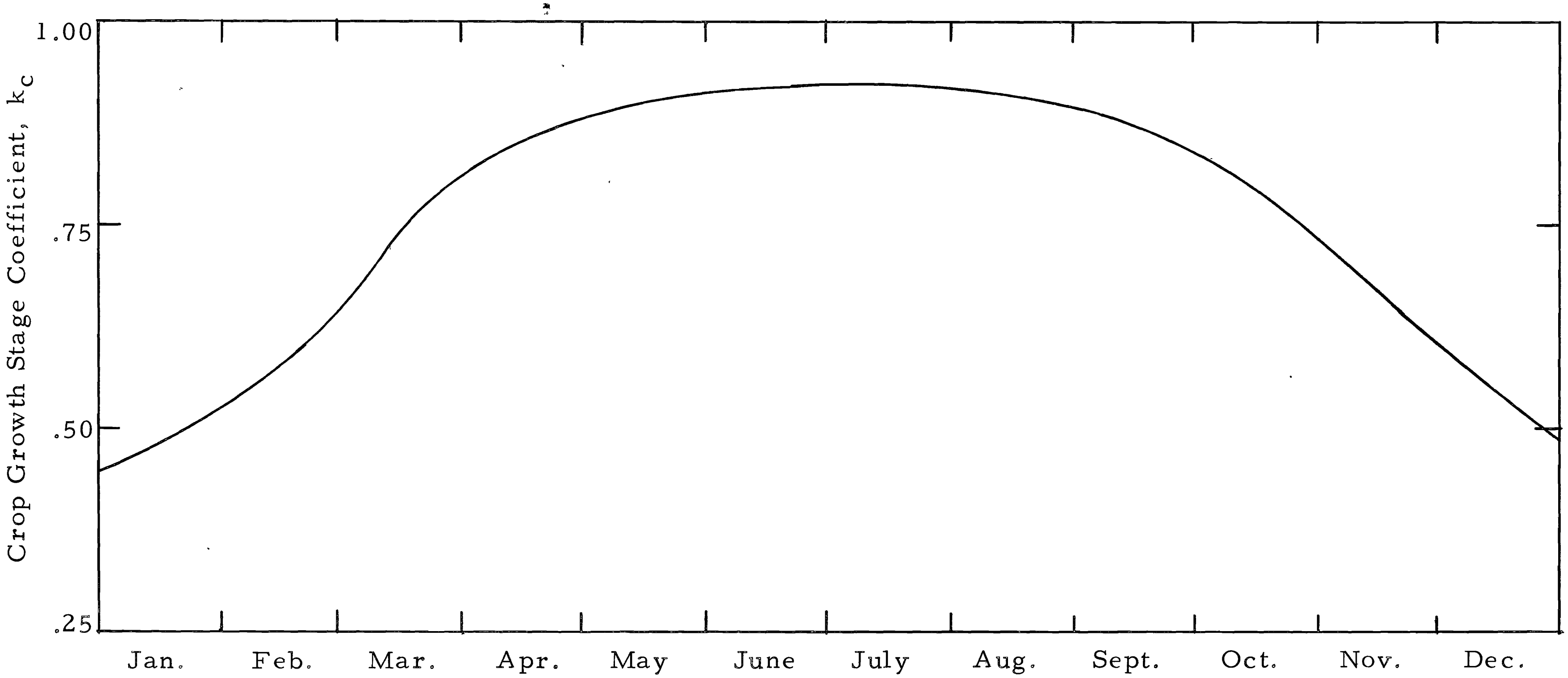

Figure 3.15. Crop growth stage coefficient curve for grass - pasture.

occur on a watershed, the potential insolation parameter was introduced into equation 3.45, thus:

$$ET_{cr} = \frac{RI_s}{RI_h} k_c k_t \frac{T_a p}{100} \quad . \; . \; . \; . \; . \; . \; . \; . \; . \; . \; . \quad 3.46$$

in which all parameters, whether continuously variable functions or finite mean values, are applicable to the same time increment, and

RI_s = the radiation index for a particular watershed zone possessing a known degree and aspect of slope

RI_h = the radiation index for a horizontal surface at the same latitude as the particular watershed under study

It is interesting to note that in the northern hemisphere and for northerly slopes the ratio RI_s/RI_h decreases with a declination decrease, while for southerly slopes the ratio increases with decreasing declination (figure 3.4). Thus, for given values of p and T, the evapotranspiration rate on northerly slopes is less during the winter months than the summer months. For southerly slopes the reverse is true. It might be further noted from the definition of the radiation index parameter that the ratio RI_s/RI_h is equivalent to the ratio I_s/I_h in which the terms I_s and I_h refer to total potential insolation received on the sloping and horizontal surfaces respectively during a particular day.

An elevation correction based upon the results of the preceding section can also be included in a relationship for estimating evapotranspiration. In order to consider the plant influences the evaporation correction is multiplied by the crop coefficient parameter, k_c. Thus, equation 3.46 is modified to read:

$$ET_{cr} = \frac{RI_s}{RI_h} k_c \left[k_t \frac{T_a p}{100} + C_e (E_s - E_v) \right] \quad . \quad . \quad . \qquad 3.47$$

in which

C_e = the elevation correction factor applicable to the particular time increment

E_s = the mean elevation of the watershed zone in thousands of feet

E_v = the mean elevation of the valley floor in thousands of feet

In this study an average annual elevation correction factor of 0.0027 inch per day per thousand feet was applied.

The influence of soil water on evapotranspiration has been the subject of much research and discussion (45, 46). It is now generally conceded that there is some reduction in the evapotranspiration rate as the quantity of water available to plants within the root zone decreases. Thornthwaite (38) contends that this rate is proportional to the amount of water remaining in the soil. This criterion has been somewhat modified by recent studies at the U. S. Salinity Laboratory in Riverside, California (13). These indicate that transpiration occurs at the potential rate through approximately two-thirds of the range of available moisture within the rooting depth. A critical point is then reached when actual transpiration begins to lag behind the potential rate. Because soil moisture becomes a limiting factor at this point, plants begin to wilt. Thereafter, the relationship between available water content and transpiration rate is virtually linear. Average daily transpiration rates plotted as a function of water content (weight basis) for three soil types are shown by figure 3.16. Typical values of the soil moisture content at various points on these curves are shown by table 3.4. It should be noted that the soil moisture content at the point of discontinuity on the curve, M_{es}, is a function of the average soil moisture tension within the plant root zone, and is, therefore, dependent upon not only the soil type but also the extent and distribution of the root system of the transpiring plants.

Table 3.4. Typical soil moisture values, in inches per foot of soil depth, for three characteristic soil types

Soil type	Total soil moisture of field capacity	Approx. lower limit of available water for plants	Total soil moisture available to plants	Available moisture at the critical value, M_{es}
Clay	6.0	2.0	4.0	1.3
Loam	3.5	0.8	2.7	0.9
Sand	1.2	0.3	0.9	0.3

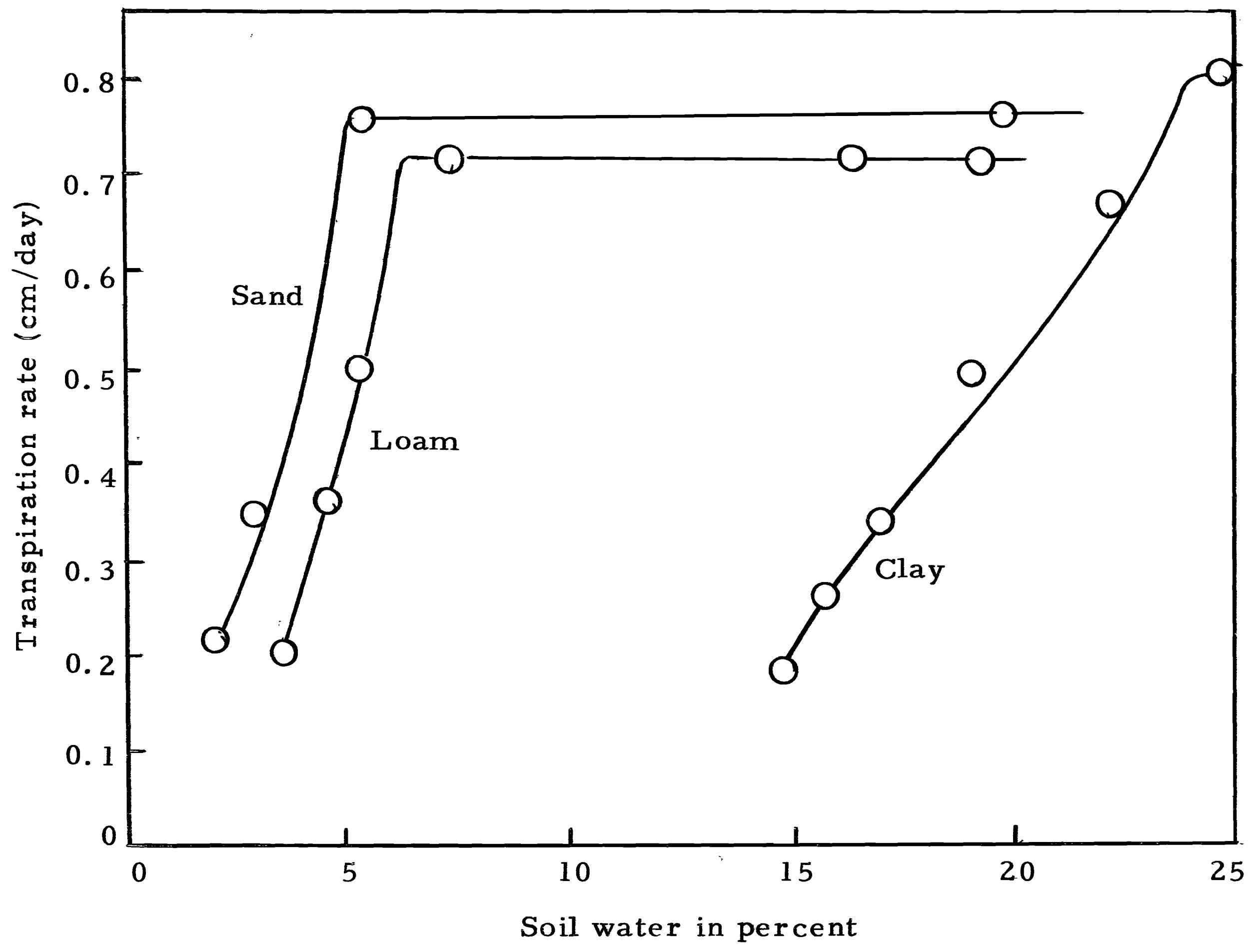

Figure 3.16. Average daily transpiration rates as functions of water content for birdsfoot trefoil in shallow containers.

On the basis of the preceding discussion, actual evapotranspiration is expressed as follows:

$$ET_r = ET_{cr} \quad , \quad [\, M_{es} < M_s(t) \le M_{cs} \,] \quad . \quad . \quad . \quad . \quad . \quad . \qquad 3.48$$

From equation 3.48 it is apparent that when the available moisture in the plant root zone is greater than a critical value, M_{es}, the actual evapotranspiration can be estimated by equation 3.47. For available soil moisture levels less than M_{es} actual evapotranspiration is given by

$$ET_r = ET_{cr} \frac{M_s(t)}{M_{es}} \quad , \quad (0 \le M_s(t) \le M_{es}) \quad . \quad . \quad . \quad . \quad . \qquad 3.49$$

This equation when integrated is exponential in nature. To demonstrate this statement, the integration is simplified by assuming that changes in soil moisture are due entirely to evapotranspiration and further that the potential evapotranspiration rate, ET_{cr}, is a constant throughout the time increment or integration period. Actually, neither of these assumptions is necessary in the analog computer program. Equation 3.49 can then be written in the form:

$$ET_r = \frac{dM_s}{dt} = -ET_{cr} \frac{M_s(t)}{M_{es}} \quad . \quad . \quad . \quad . \quad . \quad . \quad . \quad . \qquad 3.50$$

with the negative sign indicating abstraction from storage. Integrated between times t_1 and t_2 equation 3.50 appears as:

$$M_s(2) = M_s(1) \exp \left[- \frac{ET_{cr}}{M_{es}} (t_2 - t_1) \right] \quad . \quad . \quad . \quad . \quad . \quad . \qquad 3.51$$

in which $M_s(1)$ and $M_s(2)$ are the soil moisture storage values at times t_1 and t_2 respectively.

From equation 3.49, equation 3.47 can now be modified to read:

$$ET_r = \frac{M_s}{M_{es}} \frac{RI_s}{RI_h} k_c \left[k_t \frac{T_a p}{100} + C_e (E_s - E_v) \right],$$

$$(0 \leq M_s \leq M_{es}) \quad . \quad . \quad . \quad . \quad . \quad . \quad . \qquad 3.52$$

This is a general equation for estimating evapotranspiration rates. Under the particular conditions when $M_s > M_{es}$, $ET_r = ET_{cr}$ and equation 3.52 is of the particular form shown as equation 3.47.

<u>Computation of evaporation from water surfaces.</u> Evaporation rates, E_{cr}, from interception and surface depression storage within the watershed zone are estimated by equation 3.47. In the case of water surfaces a k_c factor of 1.0 is applied (26, 27) whereas for snow and bare ground this factor is assumed to equal 0.25 (14, 34). Evaporation losses from interception and surface depression are assumed to occur concurrently. During snow accumulation periods as indicated by an air temperature of less than 35° F soil moisture content is assumed not to influence evapotranspiration rates. During these periods equation 3.47 applies regardless of the soil moisture level within the plant root zone. Thus,

$$ET_r = ET_{cr} \quad , \quad (T < 35^{\circ} F) \quad . \quad . \quad . \quad . \quad . \quad . \quad . \quad . \qquad 3.53$$

Several studies have been carried out in which the evaporation loss from the top surface of a snow pack was investigated (14, 40, 47, 49, 50). Typical rates vary from 0.01 inch per day to 0.03 inch per day, depending upon the degree of exposure of the snow surface. In cases where lake or pan evaporation data are available, close estimates of snow surface evaporation rates are obtained by assuming about one-third those of the lake or one-fifth the pan rates.

Deep percolation

Deep percolation is defined as the movement of water through the soil from the plant root zone to the underlying groundwater storage basin. This movement occurs under the influence of both gravity and capillary potential fields. For saturated flow gravity is the dominant force, while in the case of unsaturated flow the capillary field becomes the important potential. Thus, deep percolation exists even though the moisture content of a soil is below field capacity (30, 48). In general terms the relationships for deep percolation losses in the saturated and unsaturated states are expressed as follows:

$$G_{rs} = f(k_h) \quad \ldots \ldots \ldots \ldots \quad 3.54$$

$$G_{ru} = f(k_u, \theta) \quad \ldots \ldots \ldots \ldots \quad 3.55$$

in which

G_{rs} and G_{ru} = the saturated and unsaturated rates of deep percolation losses respectively

k_h = the hydraulic conductivity or permeability of the soil

k_u = the capillary conductivity of the soil

θ = the soil moisture content

Equations 3.54 and 3.55 can be approximated by the empirical expression:

$$G_r = -k_g M_s(t) \quad , \quad (0 \leq M_s(t) \leq M_{cs}) \quad . \quad . \quad . \quad . \quad . \quad . \qquad 3.56$$

in which the negative sign indicates outflow or storage loss and k_g is a constant of proportionality, depending upon the porosity of the soil. $M_s(t)$ is given by equation 3.26. At field capacity $M_s(t) = M_{cs}$, and if deep percolation is assumed to be vertical (gradient = 1), equation 3.54 can be written in the form $G_{rs} = k_h$. Now, if the capillary component of flow is neglected at field capacity, this expression can be combined with equation 3.56 to yield

$$k_g M_{cs} = k_h$$

or

$$k_g = k_h/M_{cs} \quad . \quad . \quad . \quad . \quad . \quad . \quad . \quad . \quad . \quad . \quad . \quad . \quad . \quad . \qquad 3.57$$

Interflow

Interflow is defined as that portion of the soil seepage water which does not enter the groundwater basin but rather which moves largely in a lateral direction through the upper and more porous portion of the soil profile until it enters a stream channel. It is assumed that no interflow occurs until the available moisture holding capacity of the soil root zone has been satisfied. Once this point is reached storage changes within the root zone are insignificant, so that interflow rate is given by the following expressions:

$$N_r = 0 \quad , \quad (M_s < M_{cs}) \quad . \quad . \quad . \quad . \quad . \quad . \quad . \quad . \quad . \quad . \qquad 3.58$$

$$N_r = F_r - G_r - ET_{cr} \quad , \quad (M_s = M_{cs}) \quad . \quad . \quad . \quad . \quad . \qquad 3.59$$

Equations 3.56 and 3.59 can be combined to yield:

$$N_r = F_r - k_g M_{cs} - ET_{cr} \quad . \quad . \quad . \quad . \quad . \quad . \quad . \quad . \quad . \qquad 3.60$$

The total interflow quantity which is available during a time period, n, is given by the integration of equation 3.60.

$$\int_{t_{cr}}^{t_n} N_r \, dt = \int_{t_{cr}}^{t_n} (F_r - k_g M_{cs} - ET_{cr}) \, dt \quad . \quad . \quad . \quad . \quad . \qquad 3.61$$

in which t_{cr} represents the time at which $M_s = M_{cs}$ and is bounded as follows: $(t_o \le t_{cr} \le t_n)$.

Subsurface routing or translation

The movement of water from one point to another within a hydrologic system is a very complicated process. Some of the characteristics of an area which influence this process are soil porosity, soil depth, surface drainage density, shape, and slope of the watershed or zone. The problem can be simplified, however, by applying a general routing relationship which is based on the premise that the rate of discharge from a storage basin is proportional to the quantity of water in storage (20), namely,

$$q = \frac{d\,s\,(t)}{dt} = -\,ks(t) \quad . \quad . \quad . \quad . \quad . \quad . \quad . \quad . \quad . \quad . \quad . \quad . \qquad 3.62$$

in which

q = the discharge rate from the basin

$s(t)$ = the storage within the basin at any time, t

k = a constant depending upon the basin characteristics. The value of k is frequently established by model verification studies.

In this model equation 3.62 is applied to the groundwater basin of the watershed in order to estimate base flow. This same equation with a different value of k is also applied to obtain an estimate of the time distribution of the interflow runoff for each watershed zone. Because interflow moves at relatively shallow depths, it does not usually travel far before emerging in an established surface channel where it combines with surface runoff. In this model where large time increments are involved surface flow is not delayed in any form of storage unless, of course, a surface reservoir exists on the watershed. Thus, in general, this flow appears in the outflow hydrograph as it occurs on the watershed so that the following expression applies:

$$q_{rs} = S_r \quad . \; . \; . \; . \; . \; . \; . \; . \; . \; . \; . \; . \; . \; . \quad 3.63$$

The following relationships apply where designated:

Base flow.

$$\left[\sum_{i=1}^{m} G_r\right] dt - Q_{rg}\, dt = d\, G_s\,(t) \quad . \; . \; . \; . \; . \; . \; . \; . \quad 3.64$$

$$Q_{rg} = k_b\, G_s(t) \quad . \; . \; . \; . \; . \; . \; . \; . \; . \; . \; . \; . \quad 3.65$$

in which m is the number of zones into which the watershed is divided, Q_{rg} is the base flow rate from the watershed, and k_b is a constant determined by verification studies.

From equations 3.64 and 3.65

$$G_s(t) = \int_0^t \left[\sum_{i=1}^{m} G_r(i) - Q_{rg}\right] dt$$

$$= \int_0^t \left[\sum_{i=1}^{m} G_r(i) - k_b\, G_s(t)\right] dt \quad . \; . \; . \; . \; . \; . \quad 3.66$$

Interflow.

$$N_r\, dt - q_{rn}\, dt = d\, N_s(t) \quad . \; . \; . \; . \; . \; . \; . \; . \; . \; . \quad 3.67$$

$$q_{rn} = k_n\, N_s(t) \quad . \; . \; . \; . \; . \; . \; . \; . \; . \; . \; . \; . \quad 3.68$$

in which

$$N_s(t) = \int_0^t (N_r - q_{rn})\, dt \quad . \quad . \quad . \quad . \quad . \quad . \quad . \quad . \quad . \quad . \quad 3.69$$

q_{rn} in these equations represents the interflow rate from a particular watershed zone.

Total outflow. Total outflow from the watershed is given by summing surface runoff, interflow, and base flow, thus:

$$Q_{rt} = \sum_{i=1}^{m} \left[q_{rs}(i) + q_{rn}(i) \right] + Q_{rg} \quad . \quad . \quad . \quad . \quad . \quad . \quad . \quad . \quad 3.70$$

in which the quantity $\sum_{i=1}^{m} \left[q_{rs}(i) + q_{rn}(i) \right]$ is designated the direct runoff.

Long transport delay times, such as the average time required for the groundwater or base flow, Q_{rg}, to move off the watershed, are simulated in the model by means of active delay networks. The required delay setting of these networks is established during the model verification studies.

CHAPTER IV

ANALOG COMPUTER IMPROVEMENTS

As indicated in Chapter I, modifications to an analog computer to increase its capability in hydrologic simulation were completed at Utah State University in November 1964 (3). This work was part of the first phase of the analog simulation program at this institution. The computer, which is shown by figure 4.1, contained 46 operational amplifiers, three x-y multipliers, two function generators, 192 switched potentiometers, a digital voltmeter, and a control console. Notable features of the equipment were the switched potentiometers which permitted the input of digital data, and the program jacks on the faces of the computing consoles. These jacks provided an easy means of incorporating into the computer programs complex arrangements of capacitors for the simulation of long storage and routing delay times. However, the computer lacked a patch panel, so that the interchange of problems was difficult and time consuming. In addition, its capacity was sufficient for only relatively small and uncomplicated simulation problems.

Under the project reported herein a considerable effort was made to match the development of the analog computer with that of the mathematical model of the hydrologic system. The philosophy inherent in this course of action is depicted by figure 2.1. As a part of the

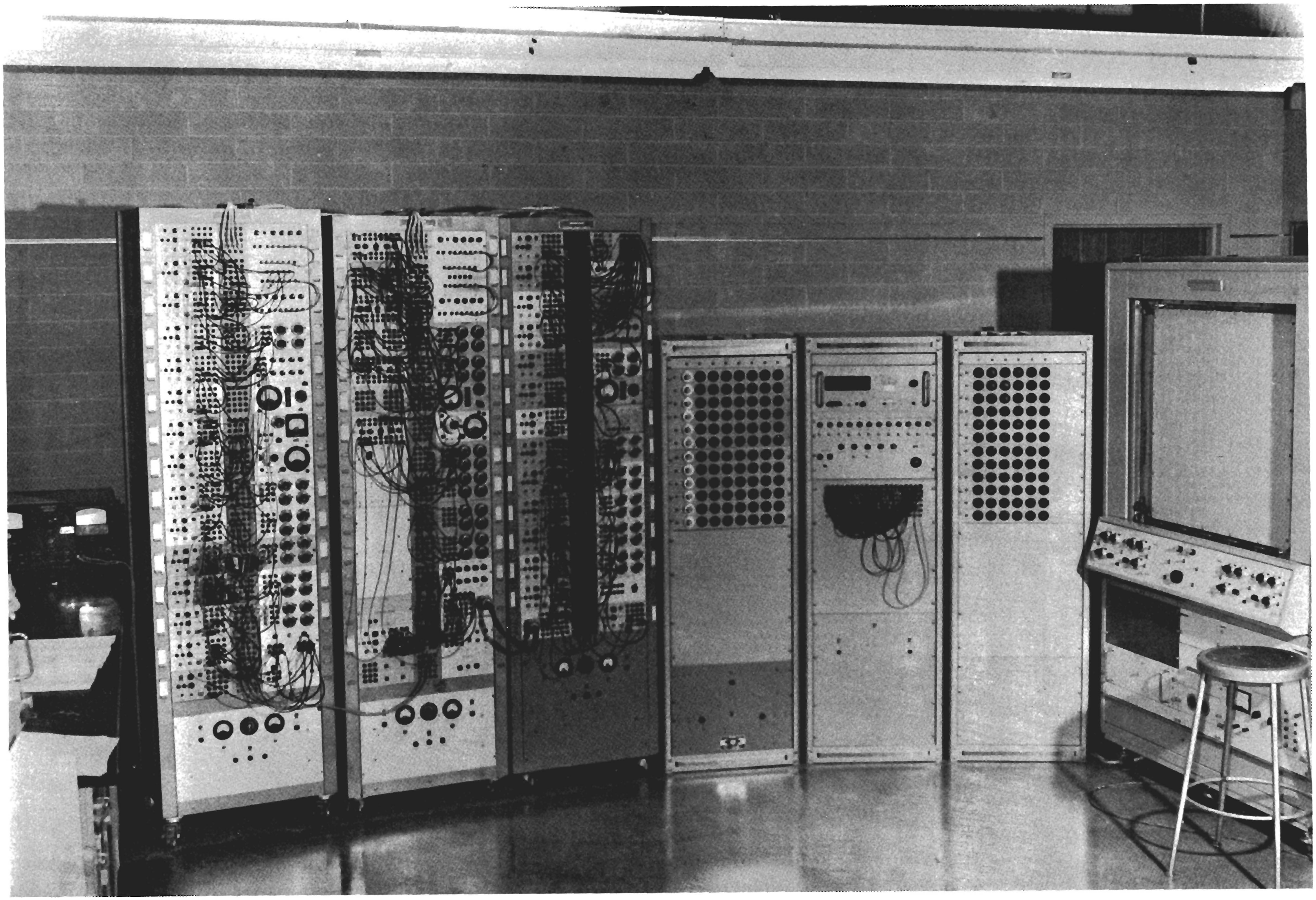

Figure 4.1. The first model of the analog computing facilities developed for simulation studies at Utah State University.

development effort, two M33 anti-aircraft fire control system analog computers containing 44 chopper stabilized operational amplifiers each were obtained from surplus U. S. Government Property. These special-purpose computers have now been modified for general-purpose application. The modifications include the complete repackaging of the operational amplifiers together with their associated power supplies and control equipment in a new console. Components added to the system include a push-button computer control mechanism, a removable programming patch board and bay, 96 coefficient potentiometers, and a digital voltmeter with a four place reading. The removable programming patch board greatly improves the flexibility and utility of the analog operation by making it possible to change problems merely by changing panels. A problem is wired in advance on a panel, thus leaving the computer free for other studies during the programming operation. Patch panels also provide a means of problem storage for later use.

As the complexity of problems increases, the need for non-linear computing equipment becomes greater. To meet this need several diode quarter square multipliers, diode function generators, and comparator relays were constructed and added to the modified M33 computer. Figure 4.2 is a picture of the M33 computer when modifications to this equipment were in a partial state of completion.

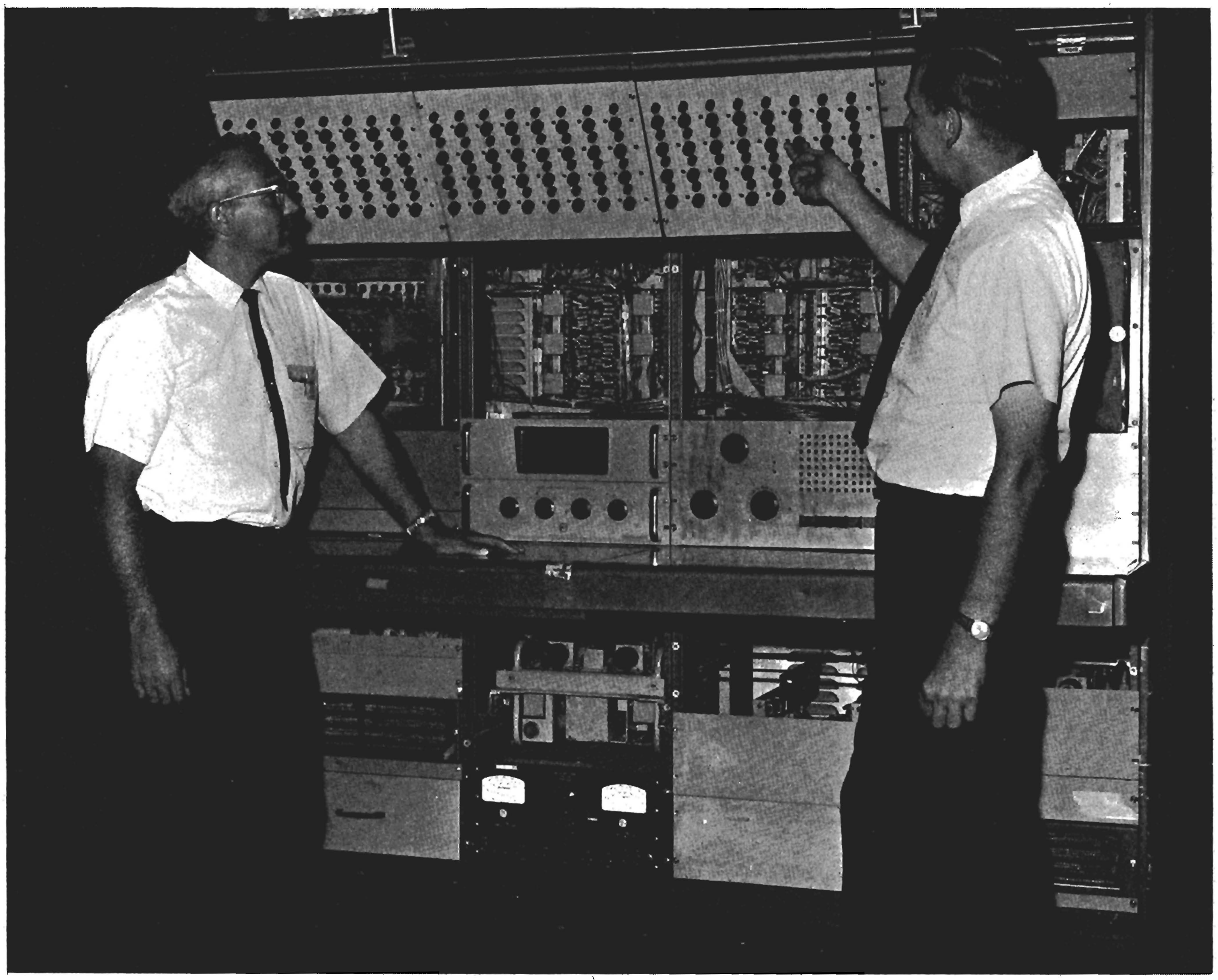

Figure 4.2. The M33 computer showing modifications in a partial state of completion.

When modifications to the M33 computing equipment were complete, the equipment was interfaced with the computing equipment of figure 4. 1. The interface provides for the operation of both computers from a single control console, and for the connection of some of the original amplifiers to the patch panel. The two computers can be operated either independently or as a single unit. The important components of the total computer now include 134 operational amplifiers, 192 switched potentiometers, approximately 170 coefficient potentiometers, and several pieces of non-linear equipment. The entire facility is shown by figure 4.3. The piece of equipment situated to the extreme right of this figure is a 30 inch by 30 inch two-arm x-y automatic plotter for recording output information. Through the modifications made under this project the capability of the analog computing equipment at this laboratory has been greatly expanded.

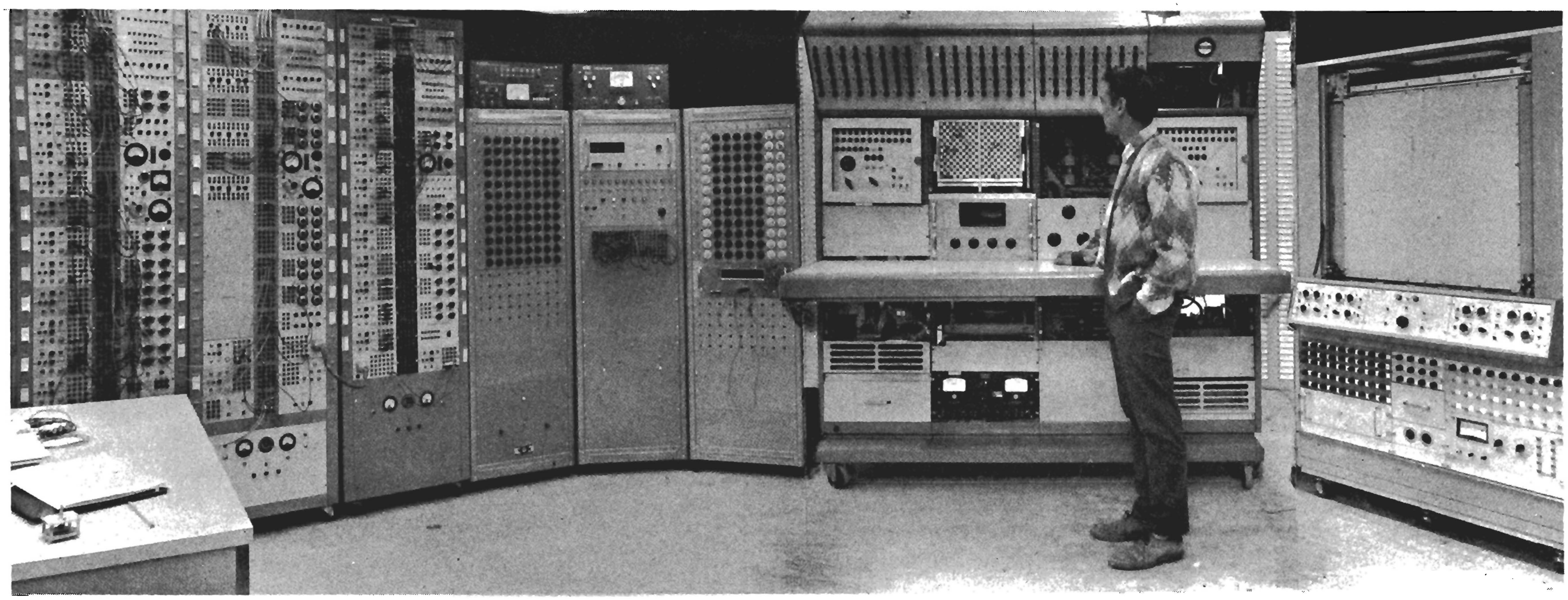

Figure 4.3. Analog computing facilities formed by interfacing the first model with the modified M33 computer.

CHAPTER V

TESTING AND VERIFICATION OF THE MODEL

In order to test and verify a hydrologic model, it is necessary to simulate an actual hydrologic unit. Of major importance in this analysis is the accuracy with which the known input and output data actually represent the various hydrologic quantities as they occur on the watershed. Frequently, the accuracy of available data is the limiting criterion which establishes the simulation accuracy for a particular watershed.

In this project, the equations presented in Chapter III and the computing equipment discussed in Chapter IV were tested by simulating a subbasin of the Sevier River drainage in central Utah. This subbasin, which is referred to as Circle Valley, contains approximately 93,000 acres. It is situated at a latitude of about 40^{o} N, and is formed by a widening of the Sevier River valley at a point immediately upstream from its point of confluence with the drainage of the East Fork of the Sevier River. Figure 5.1 shows a general outline of the subbasin. The average elevation of the valley floor is approximately 6,000 feet above sea level. On the west side of the valley the mountains rise to a peak elevation of 11,440 feet, while on the east side 11,036 feet is the maximum elevation. Circle Valley was selected for the study because its hydrologic system is relatively uncomplicated, and yet contains

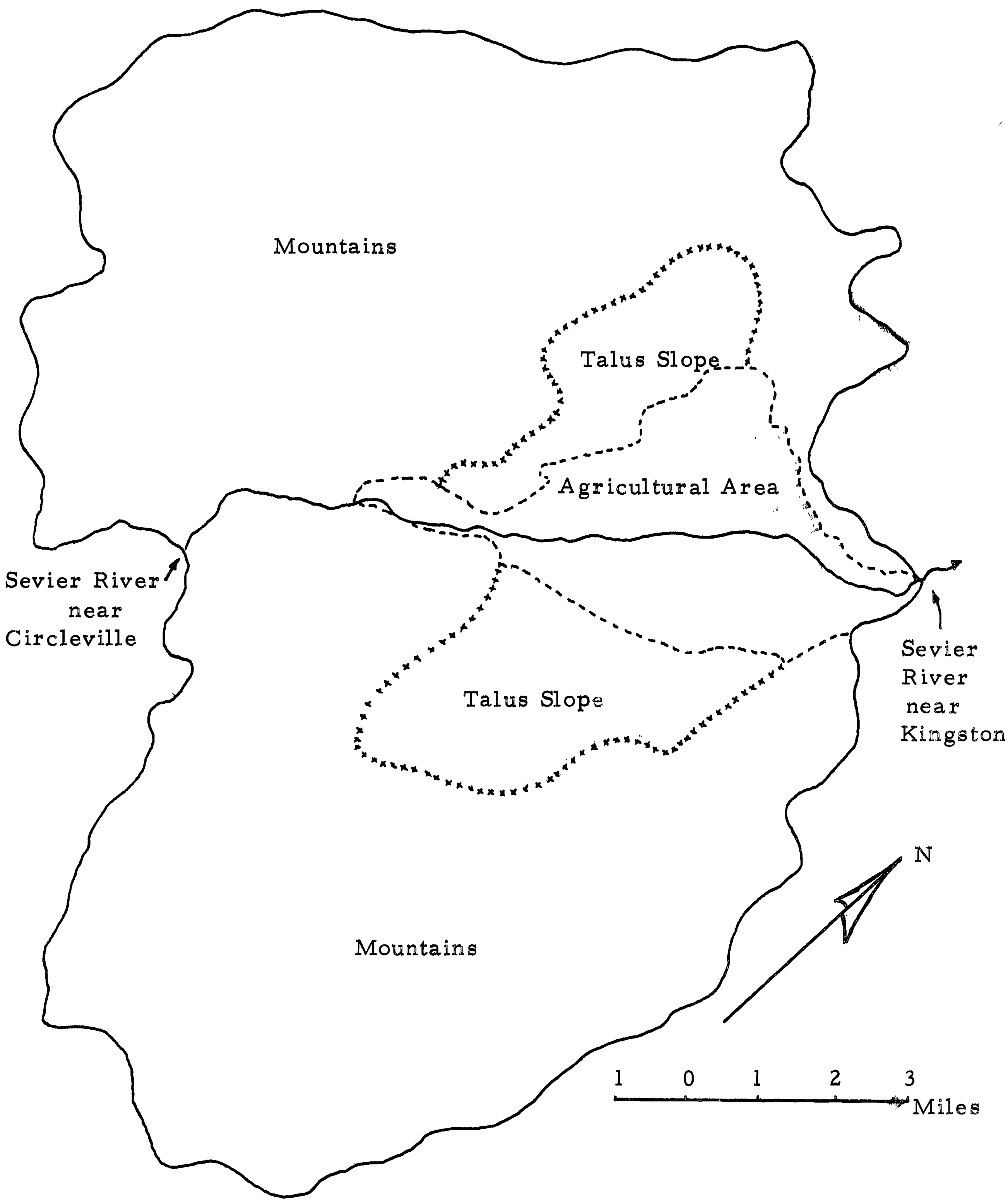

Figure 5.1. General outline of Circle Valley subbasin, Sevier River, Utah.

many of the characteristic hydrologic phenomena. In addition, there are sufficient physical data available in the subbasin to guide the formulation of a model and to provide an evaluation of its performance.

An area-elevation curve for the mountainous or watershed area of Circle Valley is shown by figure 5.2. This curve indicates the mean watershed elevation to be about 7,400 feet. The total area of the watershed or land above the elevation of the valley floor is 84,700 acres. If the watershed is considered as consisting of two general facets, that on the west side of the Sevier River has a south-east aspect and an approximate average slope of 60 percent, while corresponding values for the facet on the east side of the river are north-west and also 60 percent. The various types of watershed cover were grouped into very broad categories. The approximate areas included within each of these categories are shown by table 5.1.

Table 5.1. Watershed cover, Circle Valley, Utah.

Facet	Brush & Sage	Coniferous	Deciduous	Barren	Total
West (acres)	28,428	4,732	1,085	4,250	38,495
East (acres)	30,160	14,140	1,140	765	46,205
Totals (acres)	58,588	18,872	2,225	5,015	84,700

The dominant soil type on the watershed is a course-textured loam which in many cases contains a large number of stones. The average soil moisture holding capacity is about 0.83 inches per foot of soil.

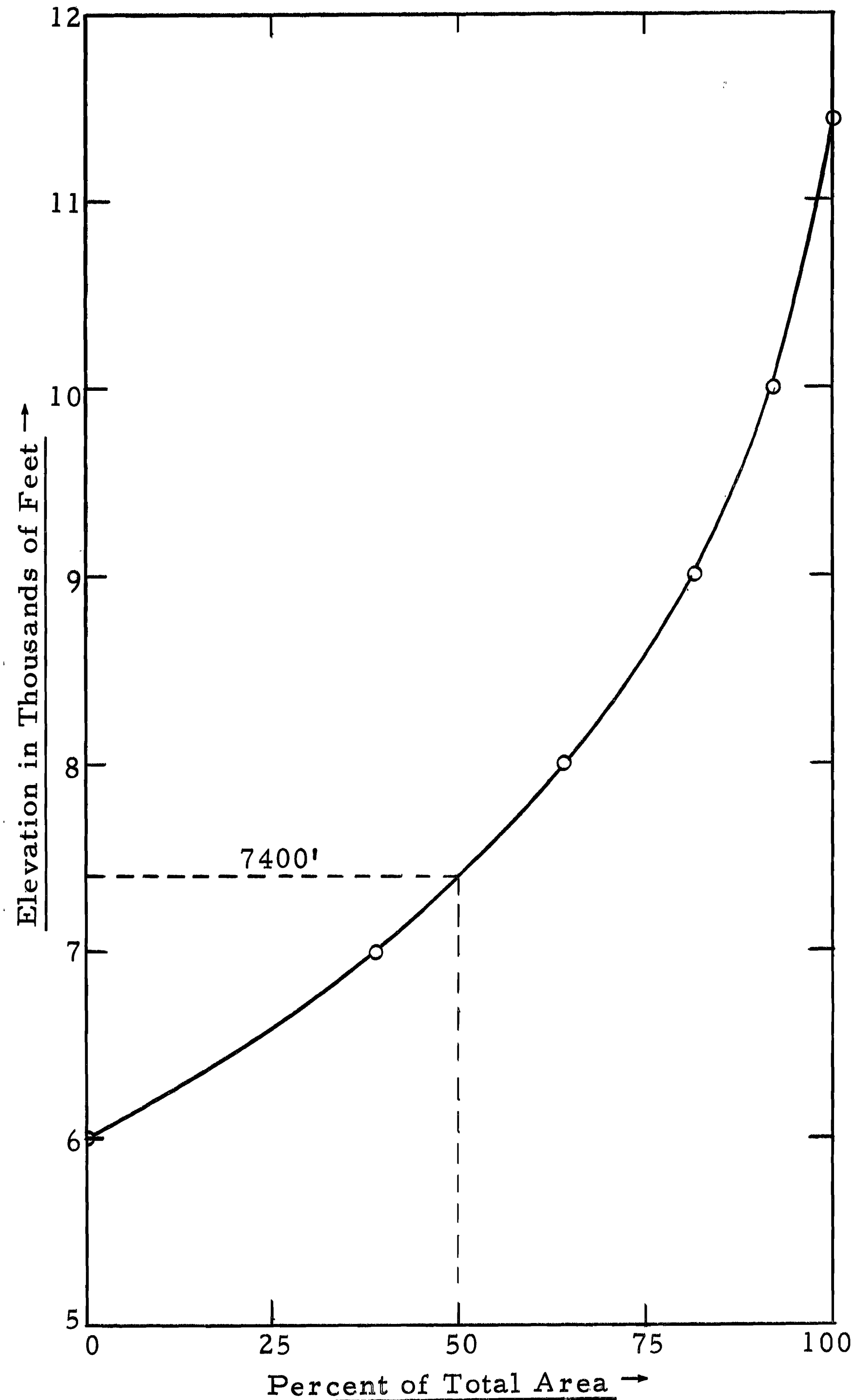

Figure 5.2. Area-elevation curve for the mountainous portion of Circle Valley basin.

The flat or bottom land area within Circle Valley is shown by figure 5.3. This sketch shows the locations of the irrigation canals and the single irrigation well within the valley. Also shown is the cropland area which contains some 4,580 acres, and a wet or swampy area of about 3,430 acres at the lower end of the valley. The primary agricultural crops within the cultivated area are grain (820 acres), potatoes (370 acres), corn (180 acres), and alfalfa (3,210 acres).

The wet area is formed by a natural subsurface barrier of low permeability material which extends across the mouth of the valley. Geologic investigations (5) have indicated that this barrier prevents any appreciable subsurface outflow from Circle Valley so that essentially all outflow is accounted for by surface measurements. The boundary between the cropland area and the wet area approximates the division between the confined and the unconfined groundwater conditions. The groundwater underlying the cropped land is unconfined, while the underground reservoir beneath the wet area is confined and subject to a hydrostatic pressure.

In formulating a model for Circle Valley, the basin was divided into four basic hydrologic subunits; namely, the watershed, the cropland, the groundwater basin beneath the cropland, and the wet area. Because of time limitations, it was necessary to model the basin before the computer modifications described by Chapter IV had yet reached the stage where there were enough amplifiers available to simulate

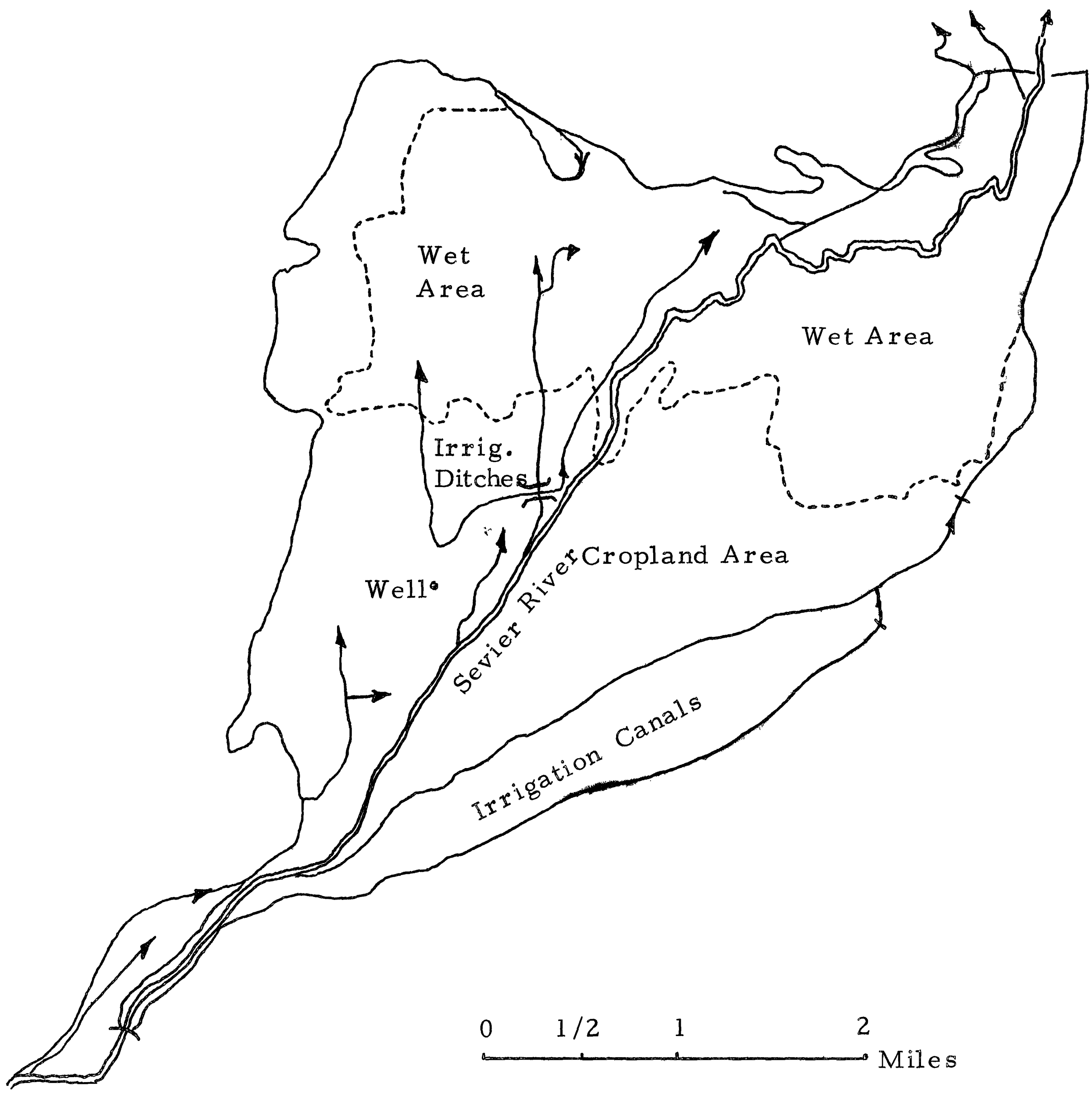

Figure 5.3. Agricultural area of Circle Valley.

the watershed area as more than a single zone. Computer equipment requirements are identical for each zone. Average values of input parameters, such as temperature, precipitation, radiation index, and soil type, were developed for the entire watershed.

Figure 5.4 is a hydrologic block flow diagram for Circle Valley. The four hydrologic subunits mentioned in the previous paragraph are shown by this diagram. Figure 5.5 is the analog flow diagram representing the simulation model of Circle Valley. This diagram represents a synthesis of the mathematical equations presented in Chapter III into the flow system depicted by figure 5.4.

Temperature and precipitation data are available from one U. S. Weather Bureau station within Circle Valley. This station is situated on the valley floor near the small town of Circleville. Because no meteorological data are available on the watershed, temperature and precipitation were lapsed from the valley station in accordance with the relationships of figure 3.2 and table 3.1 respectively. Interception losses were computed from equation 3.18 using a value of 0.4 for k_i and a canopy density of 0.5. Calculations were also based on the assumptions that only coniferous vegetation contributes to interception losses during the winter months, whereas during the summer period these losses occur on both coniferous and deciduous types. Monthly interception losses for the west facet of the watershed were estimated at 0.025 P_r and 0.030 P_r during the winter and summer

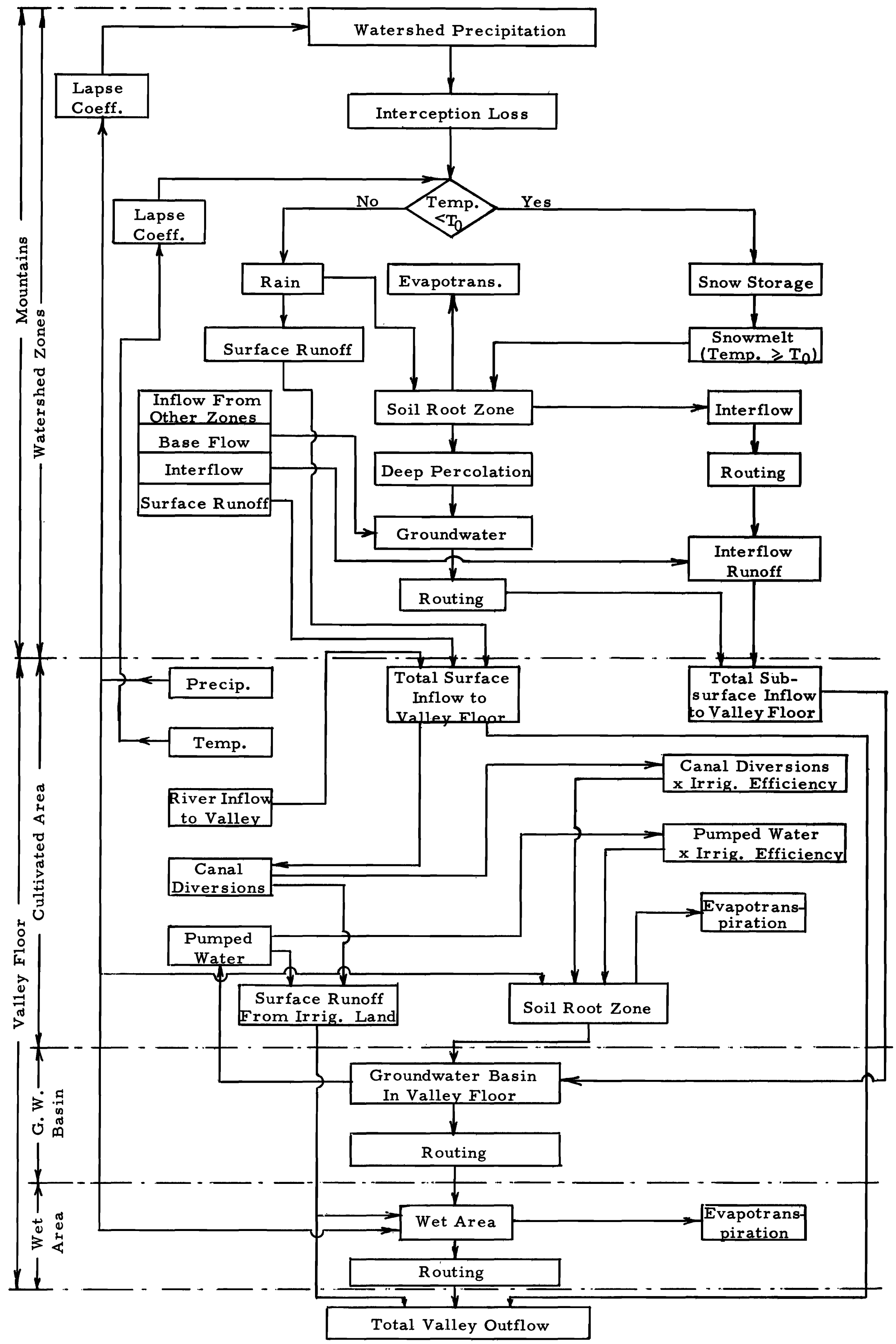

Figure 5.4. Hydrologic flow chart for the Circle Valley subbasin, Sevier River, Utah.

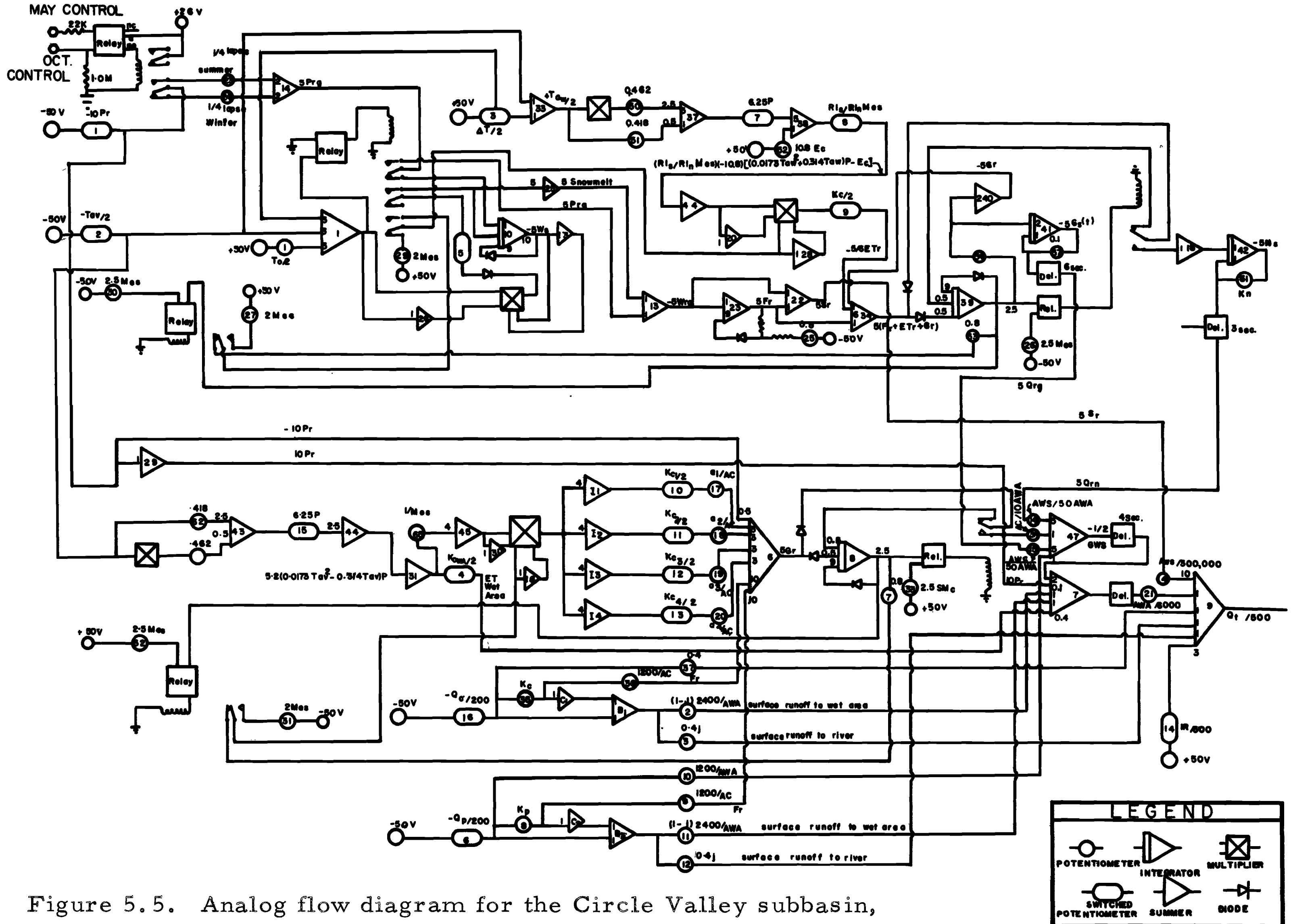

Figure 5.5. Analog flow diagram for the Circle Valley subbasin, Sevier River, Utah.

periods respectively. Corresponding estimates for the east facet were 0.060 P_r and 0.070 P_r respectively. Weighted on an area basis, monthly interception losses over the entire watershed were calculated as 0.044 P_r (winter) and 0.052 P_r (summer).

An estimate of monthly values of the radiation index applicable to the entire watershed was reached by first computing the radiation indexes for each of the two major facets into which the watershed had been divided. Since the area of each facet was approximately the same, composite values of the radiation index were obtained by a simple average of the corresponding monthly values for each of the two facets. The computations outlined in this paragraph are shown by figure B1 and table B1.

Other input values for Circle Valley are included within tables B2 and B3. Parameters which are applicable only to a particular year, such as temperature, precipitation, and flow measurements, are shown by table B4. It will be noted that the data within this table are for the calendar years 1962 and 1963.

The computed and observed mean monthly outflow values for the year 1962 are shown by figure 5.6 . This figure and all other graphs showing computer output in this chapter were plotted directly on the x-y variplotter which is connected to the analog computer. Plots of the accumulated outflow quantities occurring in 1962, both computed and observed, are shown by figure 5.7. For this year output values

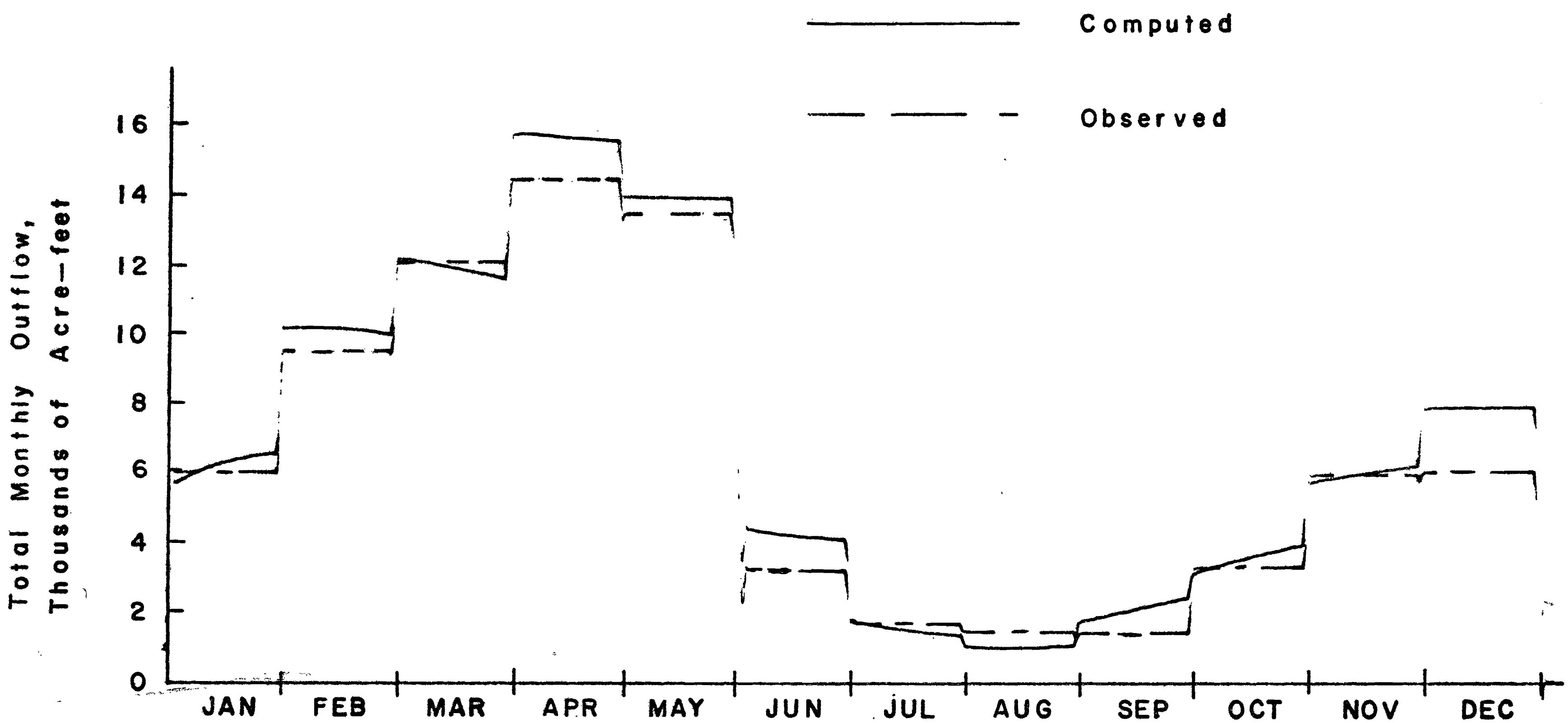

Figure 5.6. Comparison between computed and observed monthly outflow from Circle Valley during 1962.

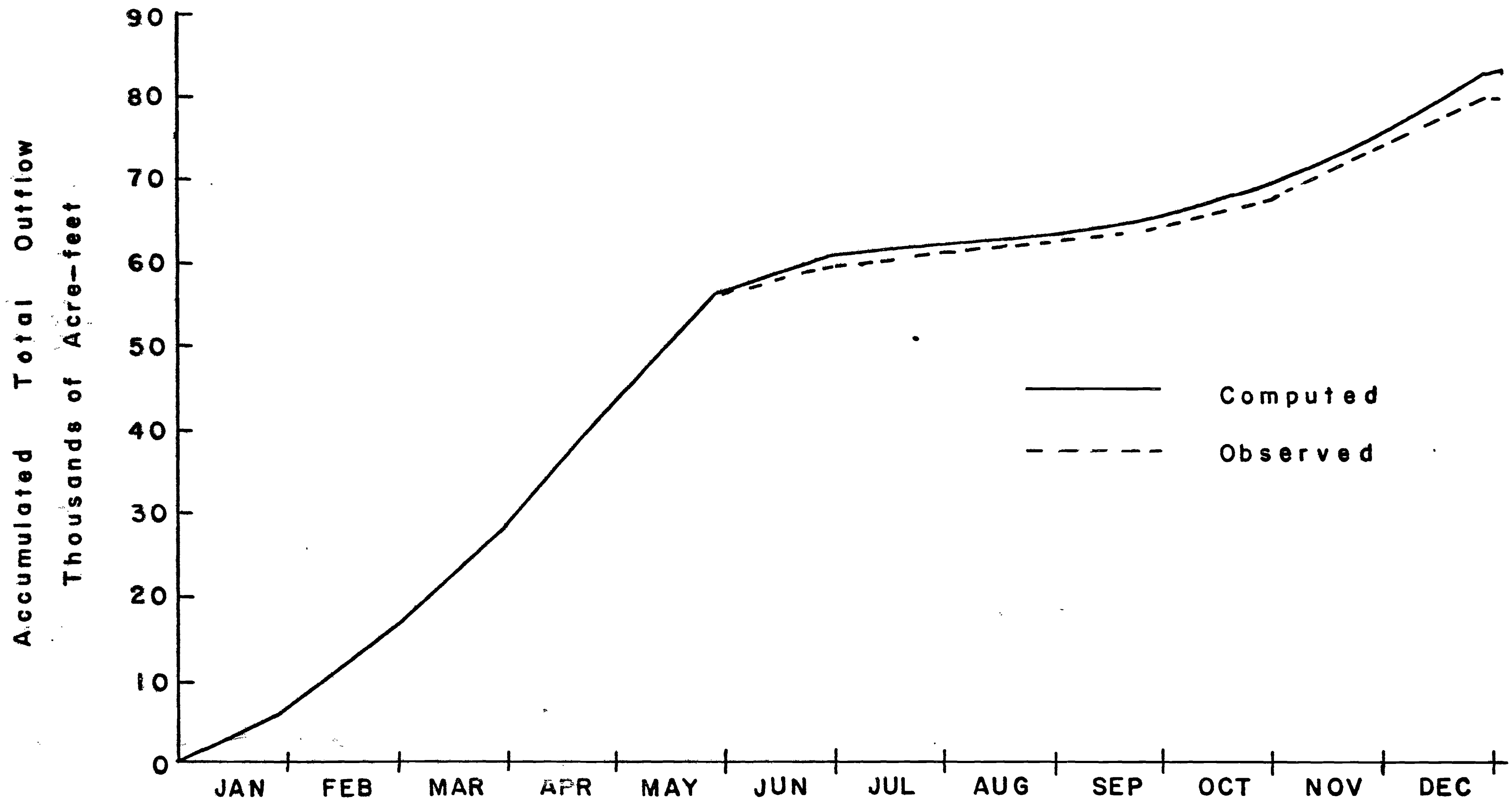

Figure 5.7. Comparison between computed and observed accumulated outflow from Circle Valley during 1962.

were also plotted at various intermediate points within the system. These plots are shown as figures B2 to B9 inclusive. Because of the absence of data, a quantitative evaluation of this model at intermediate points was not possible. The figures included within appendix B do, however, illustrate that the model simulated on a continuous basis the major hydrologic processes which occur within the prototype basin. Therefore, the operation of these processes could be examined in detail. In cases where sufficient data exists, qualitative evaluations of simulation accuracy is possible for individual processes within the system.

Conditions existing at the end of 1962, such as accumulated snow, soil moisture, and groundwater flow, were applied as initial or antecedent conditions for operation of the model over the twelve months of 1963. Monthly and accumulated plots of the computed and observed outflow values for that year are shown by figures 5.8 and 5.9 respectively. Values of computed snow storage equivalent on the watershed area during 1963 are shown by figure B10. It will be noted that during April there was no appreciable change in snow-water storage. This occurrence is explained on the basis that the mean temperature on the watershed for April was 41.2° F less a lapse of 5.9° F, or 35.3° F. Since the rate of snowmelt, as given by equation 3.22, is directly proportional to the difference $(T_a - T_0)$, a critical temperature, T_0, of 35° F yielded a negligible melt during this particular month. On the other hand, within the program precipitation during the month occurred in the form of rain.

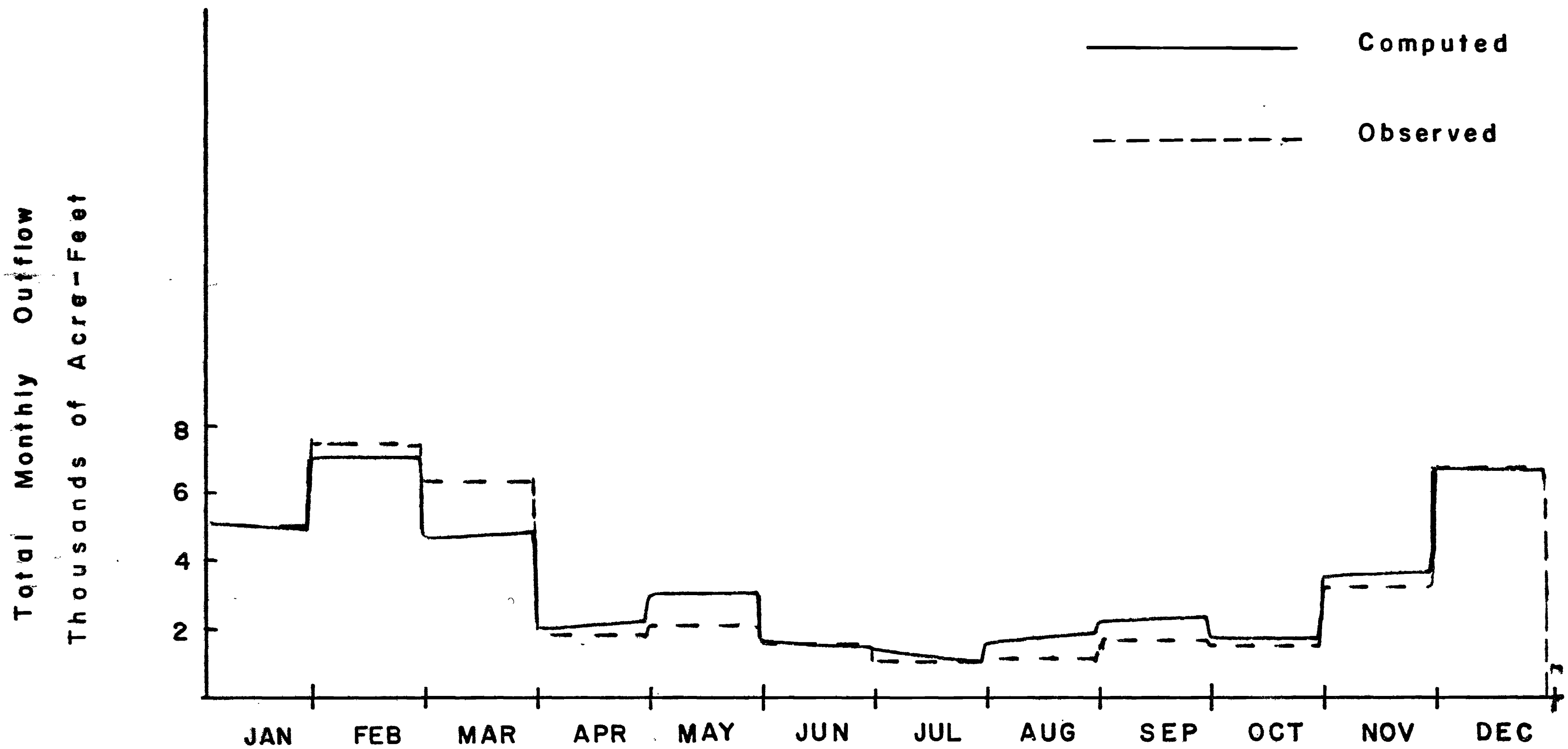

Figure 5.8. Comparison between computed and observed monthly outflow from Circle Valley during 1963.

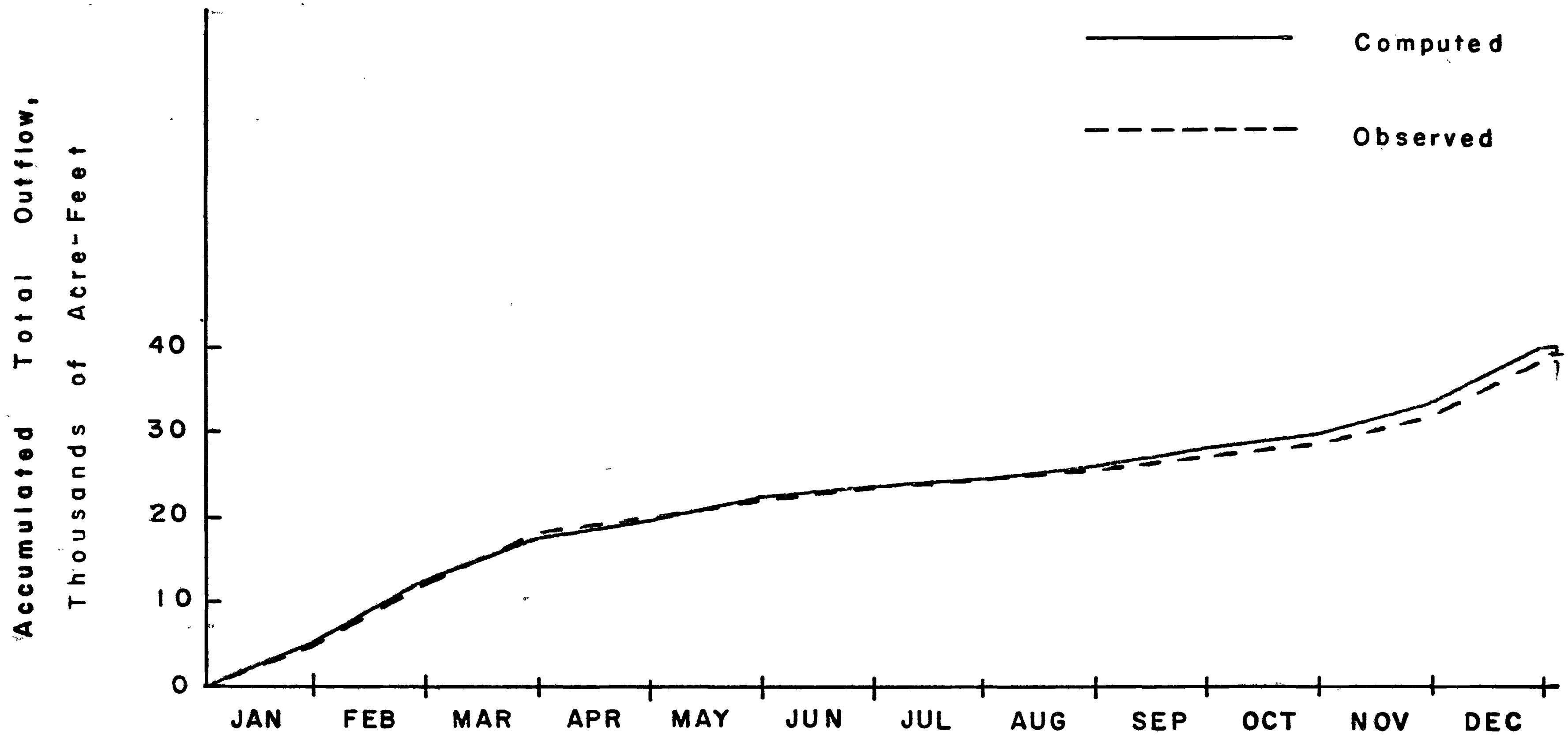

Figure 5.9. Comparison between computed and observed accumulated outflow from Circle Valley during 1963.

CHAPTER VI

SUMMARY AND CONCLUSIONS

In this report a working model of a complicated hydrologic system has been proposed. The basic components of the model are:

1. Fundamental and logical mathematical representations of the hydrologic processes.
2. An electronic analog computer which is capable of representing the individual processes and of synthesizing them into a complex system.

Electronic analog simulation of hydrologic systems has many practical applications in the areas of both research and project planning and management. As a research tool the computer is valuable in the process of investigating and improving mathematical relationships. In this respect, the computer is applied not only for its calculating potential, but also for its ability to yield optimum solutions. Simulation is also ideal for investigations of hydrologic sensitivity. Problems range from the influence of a single factor upon a particular process to the effects of an entire process, such as evapotranspiration, upon the system as a whole.

In many ways analog simulation can assist in planning and development work. Models can provide the designer with runoff estimates from the input of recorded precipitation data. In addition, simulated streamflow records from statistically generated input information enable the establishment of synthetic flow frequency distribution patterns.

In the area of water resource management, analog computer simulation will permit the rapid evaluation of the effects of various management alternatives upon the entire system. These alternatives might involve such variables as watershed treatment, including urbanization, the construction of a storage reservoir, or changes in irrigation practices within a basin.

The mathematical relationships presented in Chapter III were developed for application to areas where data are relatively sparse. For example, the basic input functions are temperature and precipitation. Parameters are included in the equations to provide for other variables such as those which are attributable to the sloping land surfaces, elevation differences, and often low available soil moisture values of a typical mountain watershed.

During this project an expansion of the capability of the analog computing equipment paralleled the improvements to the hydrologic equations. Capacity was increased through the addition of operational amplifiers and nonlinear components, and a patch panel was added to provide increased computer flexibility.

To test individual equations and to verify the model, a particular hydrologic unit was simulated. Flow records at the outlet of the subbasin provided data for qualitative verification of the model. Close agreement between computed and observed outflows was achieved on both a monthly and a total annual basis. For 1962 the computed accumulative outflow exceeded the observed by about 5 percent. Terminal conditions for 1962 were input as initial conditions for 1963 and outflow values computed. The accumulated outflow for this year exceeded the observed by less than 5 percent. Continued testing of this model will be undertaken through watershed simulation studies associated with other investigations.

In a research program of this nature certain constraints or boundary conditions limit the degree of achievement during any particular phase of the overall program. The most important of these limiting features are the extent to which research information and basic input data are available, the degree of accuracy established by the time and spatial increments adopted for the model, equipment limitations, and the necessary time limit imposed upon the investigation period.

Electronic analog simulation of hydrologic phenomena has been under active development at Utah State University for about three years. The development of this research program has followed the logical pattern of proceeding in stages to increasingly detailed modeling. The important underlying feature throughout the entire program has been that all of the separately described hydrologic processes and phenomena are interlinked into a total hydrologic system. Thus, for each model it was possible to evaluate the relative importance of the various hydrologic items, expose critical areas where data and perhaps theory were lacking, and establish guidelines for more fruitful and meaningful study in subsequent phases of the work. The first model, using monthly time increments, gave good results for interbasin effects. The second model developed under the project reported herein was designed for an investigation of in-basin problems, but still utilizing a large time increment. Under the third phase of this program a model is now being developed which will simulate the hydrologic processes over small geographic units and short periods of time. This model will involve many challenges not only in the mathematical representations of the hydrologic processes, but also in equipment requirements and modeling techniques.

Analog simulation of hydrologic systems has vast potential. For example, consideration is now being given at this institution to expanding the model of the physical system by superimposing the related dimensions of water quality and economics. Many other possibilities remain to be explored. However, present achievements at Utah State University have demonstrated the soundness and validity of this approach to hydrologic problems, and have provided a basis for future applications of analog models to the comprehensive flow systems encountered in the development and management of water resources.

SELECTED REFERENCES

(1) Anderson, Eric A., and Norman H. Crawford. The synthesis of continuous snowmelt runoff hydrographs on a digital computer. Department of Civil Engineering, Technical Report No. 36, Stanford University, Stanford, Calif. 1964.

(2) Bagley, Jay M., Robert B. Hickok, Duane G. Chadwick, Marvin J. Rosa, and D. L. Brakensiek. Report on feasibility of an electronic analog approach to Sevier River Basin investigations for water resources development and conservation planning. Engineering Experiment Station Report No. EC-51-g-1, Utah State University. 47 p. (Multi.) 1963.

(3) Bagley, Jay M., D. G. Chadwick, J. P. Riley, and R. Sampson. The development of an electronic analog device for hydrologic investigations and conservation planning in the Sevier River basin. Utah Water Research Laboratory, Utah State University, Manuscript in preparation.

(4) Blaney, Harry F., and Wayne D. Criddle. Determining water requirement in irrigated areas from climatological and irrigation data. SCS, USDA, Tech. Paper 96. 48 p. February 1950.

(5) Carpenter, Carl H., Gerald B. Robinson, Jr., and Louis J. Bjorklund. Selected hydrologic data, upper Sevier River Basin, Utah. USGS and Utah State Engineer, Basic-Data Report No. 8. 29 p. 1964.

(6) Carreker, John R. The relation of solar radiation to evapotranspiration from cotton. Journal of Geophysical Research, The American Geophysical Union. p. 4731-4741. July-December 1963.

(7) Crawford, N. H., and R. K. Linsley. The synthesis of continuous streamflow hydrographs on a digital computer. Department of Civil Engineering, Technical Report No. 12, Stanford University, Stanford, Calif. 1962.

(8) Crawford, N. H., and R. K. Linsley. Digital simulation in hydrology: Stanford watershed model iv. Department of Civil Engineering, Technical Report No. 39, Stanford University, Stanford, Calif. 1962.

(9) Criddle, Wayne D. Methods of computing consumptive use of water. Journal of Irrigation and Drainage Division, Proc. ASCE 84(IR 1):1-27. 1958.

(10) Criddle, Wayne D., Karl Harris, and Lyman S. Willardson. Consumptive use and water requirements for Utah. Office of the State Engineer, Tech. Pub. No. 8. (Revised) 47 p. 1962.

(11) Dalton, J. Experimental essays on the constitution of mixed gases; on the force of stream or vapor from waters and other liquids in different temperatures, both in a torricelliam of gases by heat. Mem. Manchester Lit. and Phil. Soc. 5:535-602. Illus. 1798.

(12) Frank, Ernest C., and Richard Lee. Potential solar beam irradiation on slopes: Tables for 30° to 50° latitude. U. S. Forest Service, Research Paper RM-18, Rocky Mountain Forest and Range Experiment Station, Fort Collins, Colorado. March 1966.

(13) Gardner, W. R., and C. F. Ehlig. The influence of soil water on transpiration by plants. Journal of Geophysical Research, The American Geophysical Union. p. 5719-5724. July-December 1963.

(14) Garstka, W. U., L. D. Love, B. C. Goodell, and F. A. Bertle. Factors affecting snowmelt and streamflow. A report on the 1946-53 cooperative snow investigations at the Fraser Experimental Forest, Fraser, Colorado. 1958.

(15) Harder, J. A., Lyle Mockros, and Ray Nishizaki. Flood control analogs. Hydraulic Laboratory, University of California, Water Resources Center Contribution No. 24. 40 p. (Multi.) 1960.

(16) Jensen, Marvin E., and Howard R. Haise. Estimating evapotranspiration from solar radiation. Journal of the Irrigation and Drainage Division, Proc. ASCE. p. 15-41. 1963.

(17) Johnson, W. M. The interception of rain and snow by a forest of young ponderosa pine. Trans. Amer. Geophysical Union, Part II, p. 566-569. 1942.

(18) Lane, Robert K. Estimating evaporation from insolation. Journal of the Hydraulics Division, Proc. ASCE. p. 33-41. 1964.

(19) Lee, Richard. Evaluation of solar beam irradiation as a climatic parameter of mountain watersheds. Hydrology Papers, No. 2, Colorado State University, Fort Collins, Colorado. 50 p. 1963.

(20) Linsley, Ray K., Jr., Max A. Kohler, and Joseph L. H. Paulhus. Hydrology for engineers. McGraw-Hill Book Company, Inc., New York. 340 p. 1958.

(21) List, Robert J. Smithsonian meteorological tables. Smithsonian Institution, Washington, D. C. 527 p. 1951.

(22) Lowry, R. L., and A. F. Johnson. Consumptive use of water for agriculture. Trans. ASCE 107:1243-1302.

(23) Morton, Fred I. Potential evaporation and river basin evaporation. Journal of the Hydraulics Division, Proc. ASCE. p. 67-97. 1965.

(24) Otoba, Kotaro, Kozi Shibatani, and Hiroshi Kuwata. Flood simulator for the River Kitakami. Simulation. p. 86-98. February 1965.

(25) Papadakis, J. Climatic tables for the world. Buenos Aires (Av. Cordoba 4564), Argentina. 1961.

(26) Pastil, Uttamrao. A study of the relationship between consumptive use of water and evaporation. Unpublished M.S. thesis, Utah State University Library, Logan, Utah. 1954.

(27) Penman, H. L. Natural evaporation from open water, bare soil, and grass. Proc. Royal Society of London, Series A. 193:120-146. 1958.

(28) Phelan, John T. Estimating monthly "k" values for the Blaney-Criddle formula. Prepared for presentation at the ARS-SCS Workshop on Consumptive Use, Phoenix, Arizona, March 6-8. 11 p. (Mimeo.) 1962.

(29) Quackenbush, Tyler H., and John T. Phelan. Irrigation water requirements of lawns. Journal of the Irrigation and Drainage Division, Proc. ASCE. p. 11-19. 1965.

(30) Reisenauer, A. E. Methods for solving problems of multidimensional, partially saturated steady flow in soils. Journal of Geophysical Research, The American Geophysical Union. p. 5725-5733. July-December 1963.

(31) Shaw, Sir Napier. Manual of meteorology, Vol. 2. Cambridge University Press, Cambridge, Massachusetts. 470 p. 1936.

(42) U. S. Weather Bureau. U. S. climatological data, material summary. Vol. 1 to Vol. 14. 1950 to 1963.

(43) U. S. Weather Bureau. Three charts showing normal precipitation for the State of Utah for the three periods October to April, May to September, and the full year based upon the period of record 1931 to 1960. Office of Utah State Engineer, Utah Water and Power Board, and SCS, USDA. 1963.

(44) U. S. Weather Bureau. Mean precipitable water in the United States. U. S. Weather Bureau Tech. Paper 10. 1949.

(45) Veihmeyer, F. J. Some factors affecting the irrigation requirements of deciduous orchards. Hilgardia 2:125-291. 1927.

(46) Veihmeyer, F. J., W. O. Pruitt, and W. D. McMillan. Soil moisture as a factor in evapotranspiration equations. Ann. Mtg. of ASAE Paper 60-202, Irrigation Department, University of California, Davis, Calif. 1960.

(47) West, A. J. Snow evaporation and condensation. Proc. Western Snow Conference. p. 66-74. 1959.

(48) Willardson, Lyman S., and Wendell L. Pope. Separation of evapotranspiration and deep percolation. Journal of the Irrigation and Drainage Division, Proc. ASCE 89(IR 3):77-88. 1963.

(49) Williams, G. P. Evaporation from snow covers in eastern Canada. Natl. Res. Coun., Div. Bldg. Res., Res. Paper 73. 1959.

(50) Williams, G. P. Evaporation from water, snow, and ice. Proc. Hydrology Symposium, No. 2, Evaporation. Natl. Res. Coun., Toronto, Canada. p. 31-54. 1961.

(51) Woods, Philip C., and Gerald T. Orlob. The Lost River system, a water quality management investigation. Sanitary Engineering Research Laboratory, University of California, Berkeley, Calif. 54 p. (Multi.) 1963.

(52) Young, Arthur A., and Harry F. Blaney. Use of water by native vegetation. Calif. Dept. of Public Works, Division of Water Resources, Bul. 50. 160 p. 1942.

APPENDIXES

APPENDIX A

Program for Computation of Radiation Index Values

Radiation Indexes

```
      DIMENSION DMON(50), DAY(50), DECL(50), AIP(50), SRISE(50), RI(50),
     1DD(50), TM(50)
       READ 1, AL, H, XS, XB, N
 1     FORMAT (4F8.0, I3)
      READ 2, (DMON(I), DAY(I), I= 1,N)
 2    FORMAT (2F5.0)
      XL = (XB - XS)/10.0
       CALL PLOT (101, XS, XB, XL, 10.0, 0.0, 180.0, 6.0, 30.0)
      PUNCH 3, AL, H
 3    FORMAT (10H LATITUDE-, 3X, F5.0, 2H N, 8X, 9H AZIMUTH-, 3X,
     1F5.0, 5H DEG.//)
      PUNCH 4
 4    FORMAT (19X, 5H MON.,1X, 4H DAY, 5X, 6H SRISE, 6X, 5H SSET,
     18X, 3H IO, 8X, 3H RI)
      V = 1.5708/90.0
      AL = AL*V
      H = H*V
      W = V/4.0
      DO 8 L = 1,N
      IF (DMON(L) - 7.0) 10,10,13
10    K = DMON(L)/2.0
      C = K
      IF (DMON(L) - 2.0) 11,11,12
11    TDAY = (DMON(L) - 1.0)*30.0 + C + DAY(L)
      AN = (80.0 - TDAY)*V
      S = -1.0
      TM(L) = TDAY + 10.0
      GO TO 22
12    TDAY = (DMON(L) - 1.0)*30.0 + C - 2.0 + DAY(L)
      GO TO 14
13    K = (DMON(L) + 1.0)/2.0
      C = K
      TDAY = (DMON(L) - 1.0)*30.0 + C - 2.0 + DAY(L)
14    B = TDAY - 80.0
      IF (ABSF(B) - 90.0) 15,15,16
15    AN = ABSF(B)*V
      TM(L) = TDAY + 10.0
      GO TO 21
16    B = 266.0 - TDAY
      IF (ABSF(B) - 90.0) 17,17,18
17    AN = ABSF(B)*V
      TM(L) = 356.0 - TDAY
      GO TO 21
18    B = 365.0 - TDAY
      IF (B - 10.0) 19,19,20
19     AN = (B + 80.0)*V
       TM(L) = TDAY - 356.0
       S = -1.0
       GO TO 22
20     AN = 90.0*V
       TM(L) = 180.0
21     IF(B) 27, 25, 27
25     DECL(L) = 0.0
```

Radiation Indexes (Continued)

```
      GO TO 26
   27 S = B/ABSF(B)
   22 DECL(L) = S*23.5*SINF(AN)*V
   26 IF (TDAY - 360.0) 24,24,23
   23 TDAY = 360.0
   24 AIP(L) = 2.0 + 0.07*COSF(TDAY*V)
      DE = DECL(L)
      DD(L) = TM(L)
      C = -SINF(AL)*SINF(DE)/ (COSF(AL)*COSF(DE))
      IF (C) 31,34,32
   34 SRISE(L) =-360.0
      GO TO 8
   31 SRISE(L) = -4.0*(3.1416 - ATANF(ABSF(SQRTF(1.0-C**2)/C)))/V
      GO TO 8
   32 SRISE(L) = -4.0*ATANF(SQRTF(1.0 - C**2)/C)/V
    8 CONTINUE
      NA = N-1
      DO 80 J = 1,NA
      K = J+1
      DO 80 JA = K, N
      IF (DD(J) - DD(JA)) 80,80,81
   81 TEMP = DD(JA)
      DD(JA) = DD(J)
      DD(J) = TEMP
   80 CONTINUE
      DO 140 J = 1,N
      DO 120 JA = 1,N
      IF (DD(J) - TM(JA)) 120,130,120
  120 CONTINUE
  130 DD(J) = JA
  140 CONTINUE
      TU = XS - 6.0
      CALL PLOT (90, TU, 0.0)
      CALL PLOT (90, TU, 180.0)
      DO 100 IA = 1,12,2
      Y = TM(IA)
  100 CALL PLOT (9, TU, Y)
      TL = XS - 10.0
      CALL PLOT (90, TL, 0.0)
      CALL PLOT (90, TL, 180.0)
      DO 110 IA = 13,24,2
      Y = TM(IA)
  110 CALL PLOT (9, TL, Y)
      DO 5 I = 10,110,10
      DI = I - 10
      PUNCH 33, DI
   33 FORMAT (7H SLOPE-, 1X, F5.0, 4H PCT)
      P = ATANF(DI/100.0)
      AR = SINF(H)*SINF(P)/(COSF(P)*COSF(AL) - COSF(H)*SINF(P)*
     1SINF(AL))
      IF (AR) 6,7,7
    6 DT = 3.1416 - ATANF(ABSF(AR))
      GO TO 9
    7 DT = ATANF(AR)
```

Radiation indexes (Continued)

```
 9 C = SINF(P)*COSF(H)*COSF(AL) + COSF(P)*SINF(AL)
   ALP = ATANF(C/SQRTF(1.0-C**2))
   DO 60 L = 1,N
   DE = DECL(L)
   C = -SINF(ALP)*SINF(DE)/(COSF(ALP)*COSF(DE))
   IF (C) 36,35,37
35 SSET = (4.0*1.5708 - 4.0*DT)/V
   GO TO 40
36 SSET = (4.0*(3.1416 - ATANF(ABSF(SQRTF(1.0-C**2)/C)))-4.0*DT)/V
   GO TO 40
37 SSET = (4.0*ATANF(SQRTF(1.0 - C**2)/C) - 4.0*DT)/V
40 AIQ = AIP(L)*(COSF(DE)*COSF(ALP)*(SINF(W*(-SRISE(L)-4.0*DT/V)) +
  1SINF(W*(SSET+4.0*DT/V)))/W + (-SRISE(L)+SSET)*SINF(DE)*SINF(ALP))
   RI(L) = 50.0*AIQ/(-SRISE(L)*AIP(L)*COSF(P))
   PUNCH 50, DMON(L), DAY(L), SRISE(L), SSET    , AIQ, RI(L)
50 FORMAT (20X, F4.0, F5.0, 2X, 4F11.3)
60 CONTINUE
   DO 90 JB = 1,N
   KB = DD(JB)
90 CALL PLOT (90, RI(KB), TM(KB))
   CALL PLOT (99)
 5 CONTINUE
   END
```

Sample of Output from Radiation Index Program

C C

LATITUDE- 40. N AZIMUTH- 45. DEG.

	MON.	DAY	SRISE	SSET	IO	RI
SLOPE- 0. PCT						
	1.	1.	-276.246	276.246	336.510	29.424
	1.	15.	-283.622	283.622	365.366	31.152
	2.	1.	-298.771	298.771	427.918	34.774
	2.	15.	-314.810	314.810	498.422	38.641
	3.	1.	-332.779	332.779	580.812	42.882
	3.	21.	-360.000	360.000	706.523	48.767
	4.	1.	-375.092	375.092	773.514	51.586
	4.	15.	-393.795	393.795	851.073	54.524
	5.	1.	-413.519	413.519	924.298	56.905
	5.	15.	-428.158	428.158	972.162	58.204
	6.	1.	-440.726	440.726	1008.371	59.023
	6.	22.	-445.594	445.594	1019.758	59.272
	7.	1.	-445.043	445.043	1017.791	59.246
	7.	15.	-439.613	439.613	1001.923	58.961
	8.	1.	-426.267	426.267	960.878	58.058
	8.	15.	-411.196	411.196	909.748	56.663
	9.	1.	-389.867	389.867	828.597	53.961
	9.	23.	-360.000	360.000	700.540	48.767
	10.	1.	-349.005	349.005	650.695	46.497
	10.	15.	-330.132	330.132	564.229	42.270
	11.	1.	-308.803	308.803	468.670	37.195
	11.	15.	-293.732	293.732	404.744	33.561
	12.	1.	-280.982	280.982	354.025	30.530
	12.	22.	-274.405	274.405	329.394	28.997
SLOPE- 10. PCT						
	1.	1.	-276.246	240.776	277.322	24.369
	1.	15.	-283.622	249.420	306.197	26.237

Sample of Output from Radiation Index Program (Continued)

2.	1.	-298.771	267.070	369.607	30.185
2.	15.	-314.810	285.634	442.211	34.454
3.	1.	-332.779	306.333	528.449	39.211
3.	21.	-360.000	337.582	662.892	45.984
4.	1.	-375.092	354.899	736.045	49.332
4.	15.	-393.795	376.395	822.241	52.939
5.	1.	-413.519	399.158	905.390	56.019
5.	15.	-428.158	416.152	960.910	57.817
6.	1.	-440.726	430.836	1003.754	59.046
6.	22.	-445.594	436.553	1017.708	59.448
7.	1.	-445.043	435.905	1015.453	59.404
7.	15.	-439.613	429.531	996.737	58.948
8.	1.	-426.267	413.951	948.699	57.608
8.	15.	-411.196	396.470	889.783	55.696
9.	1.	-389.867	371.875	798.125	52.235
9.	23.	-360.000	337.582	657.279	45.984
10.	1.	-349.005	324.968	603.533	43.342
10.	15.	-330.132	303.289	511.602	38.518
11.	1.	-308.803	278.694	411.879	32.851
11.	15.	-293.732	261.213	346.300	28.858
12.	1.	-280.982	246.331	294.968	25.564
12.	22.	-274.405	238.611	270.257	23.910

SLOPE- 20. PCT

1.	1.	-276.246	202.159	224.012	19.975
1.	15.	-283.622	212.197	252.299	21.937
2.	1.	-298.771	232.540	315.244	26.125
2.	15.	-314.810	253.766	388.453	30.712
3.	1.	-332.779	277.296	476.780	35.899
3.	21.	-360.000	312.677	617.216	43.447
4.	1.	-375.092	332.272	695.035	47.270

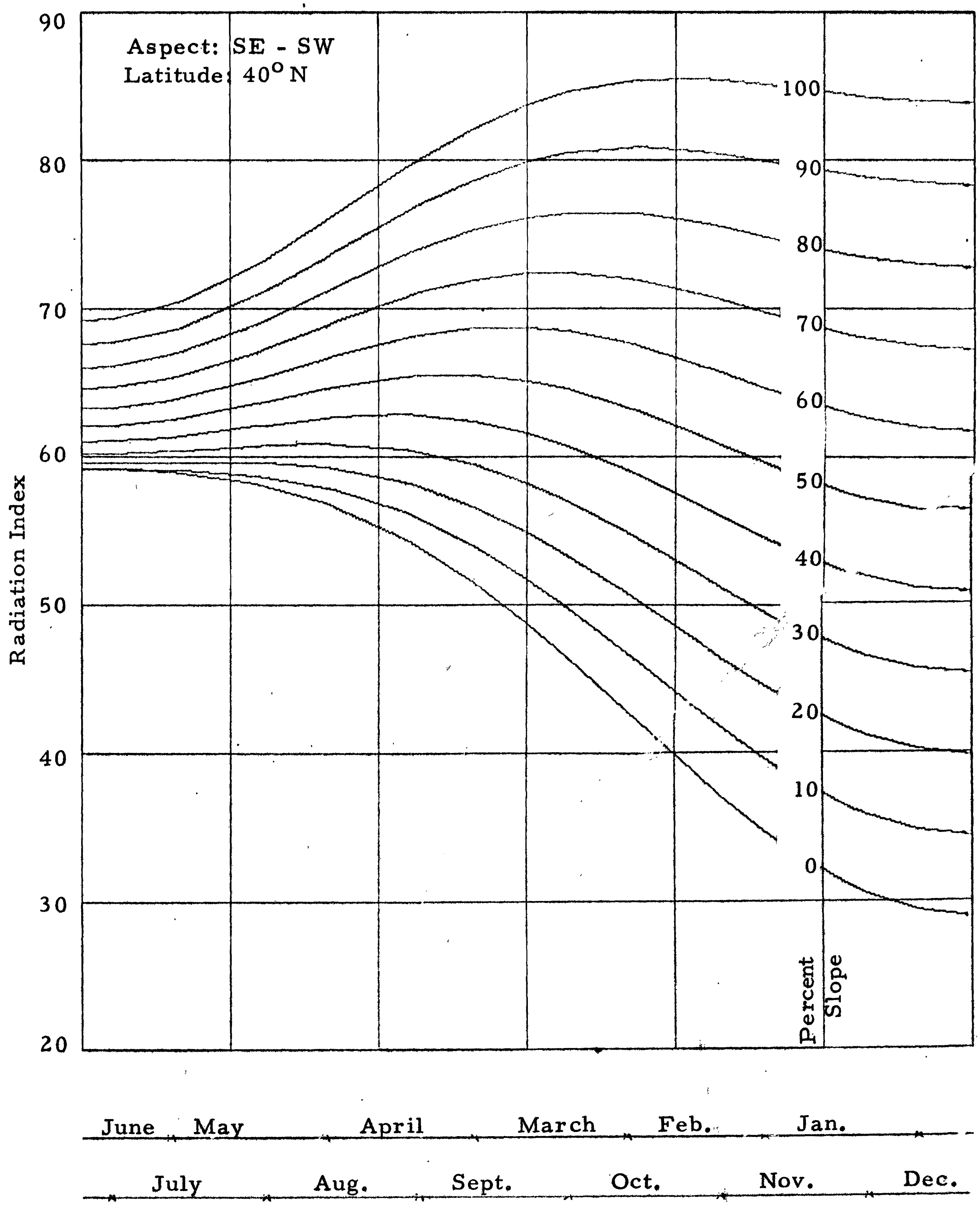

Figure A1. Radiation index values as a function of slope inclination and time of year.

APPENDIX B

Hydrologic Data for Circle Valley Model

Table B1. Average radiation index values for the Circle Valley watershed.

No.	Month	Radiation Indexes				Ratio
		S.E. Slope 60%	N.W. Slope 60%	Avg. for the S.E. & N.W. Slopes	Horiz. Surface	RI_s/RI_h col. 5 by col. 6
1	January	63.0	11.0	37.0	31.0	1.16
2	February	66.0	22.0	44.0	38.0	1.16
3	March	68.5	35.0	51.8	47.5	1.09
4	April	68.0	48.0	58.0	55.0	1.06
5	May	66.0	57.0	61.5	58.0	1.06
6	June	63.0	61.0	62.0	59.0	1.05
7	July	64.0	58.0	61.0	58.5	1.04
8	August	67.0	52.0	59.5	56.0	1.06
9	September	69.0	39.0	54.0	50.0	1.08
10	October	68.0	24.0	46.0	41.5	1.11
11	November	63.0	14.0	38.5	33.0	1.17
12	December	62.0	9.0	35.5	29.0	1.22

Table B2. Constant input values for the Circle Valley subbasin.

Symbol	Description	Value
E_c	elevation correction factor applied in the computation of evapotranspiration	0.081"/mo./1000'
j	proportion of irrigation surface runoff returning directly to the river	0.50
k_b	a constant applied in the computation of the rate of baseflow from a watershed	0.10
k_g	a constant applied in the computation of deep percolation rate	0.10
k_n	a constant applied in the computation of interflow rate	0.40
k_s	a constant applied in the computation of snowmelt rate	0.10
k_c	a surface irrigation efficiency factor for canal diversions	0.40
k_p	a surface irrigation efficiency factor for pump diversions	0.40
M_{cs}	available soil moisture storage capacity--watershed cultivated area	6" 10"
M_{es}	a limiting value of available soil moisture applied in the computation of evapotranspiration--watershed cultivated area	3" 4"

Table B3. Constant monthly input values for the Circle Valley subbasin.

Month	Temp. Lapse ^{o}F		Percent Daylight Hours		Radiation for ET ($RI_s/RI_h\ M_{es}$)		Radiation for Snowmelt $(100/15)\ k_s\ RI_s/RI_h$		Watershed Coef.	
	Actual Value	Volts[1] ($0.5\Delta T$)	Actual Value	Volts (6.25 PDH)	Actual Value	Volts	Actual	Volts	Actual	Volts ($0.5\ k_c$)
1	3.64	1.82	6.86	21.4	0.386	19.30	0.773	38.6	0.48	12.00
2	4.76	2.38	6.79	21.2	0.386	19.30	0.773	38.6	0.56	14.25
3	5.60	2.80	8.34	26.1	0.363	18.15	0.726	36.3	0.72	18.25
4	5.88	2.94	8.90	27.8	0.353	17.65	0.707	35.4	0.84	21.25
5	6.16	3.08	9.92	30.9	0.353	17.65	0.707	35.4	0.90	22.50
6	6.16	3.08	9.66	31.1	0.350	17.50	0.700	35.0	0.92	23.00
7	6.16	3.08	10.11	31.6	0.346	17.30	0.694	34.7	0.92	23.00
8	6.16	3.08	9.48	29.6	0.353	17.65	0.707	35.4	0.92	22.75
9	5.88	2.94	8.38	26.2	0.360	18.00	0.720	36.0	0.88	21.75
10	5.60	2.80	7.80	24.3	0.370	18.50	0.740	37.0	0.80	20.00
11	4.20	2.10	6.81	21.2	0.390	19.50	0.780	39.0	0.68	16.75
12	3.08	1.54	6.65	23.5	0.406	20.30	0.813	40.6	0.56	13.75

Month	Grain Coeff.		Potato Coeff.		Corn Coeff.		Alfalfa Coeff.		Wet Area Coeff.	
	Actual	Volts ($0.5\ k_c$)	Actual	Volts ($0.5\ k_c$)	Actual	Volts ($0.5\ k_c$)	Actual	Volts ($0.5\ k_c$)	Actual	Volts ($0.5\ k_c$)
1	0.25	6.25	0.25	6.25	0.25	6.25	0.68	17.00	0.70	17.5
2	0.25	6.25	0.25	6.25	0.25	6.25	0.80	19.75	0.70	17.5
3	0.25	6.25	0.25	6.25	0.25	6.25	0.88	22.25	0.75	18.6
4	0.26	6.50	0.25	6.25	0.25	6.25	1.00	24.75	0.81	20.3
5	0.50	12.50	0.25	6.25	0.26	6.50	1.08	27.00	0.89	22.3
6	1.54	38.50	0.38	9.50	0.60	15.00	1.12	27.75	1.02	25.5
7	1.12	28.25	0.90	22.50	1.28	32.25	1.10	27.50	1.18	29.5
8	0.25	6.25	1.32	32.75	1.08	27.00	1.08	27.00	1.28	32.0
9	0.25	6.25	1.32	33.00	0.42	10.50	1.00	25.25	1.29	32.2
10	0.25	6.25	0.25	6.25	0.25	6.25	0.92	23.00	1.19	29.7
11	0.25	6.25	0.25	6.25	0.25	6.25	0.80	20.25	1.04	26.0
12	0.25	6.25	0.25	6.25	0.25	6.25	0.68	17.25	0.86	21.5

[1] The computer reference voltage is 50 volts.

Table B4. Variable monthly input values for the Circle Valley subbasin for 1962 and 1963.

1962 Month	Precipitation (Inches/Month) Actual Value	Precipitation (Inches/Month) Volts[1] 10 P	Valley Temp. (°F) Actual Value	Valley Temp. (°F) Volts 0.5 T	Canal Div. (A-F/Month) Actual Value	Canal Div. (A-F/Month) Volts $0.005Q_c$	Pumped Div. (A-F/Month) Actual Value	Pumped Div. (A-F/Month) Volts $0.005Q_p$	River Inflow (A-F/Month) Actual Value	River Inflow (A-F/Month) Volts 0.002IR
1	0.75	7.5	22.2	11.1	320	1.60	---		5060	10.12
2	0.86	8.6	31.7	15.8	480	2.40	---		8690	17.38
3	0.70	7.0	34.6	17.3	590	2.95	---		11030	22.06
4	1.25	12.5	50.7	25.4	5240	26.20	---		18370	36.74
5	0.72	7.2	53.3	26.6	7410	37.05	---		18290	36.58
6	0.54	5.4	62.5	31.2	5360	26.80	---		7270	14.54
7	0.30	3.0	69.2	34.6	2890	14.45	---		3230	6.46
8	0.12	1.2	68.1	34.0	2500	12.50	31	0.155	2640	5.28
9	0.85	8.5	61.3	30.6	3390	16.95	188	0.940	3780	7.56
10	0.37	3.7	51.7	25.8	4510	22.55	166	0.830	5270	10.54
11	0.12	1.2	40.3	20.2	3390	16.95	---		6330	12.66
12	0.23	2.3	29.8	14.9	750	3.75	---		6210	12.42
1963										
1	0.34	3.4	24.0	12.0	0	0	---		4650	9.30
2	0.82	8.2	37.1	18.6	440	2.20	---		7100	14.20
3	0.32	3.2	36.3	18.2	2431	12.16	---		6120	12.24
4	0.74	7.4	41.2	20.6	3037	15.18	---		3580	7.16
5	0.11	1.1	58.2	29.1	4504	22.52	189	0.95	5350	10.70
6	0.74	7.4	60.0	30.0	1677	8.38	188	0.94	1820	3.64
7	0.46	4.6	70.8	35.4	1423	7.12	204	1.02	1600	3.20
8	3.43	34.3	67.6	33.8	2404	12.02	163	0.82	2710	5.42
9	1.31	13.1	61.8	30.9	3234	16.17	101	0.50	3780	7.56
10	0.49	4.9	54.2	27.1	2446	12.23	---		2650	5.30
11	0.62	6.2	38.5	19.2	2280	11.40	---		4430	8.86
12	0.15	1.5	25.9	13.0	450	2.25	---		6210	12.42

[1] The computer reference voltage is 50 volts.

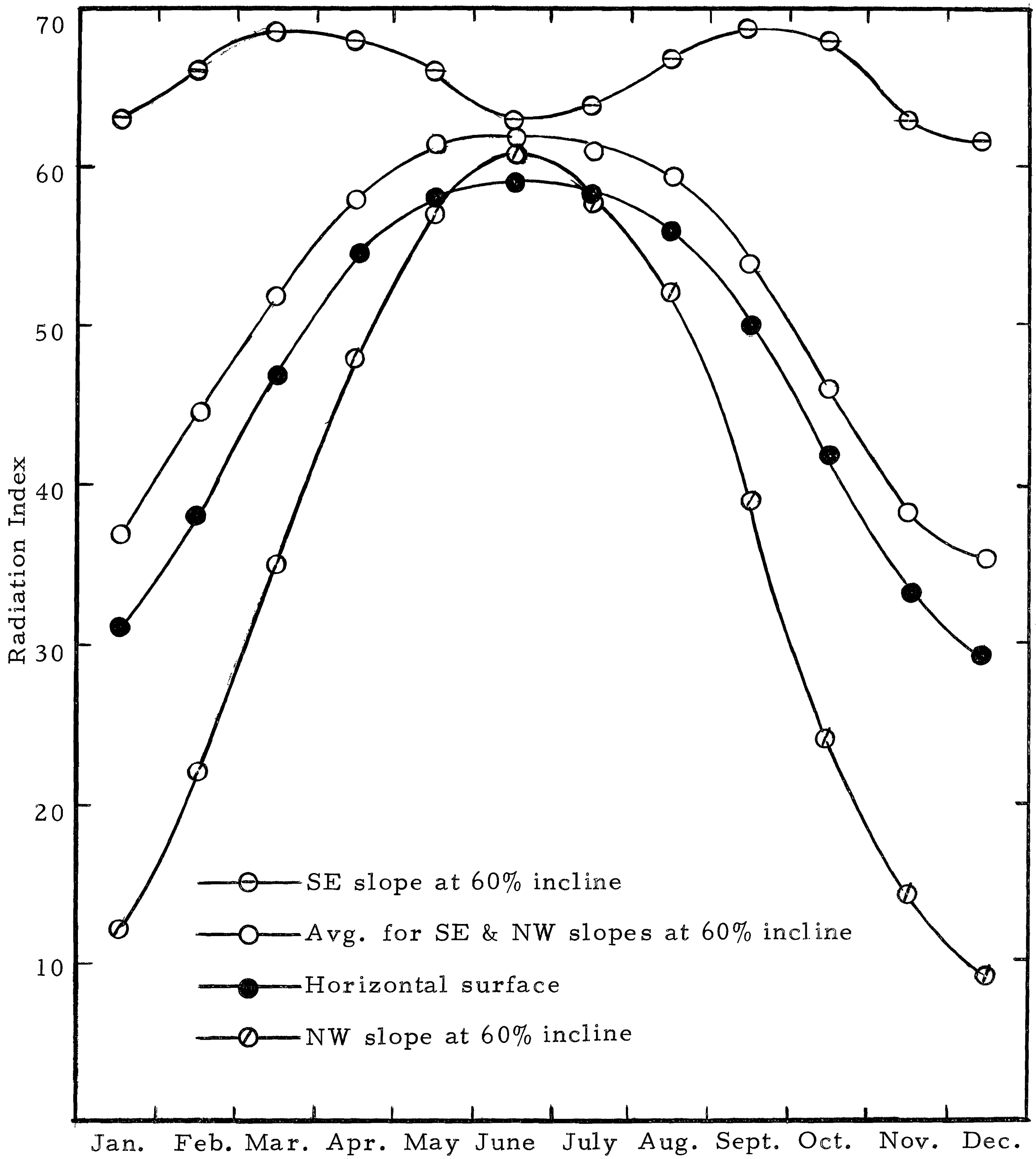

Figure B1. An average radiation index curve for the Circle Valley watershed.

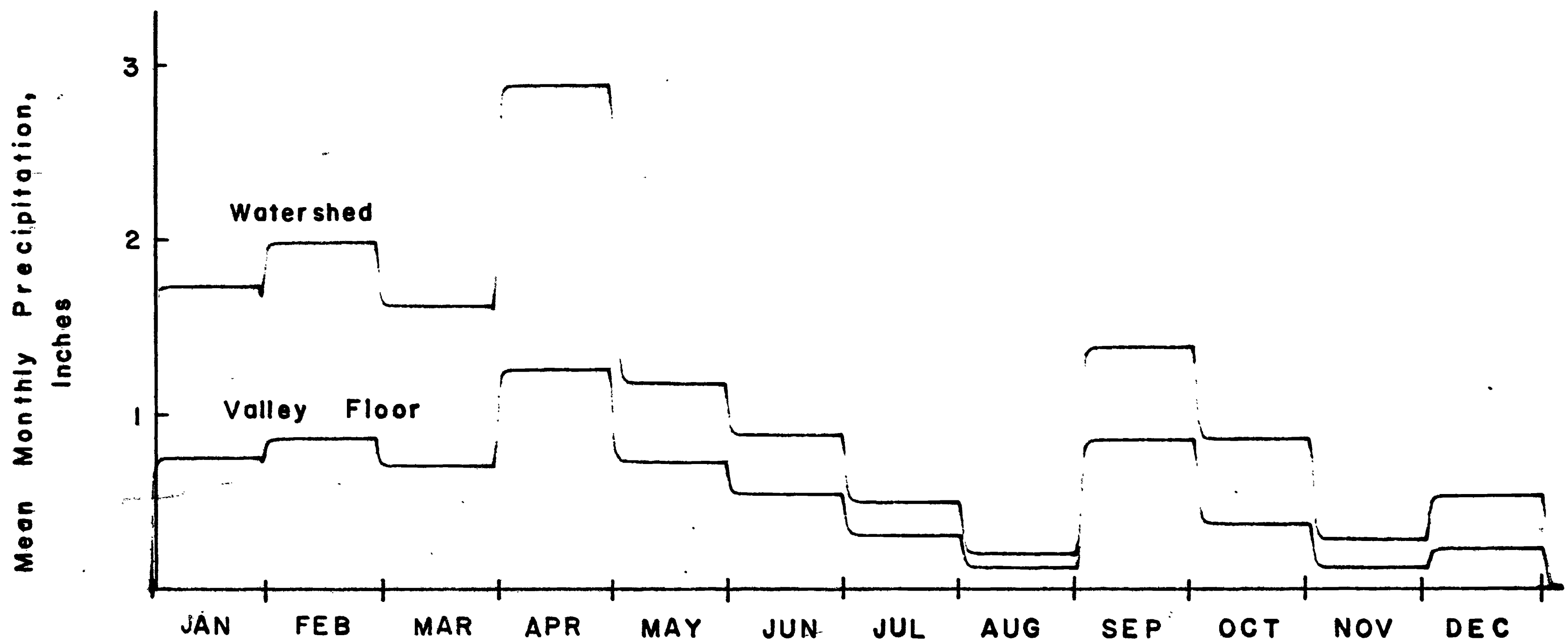

Figure B2. Mean monthly precipitation rates for the valley floor (observed) and the watershed area (computed), Circle Valley, 1962.

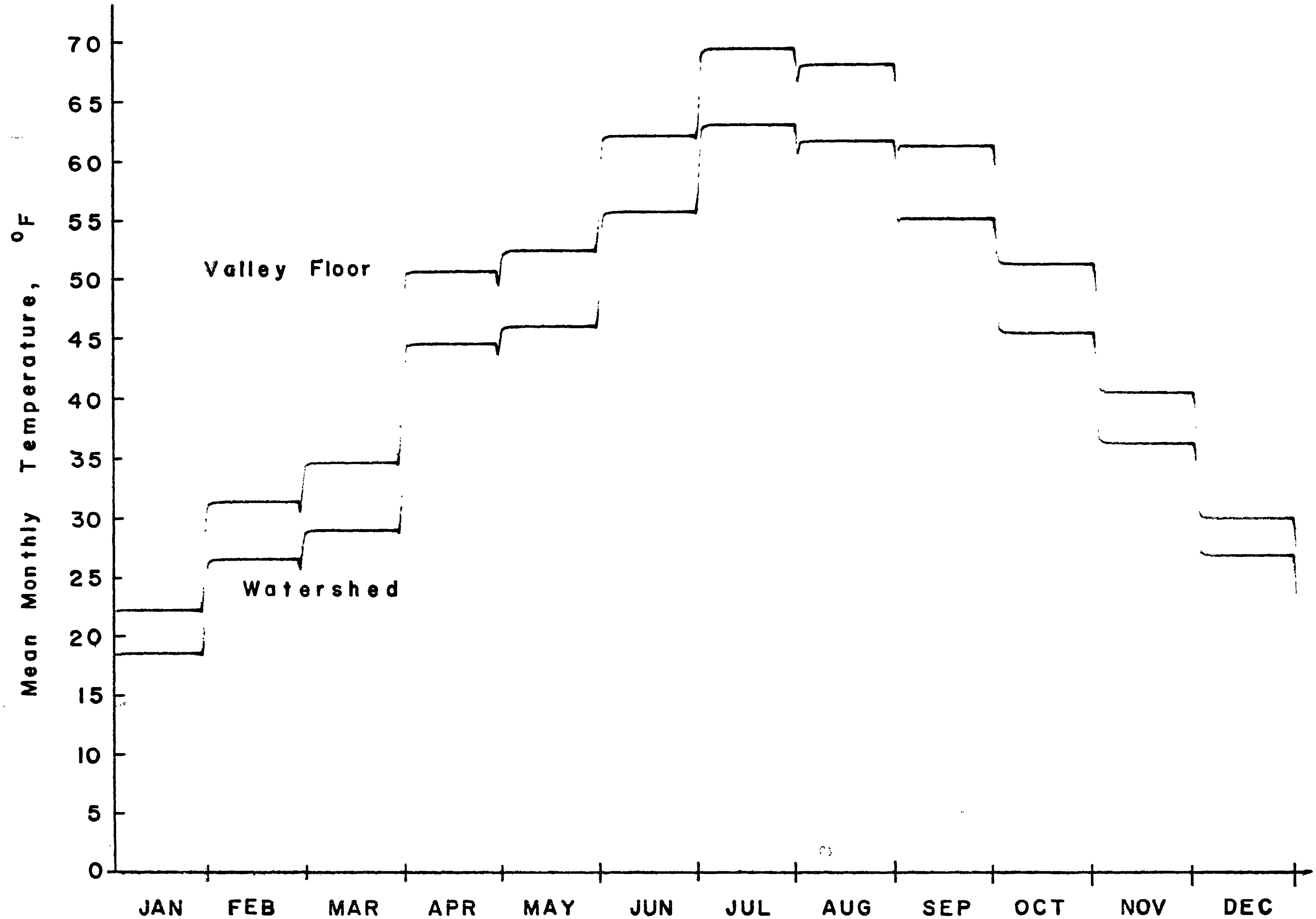

Figure B3. Mean monthly temperature for the valley floor (observed) and the watershed area (computed), Circle Valley, 1962.

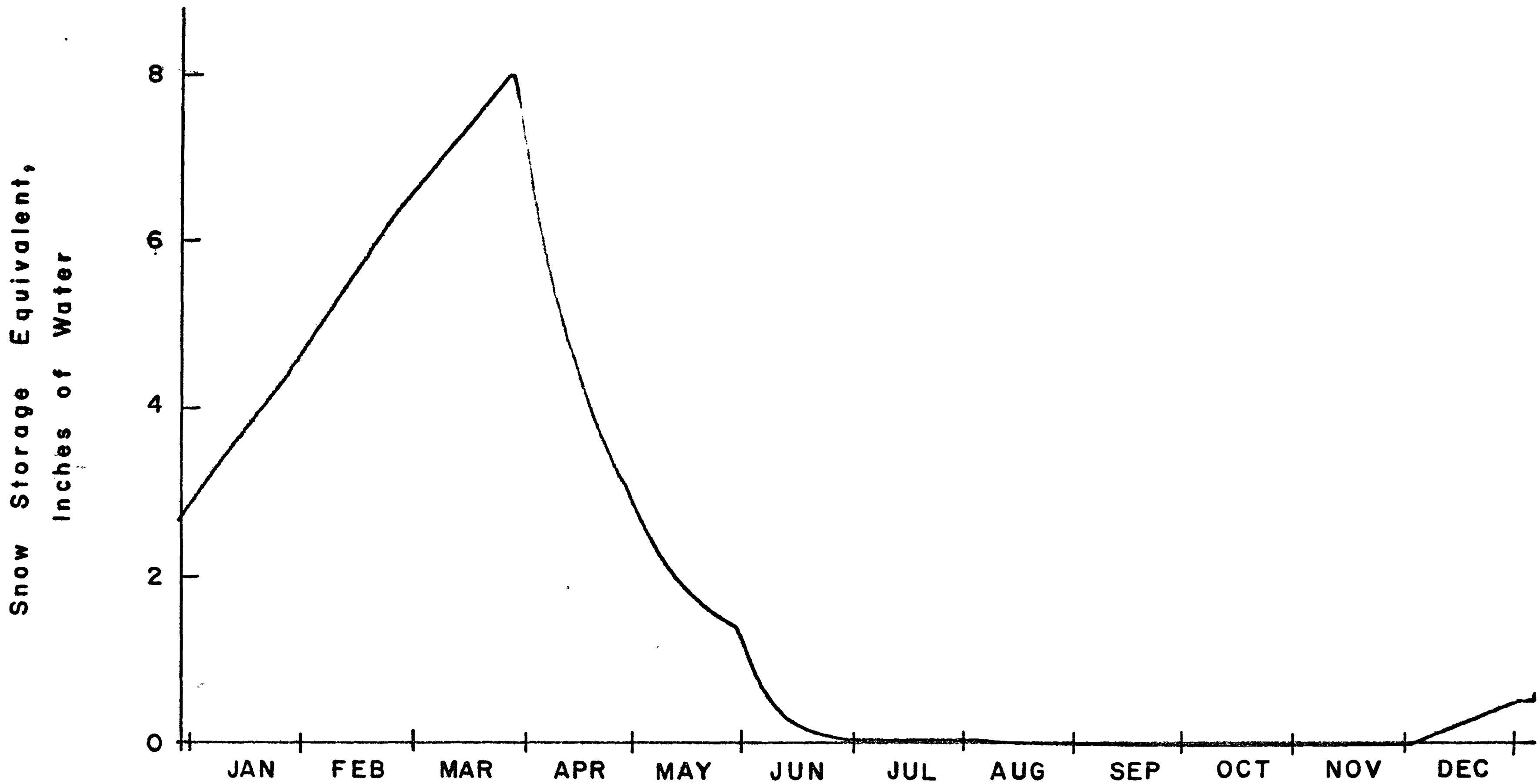

Figure B4. Computed accumulated snow storage equivalent on the watershed area of Circle Valley during 1962.

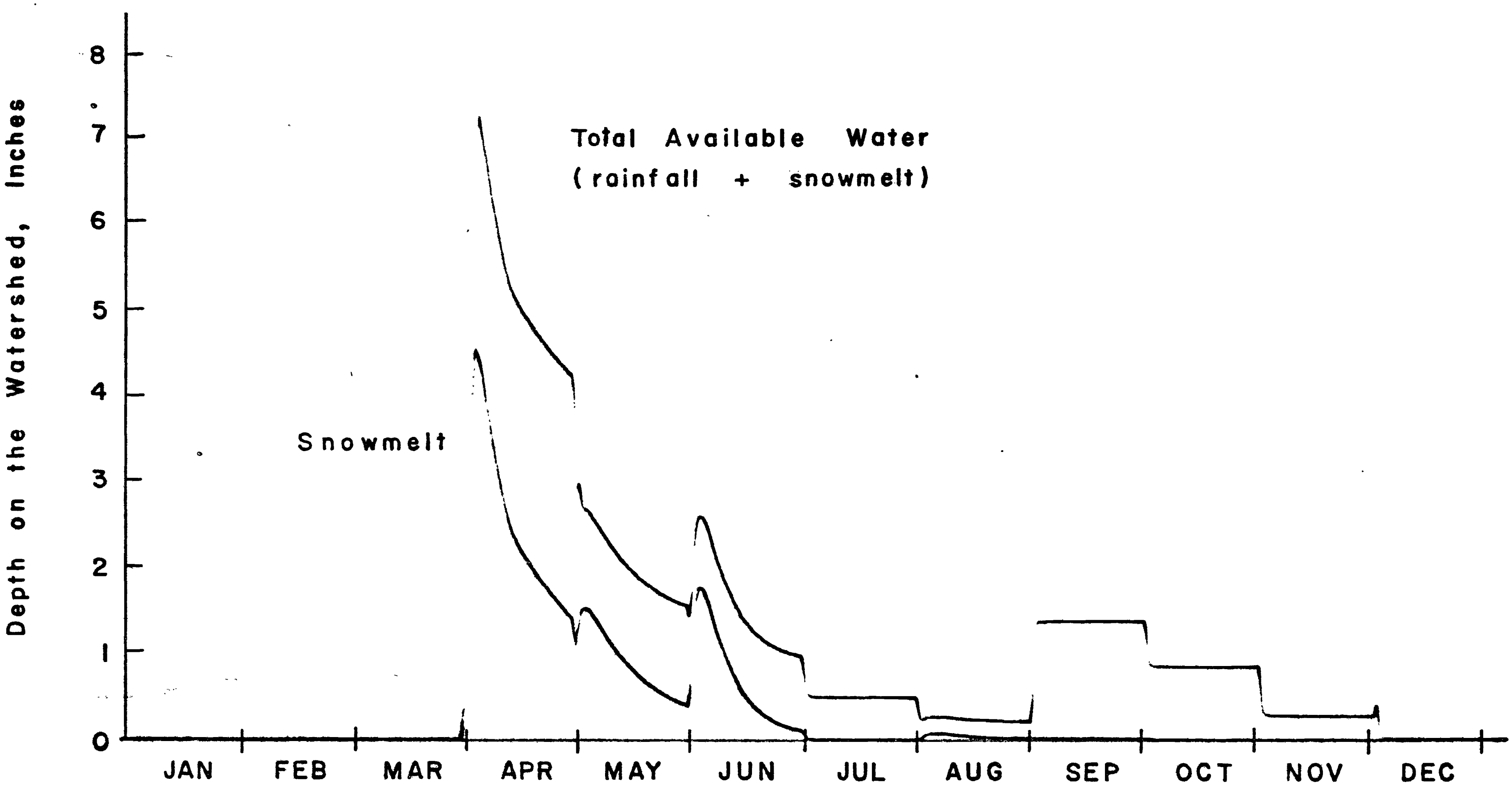

Figure B5. Computed values of available water within the watershed area of Circle Valley during 1962.

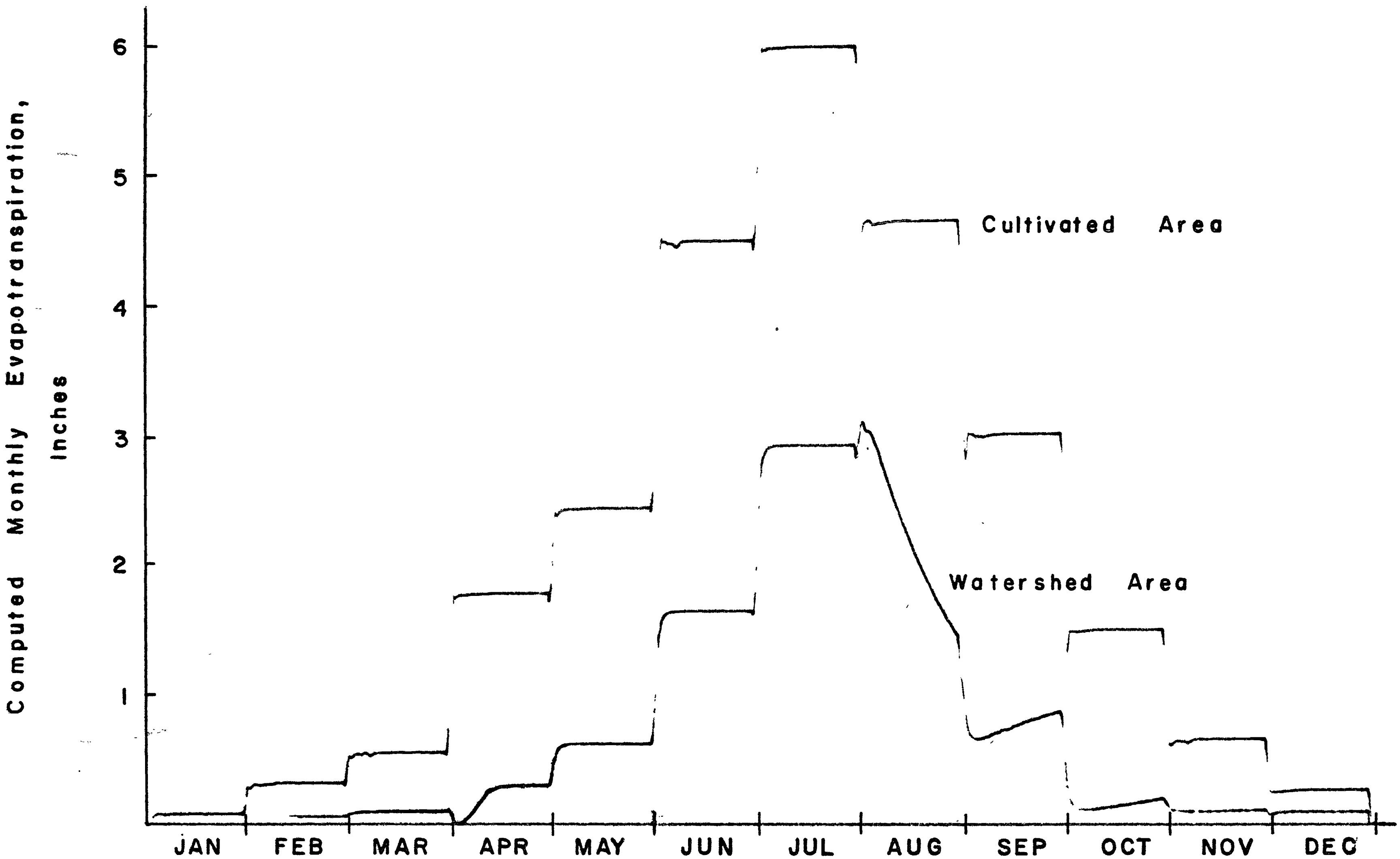

Figure B6. Computed mean monthly evapotranspiration rates, Circle Valley, 1962.

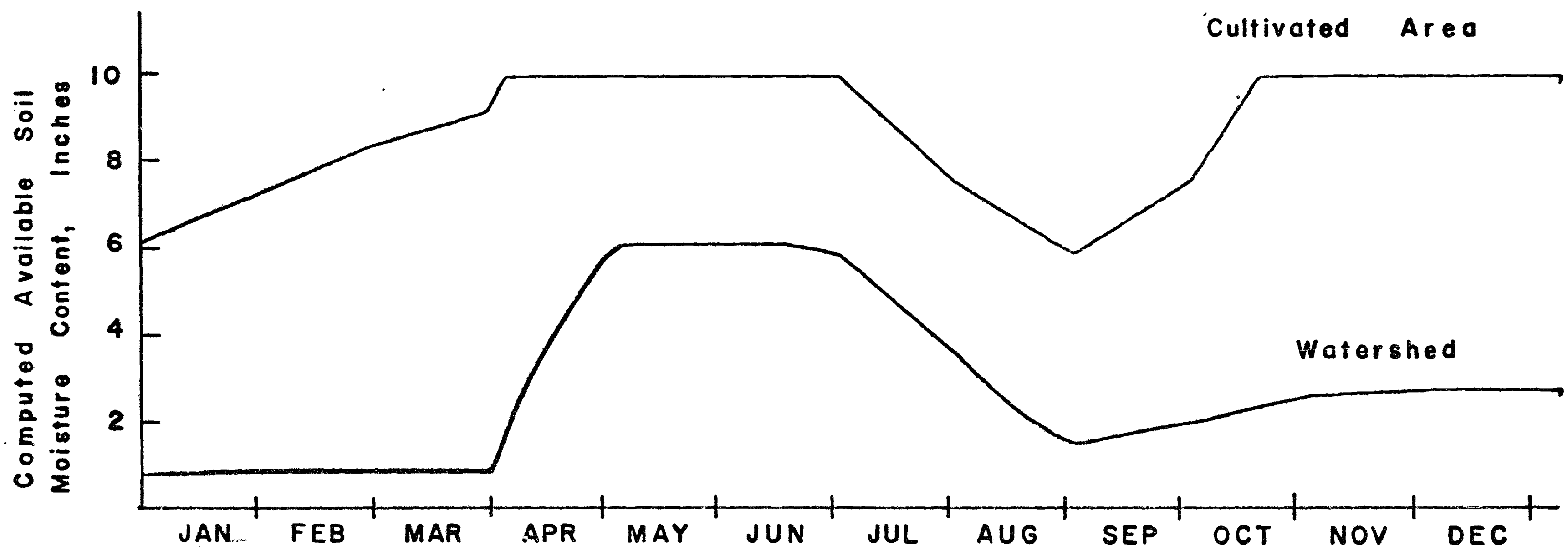

Figure B7. Computed average available soil moisture values within the cultivated and watershed areas of Circle Valley during 1962.

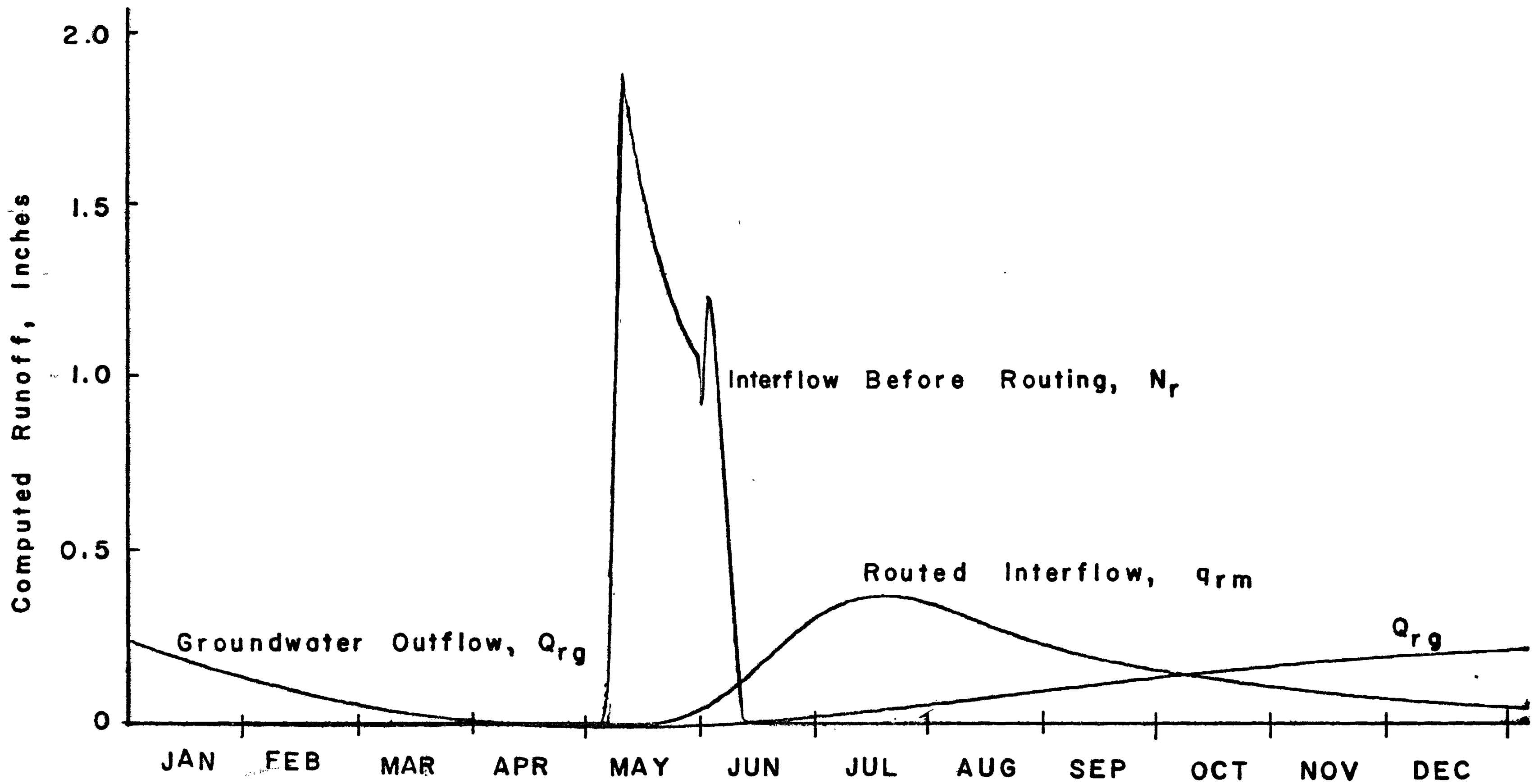

Figure B8. Components of runoff from the watershed area, Circle Valley, 1962.

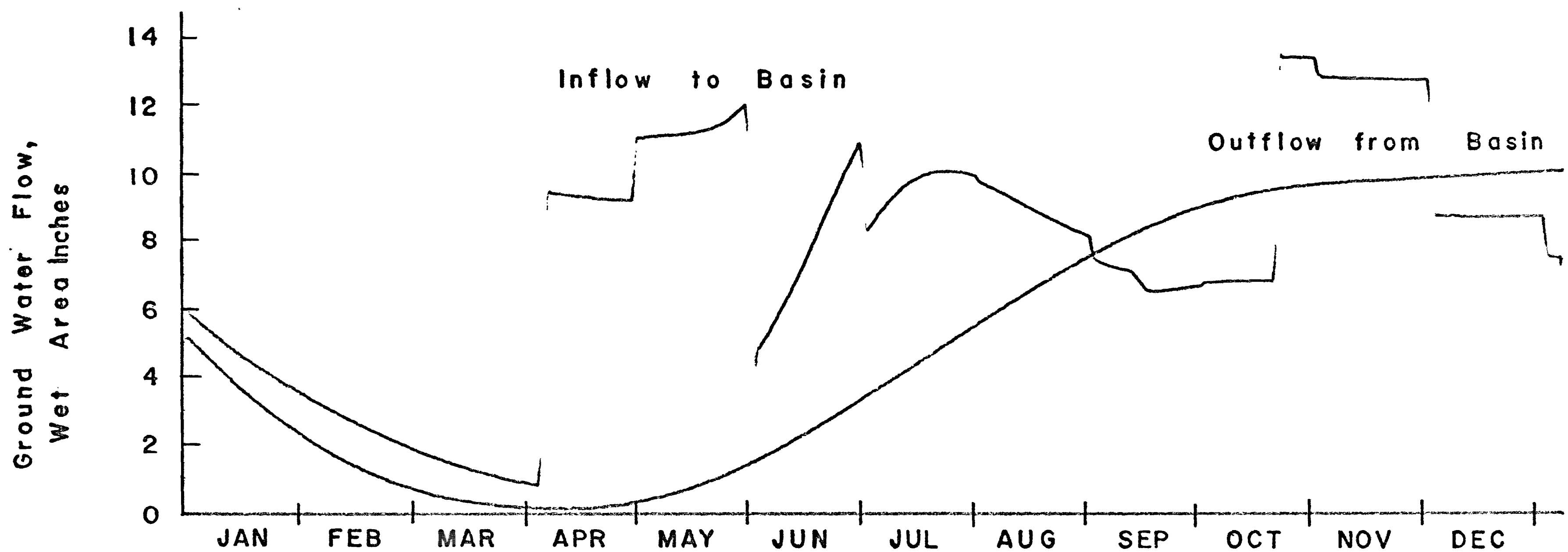

Figure B9. Computed values of inflow and outflow rates for the groundwater basin beneath the cultivated area of Circle Valley during 1962.

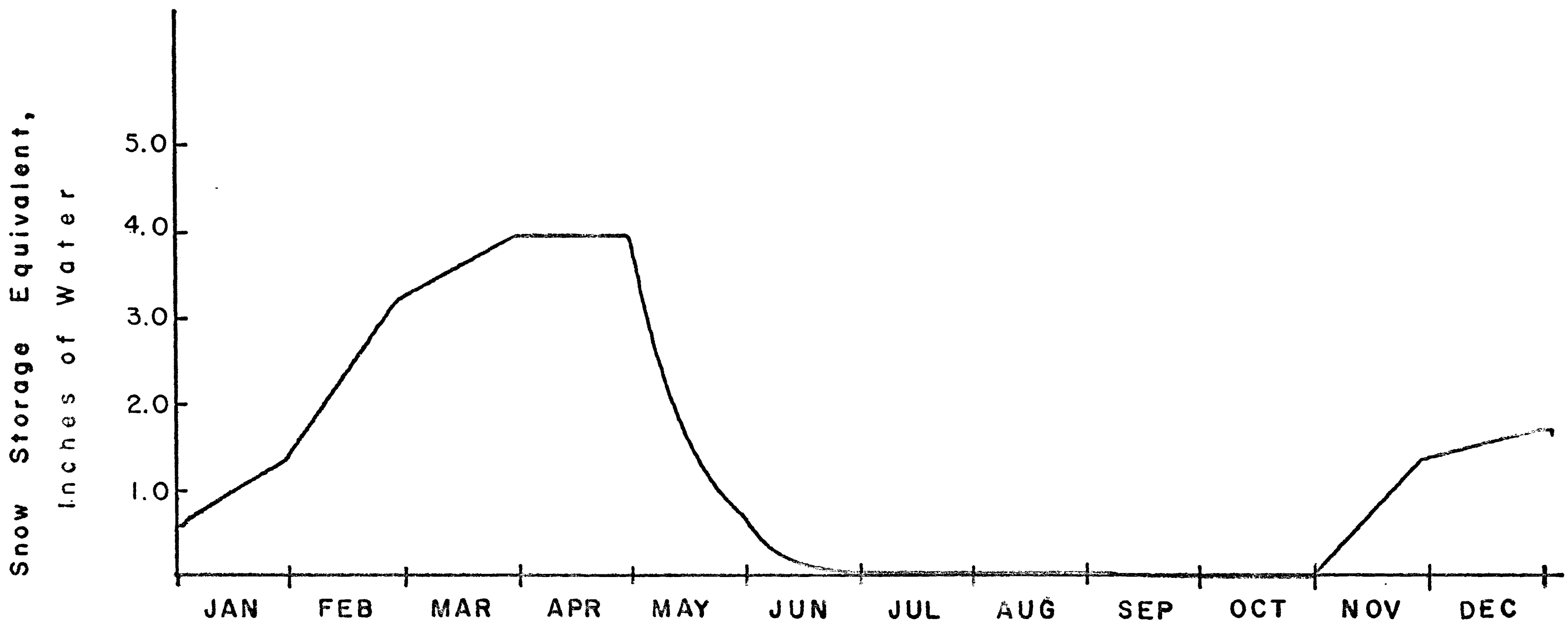

Figure B10. Computed accumulated snow storage equivalent in the watershed area of Circle Valley during 1963.